Abbass Kazemi

Fabrication and Functionalization of Nano-Micro Polymer Tubes by Using ATRP/Self-assembly Technique

and

Immobilization of Gold Particles onto Self-assembly Modified-Surfaces

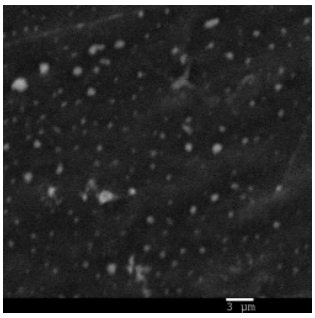

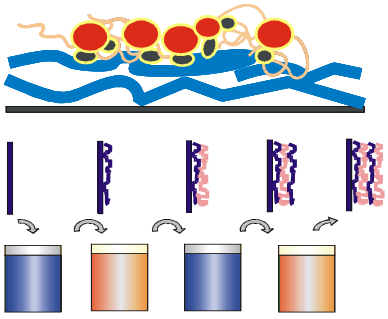

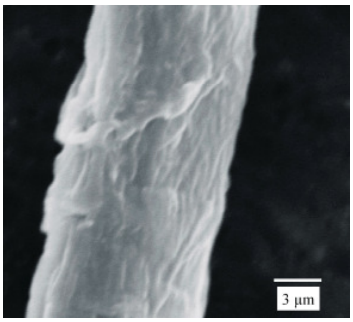

Abbass Kazemi

Fabrication and Functionalization of Nano-Micro Polymer Tubes by Using ATRP/Self-assembly Technique and Immobilization of Gold Particles onto Self-assembly Mmodified-Surfaces

Fabrication and Functionalization of Nano-Micro Polymer Tubes by Using ATRP/Self-assembly Technique
and
Immobilization of Gold Particles onto Self-assembly Modified-Surfaces

Dissertation

Zur

Erlangung des Doktorgrades

der naturwissenschaften

(Dr. rer. Nat.)

dem

Fachbereich Chemie der Pilipps-Universität Marburg

vorgelegt von

Abbass Kazemi

aus

Teheran

Marburg / Lahn 2006

Vom Fachbereich Chemie
der Philipps-Universität Marburg

als Dissertation angenommen: 26.07. 2006

Erstgutachter:	Prof. Dr. A. Greiner
Zweitgutachter:	Prof. Dr. H. J. Wendorff
Prüfer:	Prof. Dr. B. Neumüller
Prüfer:	Prof. Dr. N. Hampp

Don't try to hold on to this. You'll lose it.
Don't pull the curtain. It will end.
This moment with all of us here is paradise,
but don't try to leave this way. You'll ruin it.

Jelaluddin Rumi
(1207-1273)

CONTENTS

Table of symbols and abreviations

AIBN	Azobisbutyronitrile
ATR	Atenuated total reflaction
ATRP	Atom transfer radical polymerization
$Au_{DMAP\text{-}stab\text{-}x}$	DMAP-stabilized gold particles immobilized on the surface
$Au_{thiol\text{-}stab\text{-}x}$	Thiol-stabilized gold particles immobilized on the surface
$Au_{redAu(III)}$	Gold particles immobilized using the gold sol prepared by reduction of $HAuCl_4$
bipy	2,2´-bipyridyl
BrPPX	Brominated PPX
CD	Cyclodextrine
CVD	Chemical vapour deposition
DMAP	4-(dimethyl amino)pyridine
DSC	Differential scanning calorimetry
EDX	Energy eispersive X-ray analysis
kV	Kilo volt
IR	Infrared
GPC	Gel permission chromatography
G_{BrPPX}	Glass with a layer of BrPPX at the surface
LbL	Layer by layer
mbar	millibar
MMA	Methyl methacrylate
M_n	Number average molecular weight
Mtorr	Millitorr
M_w	Weight average molecular weight
NIPAM	N-isopropyl acrylamine
NMR	Nuclear macnetic resonance
NNDIPAAc	N,N-diisopropyl ammonium acrylate

PAA	Poly(acrylic acid)
PAH	Poly(allyl amine hydrochloride)
PD	Polydispersity
PE	Polyelectrolyte
PEI	Poly(ethyleneimine)
PEMHFs	Polyelectrolyte multilayer hollow fibers
PEMs	Polyelectrolyte multilayers
PEO	Poly(ethylene oxide)
PLLA	Poly-L-lactide
PMMA	Poly methyl methacrylate
PNIPAM	Poly (N-isopropyl acrylamine)
PPX	Poly (para xylene)
$PPXT_{end\text{-}thiol\text{-}mod}$	PPX tubes modified with thiol functionalities at the ends
PSS	Poly(styrene sulfonate)
PSS_{SDS}	Layer made by coadsorption of PSS and SDS
SDS	Sodium dodecyl sulfate
SEM	Scanning electron microscope
SH-mod-Sur-x	Thiol modifed surfaces
TEM	Transmission electron microscope
TEOS	Tetraethylorthosilicate
THF	Tetrahydrofurane
TGA	Thermal gravimetry analysis
TUFT	Tubes by template fibers
UV	Ultraviolet

1. Introduction and Theoretical Background

1.1. Introduction

Nanoscience is described as the study of objects on the nanoscale. Nanotechnology is defined as the ability to create and control individual atoms and molecules to build structures that indicate specific properties. Richard Feynman's historic talk **"Plenty of Room at the Bottom"** opened new doors to nanoscience. He expresses "The principles of physics, as far as I can see, do not speak against the possibility of maneuvering things atom by atom. It is not an attempt to violate any laws; it is something, in principle, that can be done; but in practice, it has not been done because we are too big". On the nanoscale, the way the molecules and atoms assemble into larger indicates properties of materials such as electrical, optical, and mechanical properties. Nature provides very interesting proofs in creating well-defined nano-scaled structures that makes our life better. For decades, the interdisciplinary field of nanoscience/technology has attracted interest of scientist due to the wide varieties of applications that for this field can be considered such as self assembly, nanoscale materials, ultra-sensitive biosensors, smart materials, shape memory materials, DNA template chemistry, advanced microfabrication, molecular biology, nanomedicine, nanoelectronics and carbon nanotubes.

Electrospining is a process, which was patented by Formhals,[1-3] using electrostatic forces to spin fibers from polymer solutions or melts. Recently, this process has become of more interest due to the potential applications of the polymer fibers in tissue engineering scaffolds, artificial blood vessels, medical and filtration industries. The great characteristic of the electrospun fibers is that they can be produced with diameters in the range of nanometer to a few microns with a high surface to volume ratio.

Polymer tubes can be produced by using the TUFT process.[4] In short, in this method, the electrospun fibers are used as template. The template fibers can be coated by poly (p-xylylene) (PPX) by means of chemical vapour deposition process. And then by selective removal of the core the tubes are obtained.

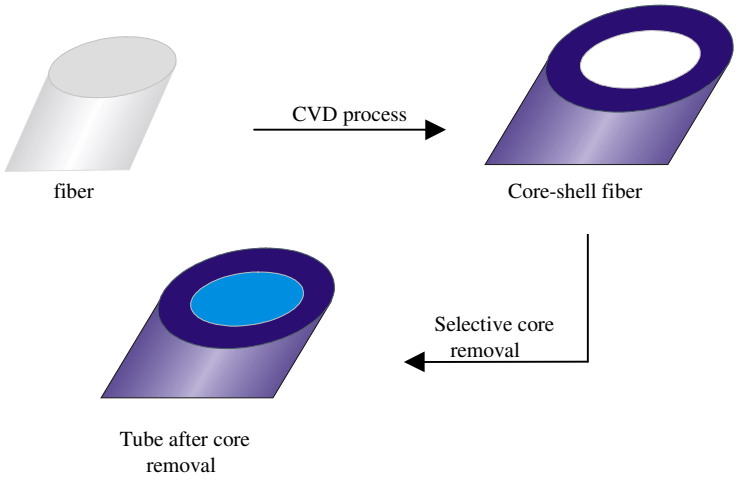

Figure 1. Schematic representation of the TUFT process.

Chemical vapour deposition process (CVD)[5-13] is a chemical process to deposit thin films onto a substrate. The deposition process is carried out on the substrate by transforming precursors in the form of thin films onto the substrate. The first report on formation of PPX films was published by Gorham.[8] The starting material was cyclic dimer of [2,2] paracyclophane, which was pyrolysed at 700-800ºC and then the polymerization was took place onto a substrate at a temperature lower than 30ºC to obtain a thin film of PPX on the substrate.

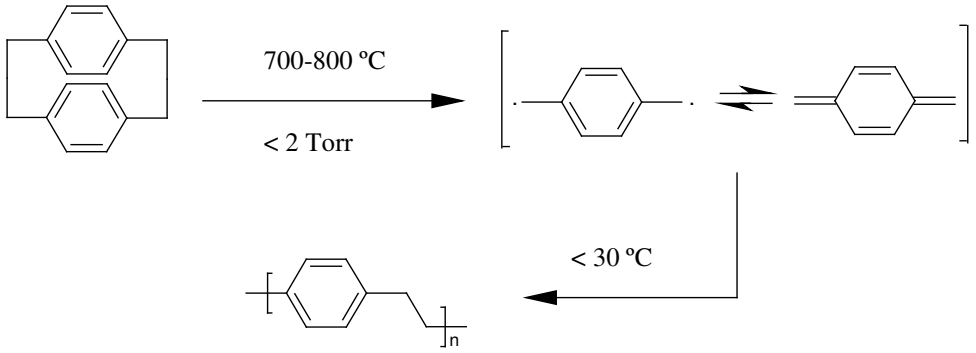

Scheme 1. Schematic representation of the formation of PPX by using chemical vapor deposition technique.

Promising chemical and physical properties of PPX make this polymer of interest of scientist. For example, high protective properties of PPX as an important property of PPX can be mentioned. PPX in the form of tubes and films can be used as surface initiator in order to obtain polymers synthesized on the surface by using atom transfer radical polymerization (ATRP). By bromination of PPX, it is converted to poly [1,4-phenylene(1-bromoethylene)], an ATRP initiator, so that ATRP can be carried out on the surface. By this mean, the surface properties can be changed by using different ATRP monomers.

Layer by layer self-assembly provides a comfortable method to build up oppositely charged polyion layers with their individual properties, which can be alternated depending on the polyelectrolytes used for multilayer build up. Decher et al.[14-15] reported a layer-by-layer self-assembly (LbL self-assembly) method for the fabrication of multilayer thin films consisting of anionic and cationic polymer layers. After each adsorption step the charge inversion of the surface could be observed. In this method charged polyelectrolyte chains are adsorbed onto an oppositely charged surface due to increasing the entropy of the system and electrostatic attraction. In general, the conformation of polymers within multilayers can be change depending changes in the environment surrounding the multilayers. Using pH sensitive polyelectrolytes make the surface to show different behaviour by changing pH.

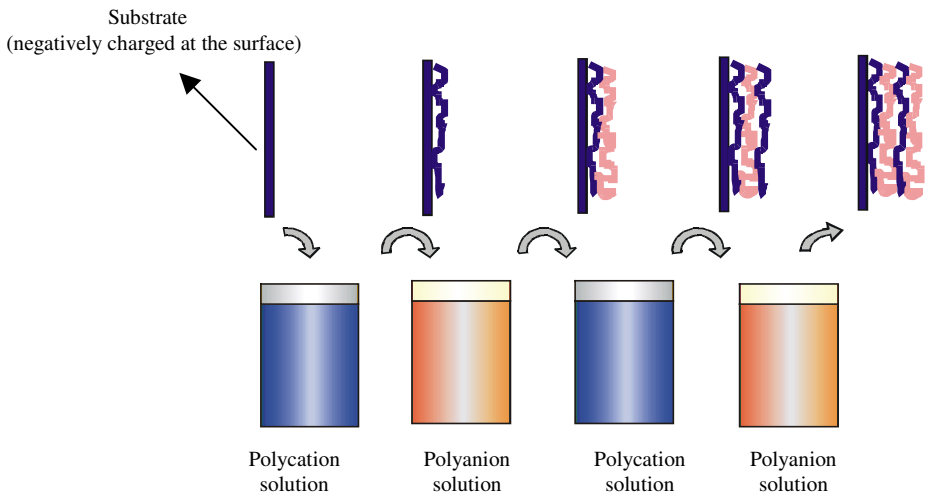

Figure 2. Shown the PEMs formation onto the surface of the substrate by L-b-L self-assembly technique.

Nowadays, by recent developments in nanoscience/nanotechnology, there are increasingly concerns to employ the self-assembly knowledge in the field of nano materials in order to modify the surface properties. Recently, the modification of the surface of nanoparticles[17,18] and carbon nanotubes[19,18] were performed by using self-assembly based technique.

Immobilization of gold colloidal monolayers onto the surfaces modified by polymer coated substrates bearing functional groups with high affinity for Au such as SH and NH_2 has been reported.[82] The gold particles can be immobilized in different patterns onto the substrates. Figure 3 shows the examples of the surfaces, which have been undertaken the immobilization of gold particles. In surface 3a, particles are immobilized separately, isolated pattern. In 3b, particles are immobilized more closely than previous surface. In figure 3c, particles are intensely packed, resulting a closed-packed colloidal monolayer. And finally in surface 3d, particles are in an aggregated form.

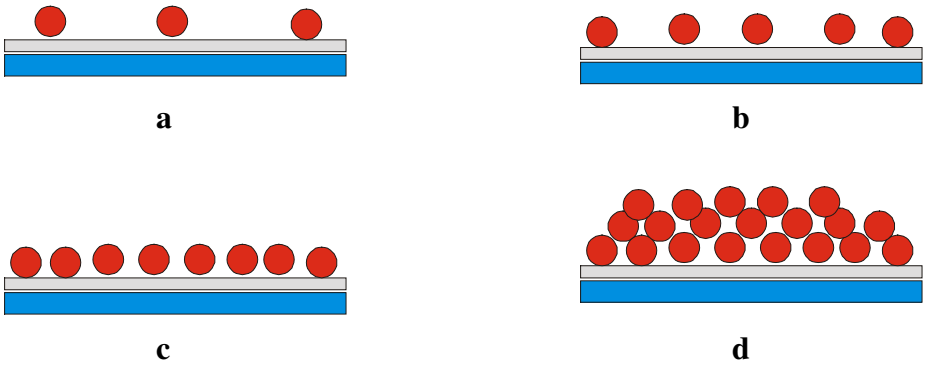

Figure 3. schematic representation of different patterns of gold particles on the substrates (a) isolated particles; (b) submonolayer; (c) monolayer; (d) bulk.

Gold substrates can be modified by self-assembly of monolayers by introducing materials with desired functional groups, which can result desirable surfaces. The surface of gold particle were modified by self-assembly of 1-dodecanethiol and other alkanethiol drivatives.

1.2. Electrospinning

1.2.1. Introduction

Electrospinnig is known as a technique for fabrication of polymer fibers. In 1930's, Formhals demonstrated a method for production of polymer fibers.[27-31] More investigation was followed by Simons,[32] showing the effect of viscosity on the length of the fibers. Later in 1971, Baumgarten reported fibers production with diameters in the range of 50-1100 nm. Relatively recently, electrospinning have increasingly gained attention due to its applications in medicine, filtration industries and tissue engineering. Various polymers has been reported to be spun into the fibers from their solution or melt.

In practice, the electrospinning apparatus is made of the following parts (figure 4): a syringe with a capillary containing a polymer solution or melt, a high voltage supplier and a collecting object. The collector can be either fixed or can be a rotating object in order to collect the fibers in oriented forms. A high voltage is used to make polymer solution or melt jet. The spinning rate can be controlled by adjusting the electric field and the flow of the polymer from the capillary.

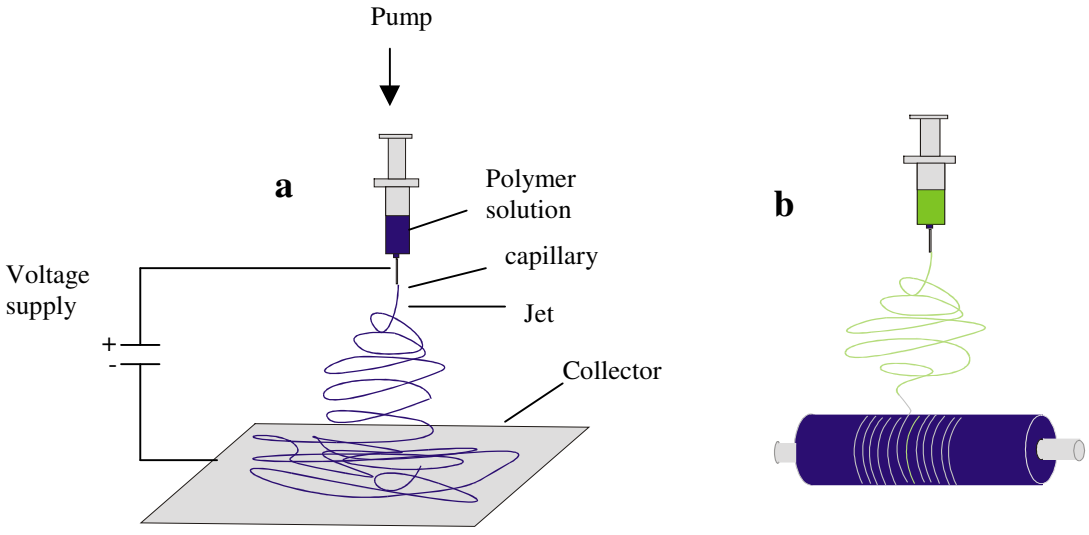

Figure 4. Shown a simple view of the electrospinning set up; (a) electrospinning onto a fixed collector; (b) electrospinning onto a rotating collector.

1.2.2. Which factors can effect the fibers characteristics?

In general, the process of the electrospinning can be effected by various parameters, which are described as follows:

- **Characteristics of polymers**

Among the polymer characteristics molecular weight, polydispersities and architecture of the polymers can influence in the electrospinning process.

- **Viscosity of polymer solutions**

In order to obtain the fibers of good appearance, the viscosity of the polymer solution should be in an appropriate range, which can differ for different polymers. For example, at high viscosity values, electrospinning will be refused due to restriction of the flow. On the other hand, if the viscosity is very low, the low cohesiveness of the solution causes the jet to break up. Investigation of the effect of the viscosity of the aqueous solutions of poly(ethylene oxide) (PEO) was performed by Fong et al..[33] Using the solution of ethanol/water, it was found that the proper viscosity are in the range of 1-20 poises in which the electrospinning was successfully performed.

- **Conductivity of polymer solutions**

The conductivity of the polymer solutions is an important factor for controlling the diameter of the electrospun fibers. An increase in the conductivity of the polymer solution can cause molecular orientation in the elctrospun fibers.[34,35]

- **Surface tension**

The liquid droplet at the capillary tip is kept by surface tension. By an appropriate intensity of the electric field the droplet can be distorted and a jet of fluid is generated. The value of the surface tension of the polymer solution should be in an appropriate range. For example, in the case of very high surface tension, electrospinning results fibers (on the collection target) to be converted to droplets before evaporation of solvent.

- **Electrical field**[36]

For electrospinning of the polymer fibers, a potential difference between the capillary tip and the collecting object is required in order to overcome the forces related to surface tension, which prevents the solution to flow. This factor can effect directly on the fibers diameters in the way that by increasing the electrical force the diameter of the fibers is decreased and vice versa.

- **Ambient parameters**

The working conditions for electrospinning process such as temerature, humidity and air velocity in the chamber can be considered as ambient parameters.

- **Distance between capillary and collection object**

In principal, by increasing the distance between capillary and collection object, fiber diameter is increased. An increase in distance with constant voltage results in a decrease in electric field, a smaller driving force on the initiated jets, and therefore, larger diameter of the fibers.

- **Collection object**

The collection object (collector) is a fixed or rotating object on which the fibers can be spun. For example, by using a rotating cylinder collector, the fibers can be obtained in an oriented form.

In practice, a mixture of the factors mentioned above can influence the fibers properties. The main achievements in the electrospinning of the fibers that one wants to obtain can be mentioned as: controllable diameters of the fibers, defect free/controllable surface of the fibers and continuous single fibers. It was established that the diameter of the fibers can be influenced by splitting the solution jet while it travels from the capillary onto the collector. [37-45] Viscosity of the polymer solution plays an important role in the fibers diameters.[46-48] Concentration of the solution, which is proportion to the viscosity, can effect on the fibers diameters.[49,50] Electric voltage used during electrospinning can also effect the fibers diameters. For example, by using higher voltages for electrospinning the smaller fibers diameters can be obtained.[50] Controlling the quality of the fibers is also important in the

electrospinning process. Non-uniform diameter[50] of the fibers and defects[51,52] are among the problems that very often cab be appeared for electrospun fibers. Demir et al. demonstrated the effect of temperature on the uniformity of the fibers that at higher temperatures the electrospinning of the polymer solutions with the same concentration results fibers with more uniform diameters.[50] Another group reported that the concentration of the solutions have influence in beads formation. The higher concentration of the polymer solutions ends up with decrease in the number of beads. In order to obtain bead-free fibers, the polymer solutions with filler materials can be used.[53] It was observed that by using salt in the polymer solution, bead-free fibers can be obtained. The reason for this were described as existence of the higher charge density on the surface of the solution jet. Producing the fibers by electrospinning using solutions containing organic and inorganic materials has been taken into consideration. Using a solution of polyacrylnitrile (PAN)/TiO_2[54] and Nylon6/montmorilonite (Mt) for production of nano-meso fibers are among the examples of the fabrication of the ultrafine fibers using the composite solutions.

1.3. Preparation of PPX by Chemical vapour deposition (CVD) process

1.3.1. An introduction to PPX formation

For the first time chemical vapor deposition was performed by Szwarc in 1974.[55-57] In CVD process for preparation of the films of poly(para-xylylene), as a precursor, [2,2] paracyclophane is used in the gas phase, which is then deposited onto a surface. The intermediate substance in the gas phase are para-xylyene monomers, which can be formed at high pyrolysis temperatures (>550 ºC). The method introduced by Szwarc was not efficient due to the low yield of the process. In 1966, Gorham improved the CVD process to make it a more efficient technique by using a vacuum pyrolysis of a cyclic dimer of di-para-xylylene.[58] [2,2]paracyclophane can be converted to para-xylylene monomers at temperatures higher than 550 ºC and at pressure below 1 Torr. Then, the intermediate precursor is deposited as a thin polymeric film of poly(para-xylylene) onto a surface at room temperature (see scheme 2).

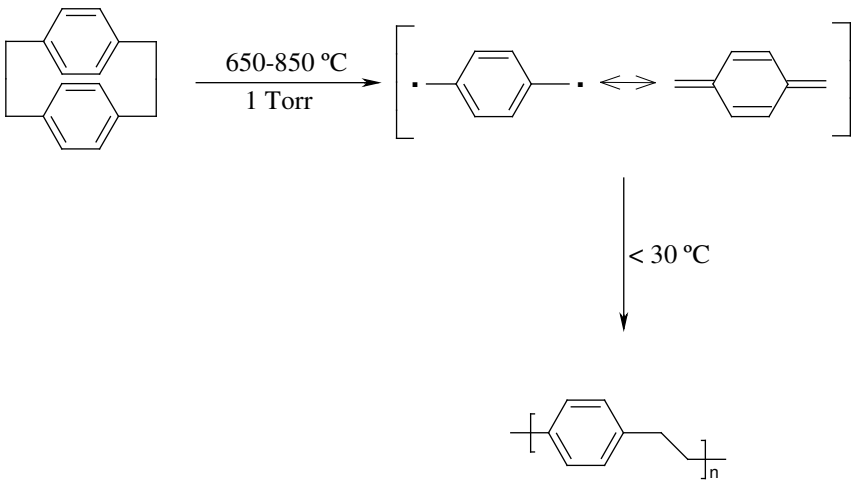

Scheme 2. Schematic illustration of PPX formation reported by Gorham in 1966.

[2,2]Paracyclophane can pyrolyzed at 600 ºC and presure below 1 Torr, resulting two intermediate molecules of p-xylylene. The reason for pyrolysis of [2,2]paracyclophane at high temperature is the strain in the molecular structure of [2,2]paracyclophane. The condensation of the gaseous intermediates (p-xylylene) results a polymeric compound of poly(p-xylylene) (PPX).[59,60]

1.3.2. CVD machine

CVD apparatus consist of different parts namely vaporizer, pyrolysis furnace, deposition chamber, cold trap and mechanical vacuum pump. To describe what is happening during the CVD process briefly:

[2,2]Paracyclophane in its dimer form, is sublimed in the vaporizer chamber while the system is "pumped down" to a pressure below 1 mbar. After the precursor gas was arrived to the pyrolysis zone, the precursor is pyrolysed at appropriate temperature 650-700 ºC and in this

way, is converted to the intermediate component p-quinodimethane. By condensation of the p-quinodimethane on the substrate at temperature < 30 ºC, the polymeric film of PPX is formed.

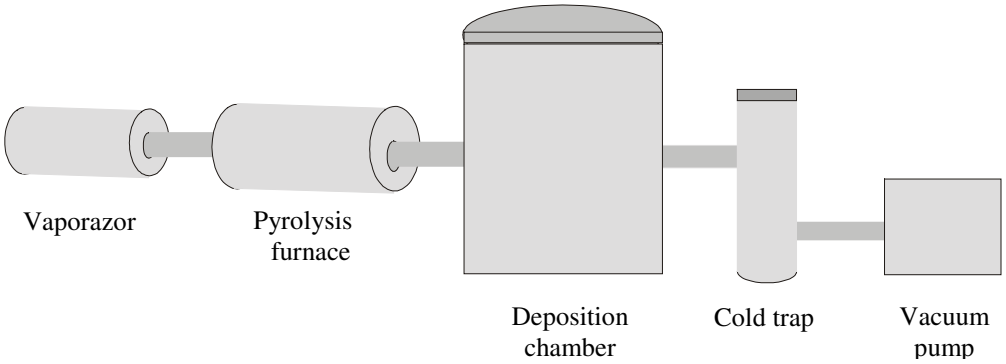

Figure 5. CVD apparatus for synthesis of PPX.

1.4. TUFT process[4]

This method gives us a way to obtain tubular fibers in nano/meso scales. Starting from electrospinning, by production of the fibers, which can be used as templates. Then, the electropun fiber templates can be coated with PPX by CVD process. After the selective core removal of the core-shell fibers, the tubes are obtained. The core removal can be done by heating or by solvent extraction. Since, the decomposition temperature of PPX is high and does not dissolve in the most solvents, PPX can be considered as an excellent coating material. Figure 6 gives a schematic illustration of the TUFT process.

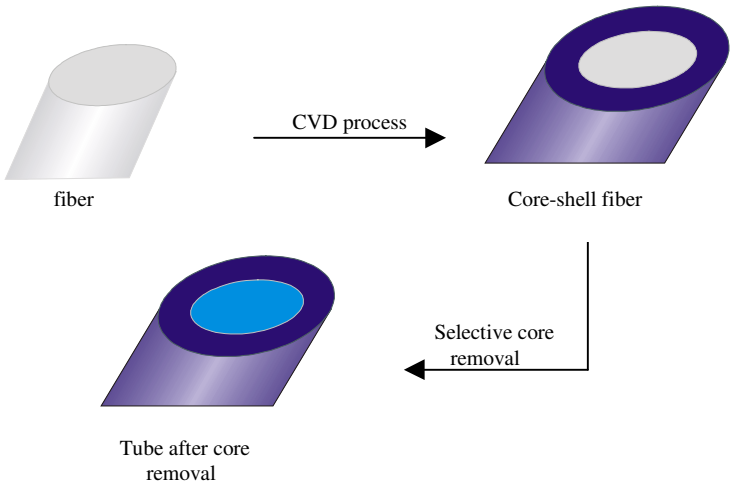

Figure 6. Shown TUFT process.

1.5. Atom transfer radical polymerization (ATRP)[61]

1.5.1. Introduction

To obtain polymers with well-defined structures, living/controlled polymerization can be employed. The living/controlled polymerization can be performed by using different techniques such as ionic polymerization and controlled radical polymerization. In this work, the focus is on a controlled polymerization technique known as ATRP. Recently, ATRP became of interest because of its capability in controlling the structure of the polymers.[62-68] In addition, this polymerization technique is very suitable for modifying the surfaces. The surface initiated ATRP was performed by several research groups. ATRP includes two steps in which the propagating chains become activated and deactivated. In conventional radical polymerization, the termination reactions takes place, which is because of the existence of the radical species. Comparing to the conventional radical polymerization, in ATRP, termination occurs in a very small amounts so that this polymerization acting almost like living

polymerization. In the following sections, the mechanism of the copper catalyzed ATRP as well as the suface-initiated ATRP will be described.

1.5.2. General procedure of ATRP

As can be realized from the name of ATRP, the most responsible reaction is occurred in the atom transfer stage, leading to a uniform growth of the propagating chains. For ATRP, the components required are monomer, initiator, catalyst (a complex of a transition metal capable to be on different redox stages and suitable ligands) and in some cases additives can be used for better performance of ATRP. In the following steps, ATRP as a controlled radical polymerization is discussed in more details:

1.5.3. Mechanism of ATRP

The mechanism of ATRP is based on the atom (halogen) transfer between propagating chains and transition metals used as catalyst. Scheme 3 shows the schematic illustration of the mechanism of ATRP.

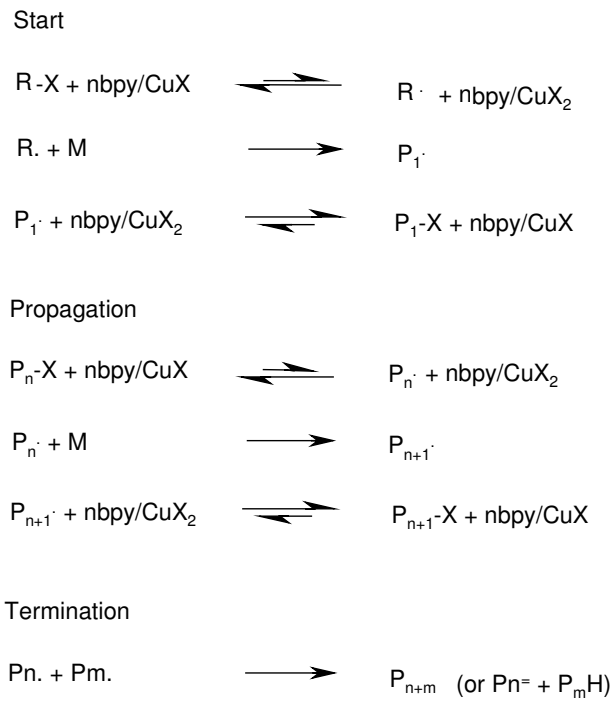

Scheme3. Schematic illustration of the different stages of ATRP.

Intiators in ATRP contain a halogen atom in their structures so that, they can react with transition metals used as catalyst in their lower oxidation states, for example cupper(I)bromide (CuBr). By oxidation of Cu(I) to Cu(II), the initiator is converted to radical species, which can initiate the polymerization. Cu(II) can be reduced reversibly to Cu(I) so that the bromine is transferred to the radical specie (the propagating chain) and in this way the growth of the propagating chains is controlled. The propagating chains in ATRP can be controlled between activated and deactivated forms. This causes that the polymers synthesized by ATRP display specific properties known for the polymers obtained from living polymerizations.

1.5.4. Characteristics of the polymers synthesized by ATRP

The molecular weights and polydispersities of the polymers synthesized by ATRP show similarities to those of the living polymerization. The theoretical degree of polymerization can be calculated from the equation below:

$$DP = [M]_0/[\text{initiator}]_0 \times \text{conversion}$$

The narrow polydispersities of the polymers obtained from ATRP (PD = 1-1.5) can be defined as one of the important characteristics of ATRP. Well-defined polymers (end-functionalized polymers and copolymers) have been synthesized by ATRP. It should be noted that termination reactions and other side reaction can occur at high molecular weights so that a variation from the usual characteristics of polymers synthesized by ATRP can be observed at high molecular weights.

1.5.5. Monomers

Monomers used in ATRP cover a wide range of monomers with different fanctionalities namely (meth)acrylates, (meth)acrylamides and styrene.

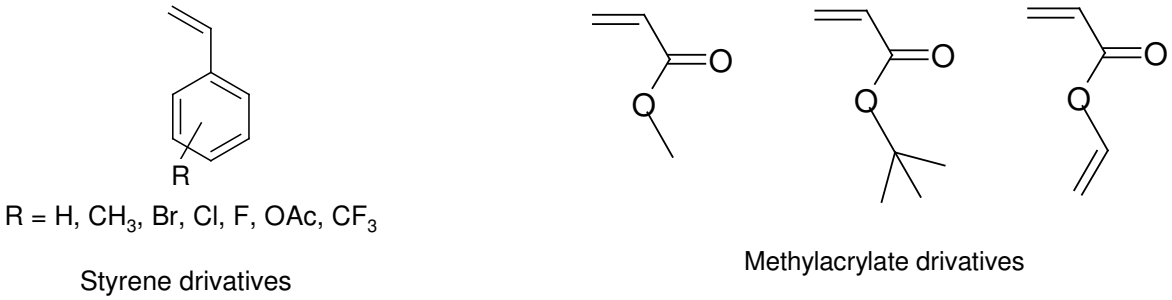

Scheme 4. Shown the chemical structures of some monomers that can be used in ATRP.

Not all the monomers can be used for ATRP successfully. Performing ATRP with nitrogen containing monomers like acrylamide and its derivatives using 1-(bromoethyl)benzene as the initiator indicate very low ATRP equilibrium constant than other usual ATRP monomers such as acrylates and styrene.[69] The reason for this might be because of the inactivation of the catalyst by olygomers after the reaction is started, resulting ATRP to be stopped at early stages of the polymerization. In addition, as the second reason for preventing the ATRP at early stages, the amide groups can be replaced instead of the terminal halogen atom.[70] Nevertheless, there are some reports on performing successfull ATRP of nitrogen containing monomers using surface initiators.[63]

Another group of the monomers that can not be directly used in ATRP are acid monomers. The acid groups can poison the catalyst. So, using acid monomers directly, the polymerization is stopped at early stages. To overcome the problem, one should chose the right initiator and pH of polymerization. Ashford et al. reported a successfull ATRP of acrylic acid using a macroinitiator.[71] The polymerization was carried out at pH between 8 and 9. In one of the attempts, ATRP of acrylic acid monomer in its salt form N,N-diisopropyl ammonium acrylate was successfully carried out using BzBr as initiator.[72]

1.5.6. Solvents

ATRP is the polymerization that can be performed in different conditions. Considering the polymerization environment, ATRP can be done as bulk polymerization, solution polymerization and even can be carried out in an heterogeneous media. A wide range of solvents can be used in ATRP. For example, tetrahydrofurane (THF), acetone, benzene, anisole, alcohol and water can be named as suitable solvents for ATRP. Using solvent become necessary for ATRPs in which the polymers synthesized are insoluble in their monomers. Choosing the right solvent is important, since some solvents can poison the catalyst[73] or can facilitate the side reactions.[74] Solvents in ATRP can effect the rate of polymerization by their effect on the catalyst structure.[75-78]

1.5.7. Catalyst

The ATRP catalyst composed of a transition metal and ligands in a complex structure. The formation of the complex is essential for a successful polymerization. The metal center causes an electron transfer reaction in order to activate the propagating chains (radicals) and deactivate the chains (dormant species). For example, copper and iron in their salt forms respectively CuBr and $FeCl_2$ are among the transition metals used in the structure of the ATRP catalyst. Various ligands can be used in the complex structure such as nitrogen and phosphorous ligands. By using ligands, the transition metal within the complex structure become soluble in the polymerization media. In addition, the ligands can provide the reactivity of the transition metal for an appropriate ATRP.

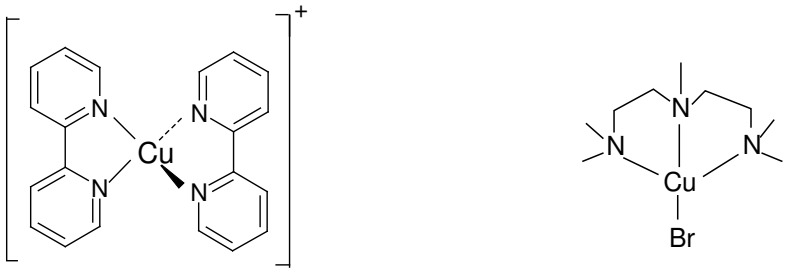

Scheme 5. Shown two complex structures of the ATRP catalyst.

1.6. Polyelectrolytes

Polyelectrolytes are polymers that their repeat units bear electrolytes, which can be charged in aqueous solution. The polyelectrolytes indicate both properties of electrolytes and polymers. The polyelectrolytes are divided into two groups of weak and strong polyelectrolytes. The strong polyelectrolytes are those, which are able to dissociate completely in aqueous solutions for a wide range of pH, whereas the weak polyelectrolytes show a partially dissociation at intermediate pH. For weak polyelectrolytes a dissociation degree can be defined, which can be changed by changing pH. Conformation of the polyelectrolytes can be effected by the charge density on the chains. The electrostatic repulsive forces cause the polyion chains to show up an expanded, rigid-rod-like conformation.[79] Scheme 6 shows the chemical structure of some examples of polyelectrolytes.

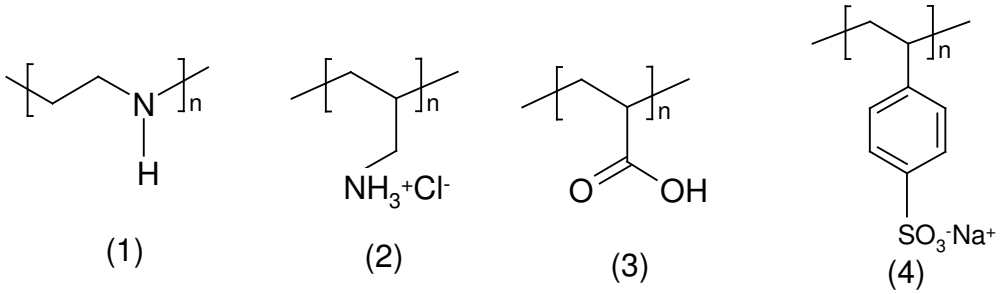

Scheme 6. The structure of polyelectrolytes: (1) Poly(ethyleneimine) (PEI); (2) Poly(allylamonium hydrochloric acid) (PAH); (3) Poly(acrylic acid) (PAA); (4) Poly(styrene sulfonate) (PSS); the structures 1, 2 and 3 are weak polyelectrolytes whereas 4 is a strong polyelectrolyte.

2.7. Layer by layer (LbL) self-assembly of polyelectrolytes

In general, self-assembly is a method, which can be described as interaction of the molecules to form larger structures. The interaction can be of non-electrostatic nature like hydrogen bonding, covalent bonds, etc. Nevertheless, using electrostatic forces make the PEM build-up very stable. Using LbL self-assembly technique, polyelectrolyte multilayers (PEMs)

can be built up. PEMs have become a challenging subject due to their potential applications in academical research and industries. LbL self-assembly is a method that can be simply applied for surface modification. In fact, the formation of PEMs on the surface changes the surface properties, depending on the types of the polyelectrolytes used in the PEM structure. In 1992, Hong and Decher proofed the concept of LbL self-assembly of oppositely charged polyelectrolytes.[87] In this method, charged polyelectrolyte chains are adsorbed onto a oppositely charged surface due to the increase in entropy of the system and the electrostatic interactions between opposite charges at the surface. The films formed on the surface are highly stable. It is known that the PEM layers do not arrange separately so that there is no specific boundary between the layers of PEMs. Polyions chains of opposite charges entangle into each other. The preparation conditions of PEMs with which the properties of the PEM films can be controlled, are salt concentration, dielectric constant of the solvent (in which the deposition process takes place), type of salt, deposition time, polyelectrolyte concentration, molecular weight of polyelectrolytes and charge density or degree of ionization along the chains.

One of the important factors that can influence the structure properties of the multilayers is the salt concentration of the dipping solutions of polyelectrolytes. The adsorption of the polyions from the salt solutions causes the changes in the thickness of the multilayer films. The existence of salt causes the charges of the polymer chains to be screened and to form coiled-structures in the solution, resulting an increase of the thickness of the layers after deposition on the surface.[80]

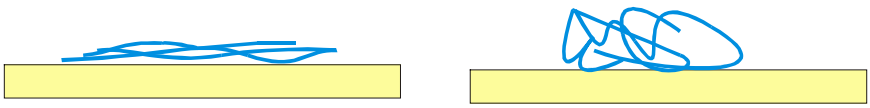

Figure7. Schematic illustration of polyelectrolytes on the surface: left, if the polymer layer is adsorbed onto the surface from a dipping solution without salt; right, if the dipping solution contains salt, the polyelectrolytes are appeared in a coiled-structure, which causes a thicker layer.

Another important factor that can effect the structure properties of the PEM films is pH of the dipping solutions from which polyions are adsorbed onto the surface. Using weak polyelectrolytes, pH of the dipping solution can effect the conformation of the chains in the solution and also can effect on the layer structure after adsorption of polyions onto the surface. For example, having a weak polyanion (PAA), by increasing the pH of the dipping solution, the charge density on the polyelectrolyte chains is increased, which means that the chains gain more negative charges. The increase of negative charges on the chains leads to more electrostatic repulsive forces within the chains, resulting the chains to be more extended, which cause a decrease of the thickness of the adsorbed PAA layer. By decreasing, pH, the process is reversed and the chains will be more coiled and the thickness of the deposited layer is increased (see figure 8).

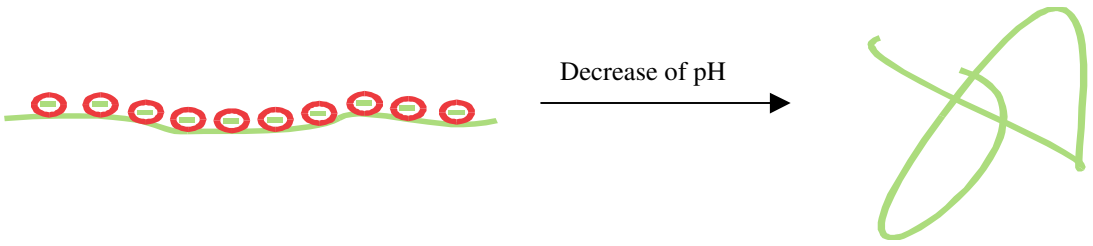

Figure 8. The polyanion chain was assumed to be a weak polyelectrolyte chain with acidic groups. The chain at low pH is protonated and the charge density on the chain then is decreased and the chain turns to a coiled structure.

1.8. Immobilization of gold on the self-assembly-modified surfaces

1.8.1. Introduction

Research in the field of nanoparticles is considered as a very interesting topic in chemistry, physics and also biology. The metal nanoparticle can be prepared in a wet condition and this make them applicable in the different fields of the science. Over hundred years ago, Faraday introduced a method for wet preparation of the metal nanoparticles. He prepared a gold hydrosol, which was stable with a red wine color. The research in the field of nanoparticles has been increasingly growing from 1990's. Schiffrin et al. introduced a preparation of stabilized-gold nanoparticles. The properties of the metal nanoparticles are highly in dependent of their size and the ratio of the numbres of atoms appeared at the surface and inside the particles. Interesting is that the electronic properties of the metal changes from a bulk to its nanoparticle form.

1.8.2. Immobilization of gold nanoparticles onto the modified-surfaces bearing thiol (mercapto) groups

Immobilization of the gold particles is based on the chemical reactivity of the thiol functionalities towards gold particles. Scheme 7 shows the possible reaction between he molecules bearing the thiol (mercapto) functional goups and gold.[81]

Scheme7. Reaction of gold with molecules bearing thiol functional groups.

If the surfaces has been modified by materials with thiol functionalities, gold particles can react with the thiol groups at the surface of the substrate and consequently can be immobilized onto the surface. There are several published works for immobilizing the gold particles on the surfaces. Grabar et al. reported a successful immobilization of gold particles on the surfaces bearing CN, NH_2 or SH fuctionalitis in which the formation of the gold monolayers are based on the covalent bands of the gold particles with CN, NH_2 or SH functional groups.[82]

One of the goals of this work, is to immobilize different types of gold particles onto the modified-surfaces, which were prepared by using the self-assembly based technique. In this method the surface was coated with monolayer of PEI and then 1-dodecanethiol by using the self-assembly technique. And then the gold particles were immobilized on the surface. The gold particles on the surface was bounded to the surface with covalent bound of the gold particles with thiol groups of 1-dodecanethiolmolecules. Figure 9 indicates the representative illustration of the surface before and after gold immobilization on the thiol-modified-surface.

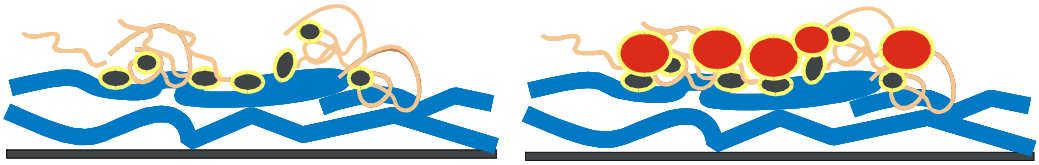

Figure 9. The preparation method of the gold-immobilized-surfaces will be described in this thesis.

1.9. Motivation

An interesting subject in nano-scaled science is to be able to handle nano-objects and to create new modified materials with new properties applications. Recent developments in characterization methods of nanomaterials make us to go further in this field to deal with nano-objects not as a whole but on the specific area of them.

The aims of my thesis is summarized (or described) as follows:

a) Sealing PPX tubes by polymers with pH/thermo-sensitivity by using either surface-initiated atom transfer radical polymerization (ATRP) or by selfassembly of polyelectrolytes onto the surface of the tubes.

b) Another objective of this thesis is to fabricate hollow fibers made of polyelectrolyte multilayers. For this mean, electrospun silica fibers were prepared and used as substrate to assemble polyelectrolytes onto the surface. After the removal of the silica from the core-sell fibers, the PEM hollow fibers can be obtained.

c) In order to modify the surface of PPX tubes, the LbL self assembly process can be employed to have the propertied of the surface altered.

d) Gold/silver particles were immobilized on the self-assembly modified surfaces of PPX films/tubes. Further experiments were carried out to deposit gold on the ends of the tubes.

2. Results and discussion

2.1. Fibers by electrospinning

2.1.1. PLLA fibers

PLLA fibers were produced using poly-L-lactide solution. The polymer chemistry of PLA make them suitable for variety of applications. Among the promising properties of PLA fibers low flammability and smoke generation, high resistance to ultra violet (UV) light and lower specific gravity, making PLA lighter in weight than other fibers. In addition, in this work, the PLLA fibers were used as fiber templates for TUFT process due to their great advantage, which can readily degrade by heating or can be dissolved by solvent.

Figure 10 shows the PLLA fibers fabricated by using ectrospinning.

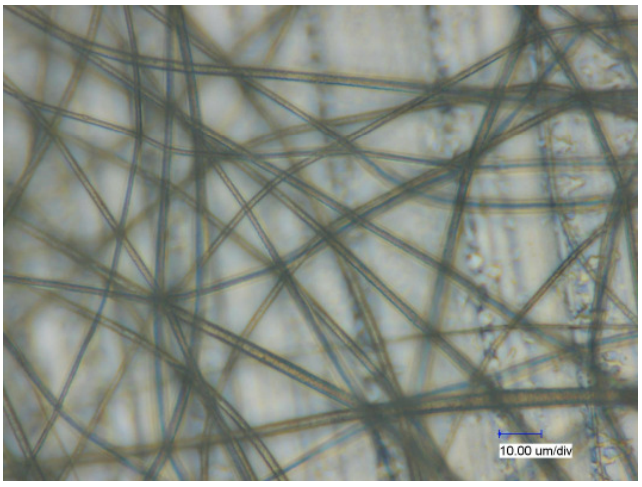

Figure 10. Digital microscope image of electrospun PLLA fibers.

2.1.2. Silica fibers

Silica fibers (SiO_2 fibers) were fabricated in order to be used as templates for production of the hollow fibers made of polyelectrolyte multilayers (HFPEMs). Since silica fibers can provide appropriate electrostatic forces for deposition of polyelectrolytes, they are used as substrate for polyelectrolyte self-assembly. In figure11, the electrospun silica fibers can seen.

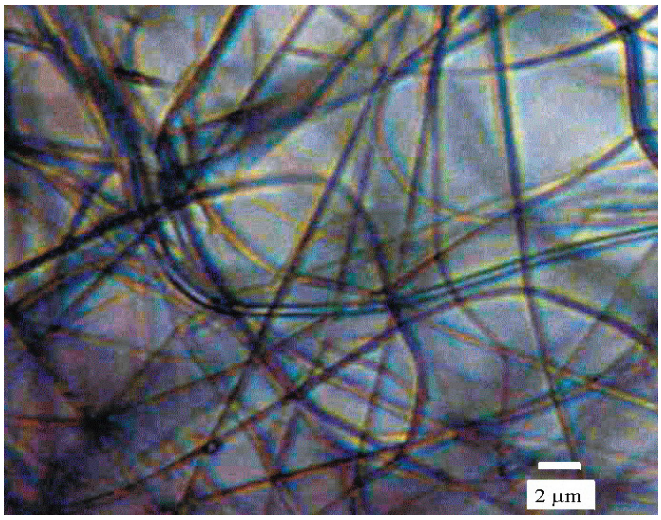

Figure11. Digital microscope image of silica fibers.

Figure 12 shows the IR spectrum of the silica fibers, which has been taken with ATR-FTIR spectroscopy.

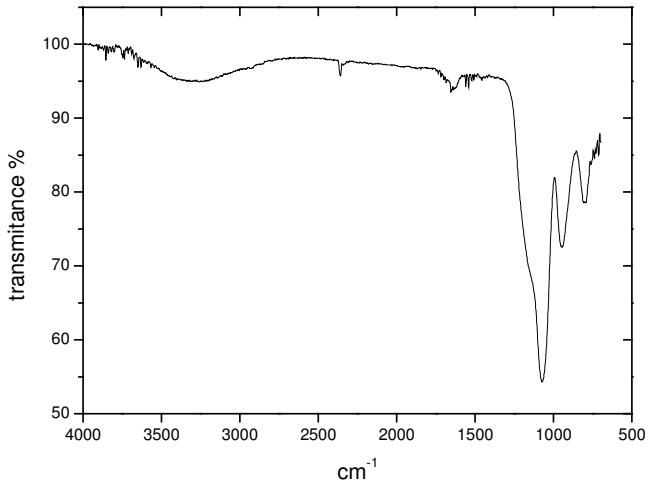

Figure 12. ATR-FTIR spectrum of the silica fibers.

In figure 12, Three characteristic peaks of the silica fibers at 1070 cm^{-1}, 945 cm^{-1}, 780 cm^{-1} can be observed, which are assigned to Si-O.

2.2. Core-shell fibers

2.2.1. PLLA fibers coated with PPX (PLLA-PPX core-shell fibers)

In order to obtain PLLA fibers coated with PPX, the chemical vapor deposition process (CVD) was employed. [2,2]paracyclophane was used as starting material for CVD process. Using 1 g of the starting material, a coated layer with nearly 1 μm thickness can be formed on the surface of the substrate. Figure 13 shows SEM image of PLLA-PPX core-shell fibers.

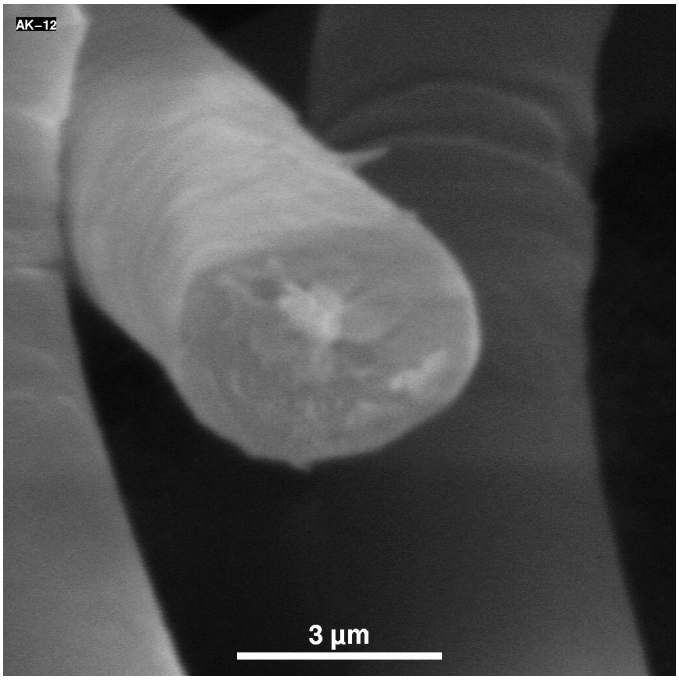

Figure13. SEM image of PLLA-PPX core-shell fibers.

2.2.2. Silica fibers coated with PEMs (silica-PEM core-shell fibers)

The layer by layer self-assembly of polyelectrolytes was carried out using silica fibers as substrate. The self-assembly process can be properly performed on the silica fibers. The first deposited layer was PEI, which was used as precoating layer. PEI has a branched structure and also is highly protonated in water. These two features of PEI make it a polyelectrolyte that could provide a high surface coverage. The new positively charged surface of PEI promotes a good adhesion to place multilayer on the surface. By knowing that the surface is now positively charged, an anionic polyelectrolyte was needed to deposit on the PEI coated surface in order to get a negatively charged layer. The procedure of deposition was followed

as described in the experimental section. Two different PEMs were deposited on the surface of the silica fibers: $(PEI/PSS_{SDS})_{30}$ and $PEI(PAA/PAH)_{29}PAA$ (see figure 14).

PEM of $(PEI/PSS_{SDS})_{30}$ contains 30 bilayers of PEI and PSS_{SDS}. SDS was added into the dipping solution of PSS in order to give the PEM special properties, which will be discussed in the section 4.2.

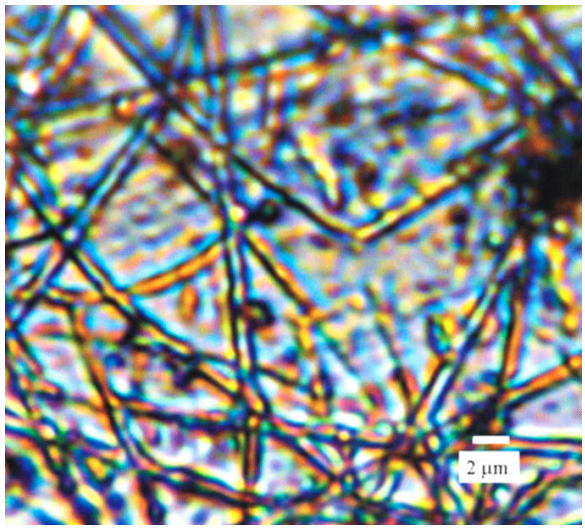

Figure14. Digital microscope image of $(PEI/PSS_{SDS})_{30}$-Coated silica fibers.

Figure15 shows IR spectra of the SiO_2 nanofibers and silica-PEM fibers (PEM: $(PEI/PSS_{SDS})_{30}$).

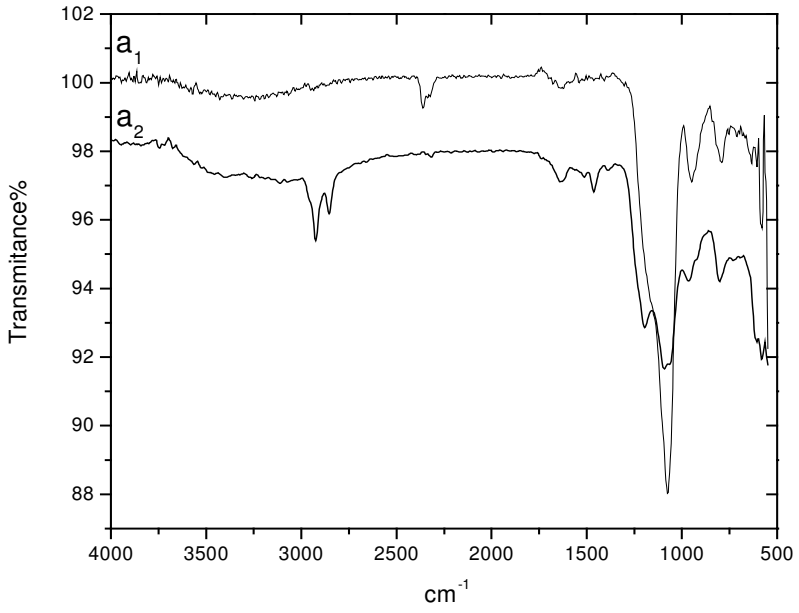

Figur 15. ATR-FTIR spectra of silica fibres and PEM-silica fibres; (a_1) silica fibres, (a_2) PEM-Sio_2 nanofibres coated with $(PEI\text{-}PSS_{SDS})_{30}$.

Further characterization of silica fibers and PEM-silica fibers was carried out by using ATR-FTIR spectroscopy (see figure 15). In the spectrum of the silica fibers, three peaks at 1070 cm^{-1}, 945 cm^{-1}, 780 cm^{-1} can be observed, which are characteristic Si–O peaks. After coating silica fibers with SDS containing PEMs, the IR spectrum (figure 2, spectrum b) exhibits new peaks. The region 3100-2830 cm^{-1} is assigned to C-H stretchs of overlapped aromatic (in PSS) and saturated hydrocarbons (in SDS, PSS and PEI). The region 2550-3660 cm^{-1} exhibits the overlapped band of –OH with the peaks of other functional groups such as C–H stretchs, –NH– and $–NH^{+}_{2}–$ (in PEI). The strong band centred at 1200 cm^{-1}, which is composed of two peaks, is signed to the $–SO_2O–$ (in PSS) and $–OSO_2O–$ (in SDS).

Figure 16 indicates the digital microscope image of the silica-PEM core-shell fibers (PEM: $PEI(PAA/PAH)_{29}PAA$).

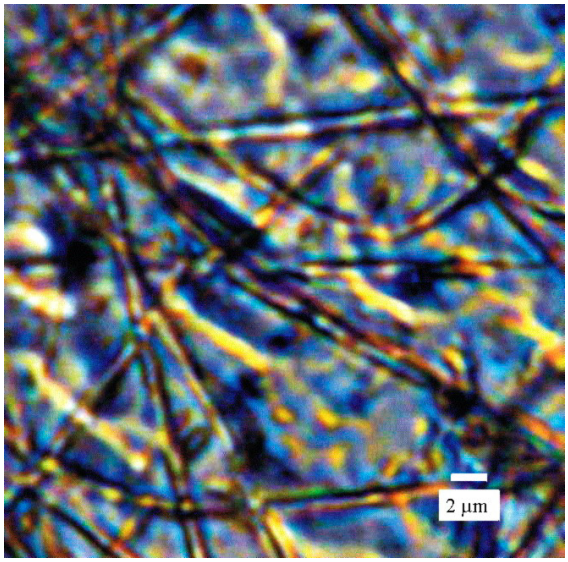

Figure 16. Digital microscope image of silica-PEM core-shell fibers (PEM: $PEI(PAA/PAH)_{29}PAA$).

The ATR-FTIR spectra of the silica fibers and silica-PEM core-shell fibers (PEM: $PEI(PAA/PAH)_{29}PAA$) are shown in figure 17.

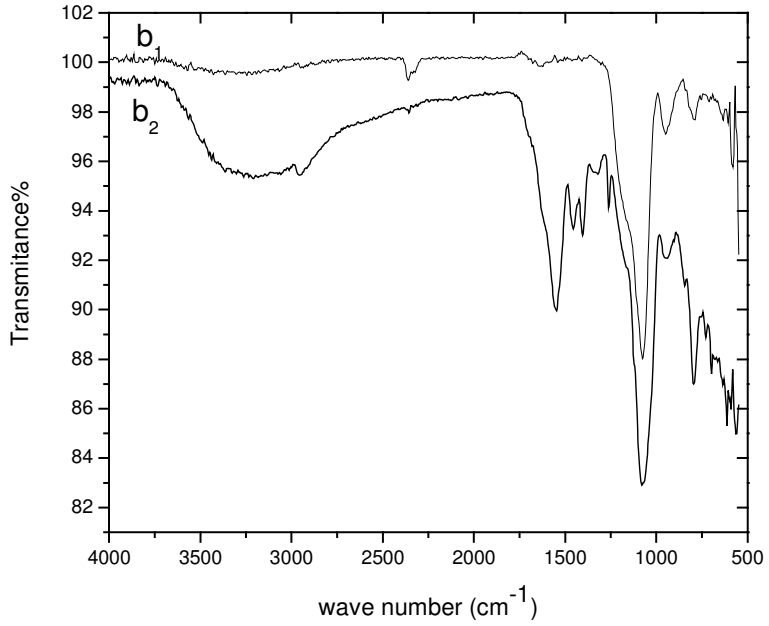

Figur 17. ATR-FTIR spectra of silica fibres and PEM-silica fibres (b_1) silica fibres, (b_2) PEM-silica fibres coated with PEI(PAA-PAH)$_{29}$PAA.

In figure 17, spectrum b_2, the spectrum of silica-PEM core-shell fibers (PEM: PEI(PAA/PAH)$_{29}$PAA), the region 1500-1750 cm^{-1} exhibits the overlapped peaks of carboxylate ions stretchs and –C=O in the carboxyl groups.

2.3. Production of hollow fibers by TUFT process

2.3.1. PPX tubes

PPX tubes were obtained by the selective core removal of the PLLA-PPX core-shell fibers using solvent extraction of the PLLA template fibers. The solvent used was chloroform. The

PLLA fibers are soluble in chloroform while the PPX coated on the PLLA fibers are insoluble in chloroform. Therefore, using chloroform as solvent results the selective removal of the PLLA fibers, leading to obtain PPX tubes. Figure 17 shows the PPX tubes prepared by the removal of the PLLA fibers.

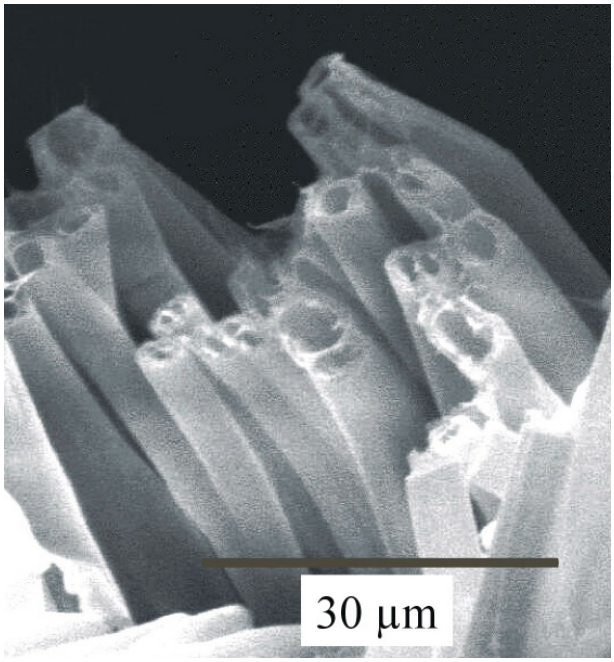

Figure 18. PPX tubes after core removal.

Since the PPX tubes are stable and insoluble in most solvents, the PPX tubes does not show any swelling or changes in their shapes (keeping their tubular shape).

2.3.2. PEM hollow fibers

In this section, a template method (TUFT)[4] is employed to obtain hollow fibers from silica fibers coated with PEMs. The LbL self-assembly technique is used in order to deposit

polyelectrolytes layers on the surface of SiO_2 fiber templates. In a second step following coating, a new generation of tubular fibers made of PEMs were fabricated after selective removal of the fiber templates.

PEMs have become an interesting subject for decades due to their various applications. Our attempt was concerned with the generation of nanotubes made of polyelectrolyte multilayers (PEMs), opening new fields of applications for nano/microtubes. The specific physical and chemical properties of PEMs make this class of materials highly applicable in different fields of science and industry such as drug delivery, sensors, electrical and optical devices.[75-79] Among properties of PEMs, the formation of PEMs with high conductivity and pH sensitivity can be mentioned.[80-82] Park et al.[80] were reported formation of pH-Sensitive bipolar ion-permselective films of polyelectrolyte multilayers. The properties of mixed surfactant-polyelectrolyte structures in solution have already been studied extensively.[84-86] The formation of PEMs containing surfactant was reported by Johal and coworkers.[87] The self-assembly and spin coating technique was employed in order to construct multilayer films using the polycation PEI and the mixture of SDS with the polyanion poly[1-[4-(3-carboxy-4-hydroxyphenyazo) bezenesulfonamido] –1,2-ethanediyl, sodium salt. The results have indicated that both SDS and polyanion can be coadsorbed onto the PEI layers. Recently, modifying surface properties of carbon nanotubes has been became an interesting subject to improve their potential applications. The layer–by-layer (LbL) self-assembly based technique has been employed to deposit PEMs on the surface of nano particles[87,88] and carbon nanotubes[89-95] and electrospun fibers[96] in order to alter their surface properties.

2.3.2.1. Hollow fibers made of PEMs of $(PEI/PSS_{SDS})_{30}$

Hollow fibers made of PEMs (PEMHFs) of $(PEI/PSS_{SDS})_{30}$ (PSS_{SDS}: these layers were coadsorbed from the solution containing PSS and SDS) were prepared. The hollow micro-sized pH sensitive tubular fibers made of PEMs were successfully fabricated, showing interesting structural properties caused due to existence of surfactant within the PEM layers. These tubular fibers have very flexible walls and are stable at very low pH of the environment.

PEMHFs were produced after dissolving the silica fiber templates in HF solution. ATR-FTIR spectra and digital microscope images of PEMHFs were analysed to confirm the removal of the fiber templates.

As can be seen from figure 19, the diameter of PEMHFs made of $(PEI\text{-}PSS_{SDS})_{30}$ multilayers (SDS-PEMHFs) is about 10 times larger than the diameter of PEM-silica fibers before HF treatment. This is due to a pronounced swelling of the structures upon HF treatment.[97-99]

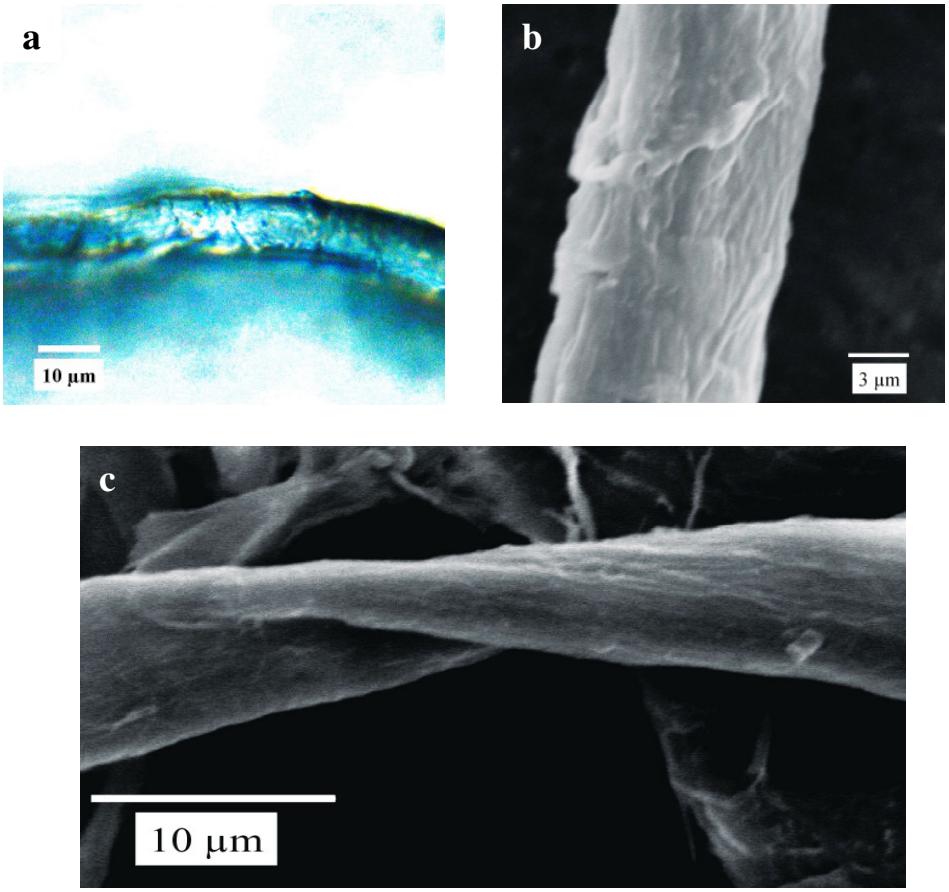

Figure 19. Digital miroscope and SEM image of PEMHFs coated with $(PEI\text{-}PSS_{SDS})_{30}$ after HF treatment; (a) Digital miroscope image of PEMHFs; (b) and (c) SEM image of PEMHFs.

Figure 20 shows a digital microscope image that indicates that light can pass through the tubes while microscope was focused on the surface of aluminium foil, which was used as background. It can be obviously seen that light is diffracted while passing through the sample.

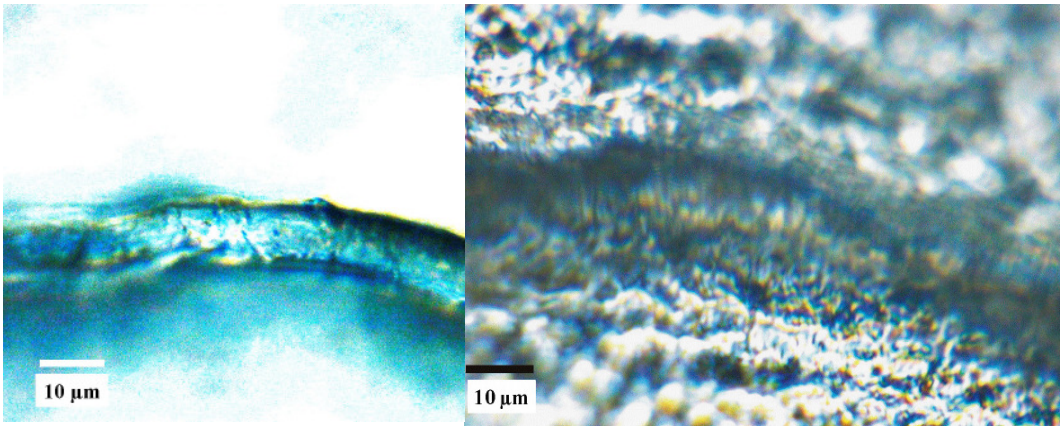

Figure 20. Shown digital microscope image of the HFPEM; left, PEMHF; right, in order to see how the tubes are transparent microscope was focused on the surface of aluminium foil, which was used for holding the sample.

Figure 21 shows the ATR-FTIR spectrum of PEMHFs after removing silica fibres in a comparison with IR spectrum of silica fibres and PEM-silica fibers ($(PEI\text{-}PSS_{SDS})_{30}$)to obtain information about the core removal of the core-sell fibers. The characteristic band of Si-O-Si can be seen in the spectra of silica fibers and PEM-silica fibres as a strong band at 1070 cm-1 while this band is disappeared in the case of PEMHFs, confirming the successful removal of silica fibre templates by HF treatment PEM-SiO_2 nanofibers.

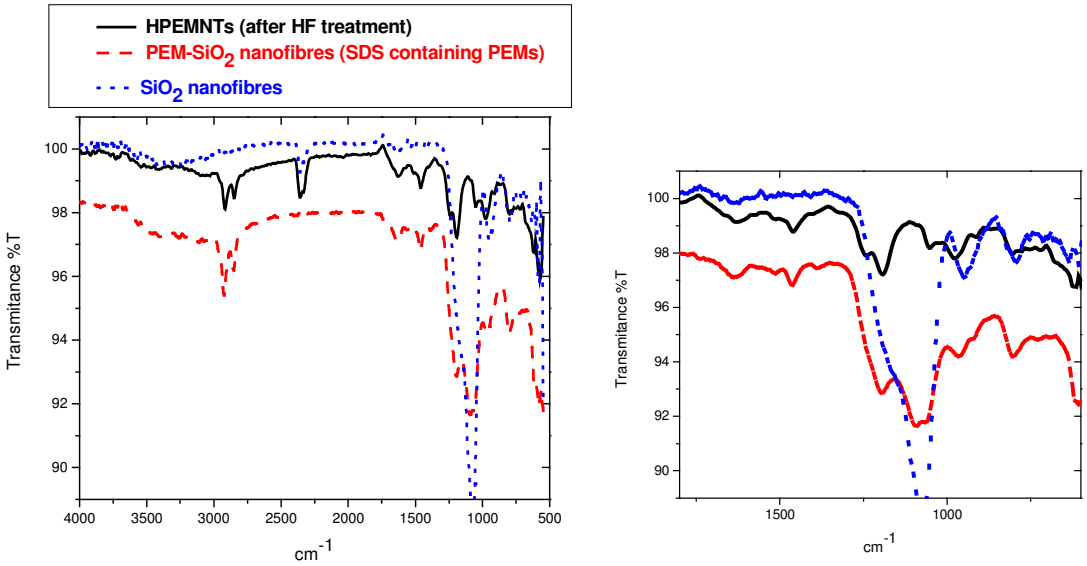

Figure 21. ATR-FTIR spectra of silica nanofibers, PEM-SiO2 nano fibers ($(PEI\text{-}PSS_{SDS})_{30}$) and PEMHFs.

The successful core removal has been demonstrated for PEMs of $(PEI\text{-}PSS_{SDS})_{30}$ coated on the silica nanofibers. SDS-PEMHFs can highly extend their structure. The swelling of the fibers ocures in a solution of hydrofluoric acid with very low pH (0.5 M HF). PEMHFs are able to expand themselves more than 10 times of their original size. The key point for this high flexibility of SDS containing PEMs is because of special structural properties caused by SDS used in the structure of PEMs. It was reported that surfactant and PEI can form some complexes with lamellar mesophase structures, which have low surface energies.[100,101] The hydrocarbon chains of SDS are short comparing to polyelectrolyte chains, leading to less entanglement of SDS with the polyelectrlytes within the complex of PEMs, so that using SDS as anionic charge carrier in a mixture with PSS causes the formation of more flexible layers within PEMs. In other words, SDS within PEM layers results a kind of temporary bridge between polyelectrolytes in the PEMs. Considering the point that the concentration of SDS in the dipping solution is far above the critical micelle concentration (CMC), a possible structural arrangement that can be suggested for SDS within PSS layers is the lamellar

structure. The suggestion of the lamellar model for SDS containing PEMs can help to explain the high flexibility of the SDS-PEMHFs of this kind. This structure property gives the PEMHFs a high flexibility and consequently PEMHFs are able to tolerate a large structure expansion.

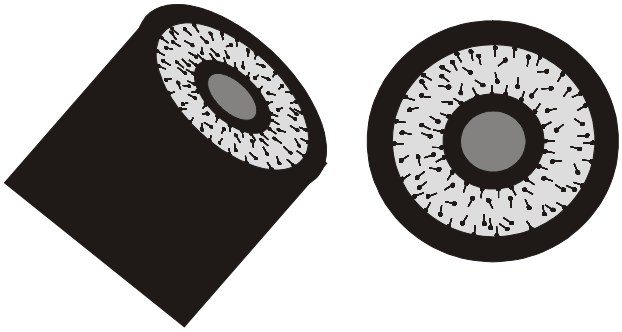

Before HF treatment

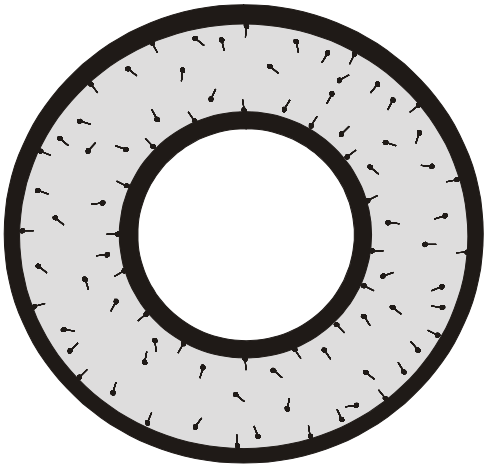

After HF treatment

Figure 22. A model structure of PEMHFs (three layers shown): formation of lamellar structures within PEMs; light gray: PSS layer; black: PEI layer; dark gray: silica fiber template.

The other factor making PEMHFs stable in solutions with low pH is the features of PSS and PEI used in PEMs. PSS is the strong polyelectrolyte so that at low pH media, the changes in the structure of PSS layers within PEMs can be very small. The extreme increase of diameter of the PEMHFs (more than 10 times increase) after HF treatment comparing to the PEM-silica core-shell fibers is due to the highly protonated PEI layers within PEMHFs, which cause more electrostatic repulsion forces along the PEI chains, leading to more expanded chains. The exsistance of SDS within the PEM layers make SDS-PEMHFs highly flexible, so that they can tolerate the large expansion of their structure.

2.3.2.2. Deformation of PEMs of PEI(PAA/PAH)$_{29}$PAA coated on the surface of silica fibers

In the case of PEM-silica fibres (PEM: PEI(PAA-PAH)$_{29}$PAA, the polyelectrolyte layers are dissolved after introducing the fibers to the HF solution. The dissolution of the coated PEMs of these core-shell fibers in the HF solution indicates low structure flexibility of this PEMs in the acidic solutions. The instability of PEMs of PEI(PAA-PAH)$_{29}$PAA in low pH environment can be explained as follows: Shiratori and Rubner[102] investigated the effect of pH of the dipping solutions (PAA and PAH) on PEMs. It was shown that by decreasing pH (pH < 4.5) of the dipping solutions, the thickness of PAA layers were decreased, whereas the thickness of PAH layers were increased. The same pH-dependant behaviour for the silica fibers coated with PEI(PAA-PAH)$_{29}$PAA might occur by keeping them in the solution of HF, which may provide entropic forces[103,104] for the deformation of PEMs. Scince the PAA charges are mostly neutralized by HF treatment (at very low pH), a lack of electrostatic forces can cause the multilayers become unstable[105], therefore the entropic forces can effectively act to decompose the multilayers.

2.4. Surface modification of PPX tubes with PEMs by using layer by layer self assembly technique

The surface modification of nano/microtubes can increase their potential applications due to the structural changes at the surface. For example, recently, the approach of altering the surface properties of carbon nanotubes can enable us to use them in different types of nanodevices. In order to obtain the tubes with modified surfaces, the self-assembly of polyelectrolytes can be carried out. The formation of polyelectrolyte multilayers (PEMs) and their properties were studied.[78,79] To coat carbon nanotubes by polyelectrolytes, the layer-by-layer assembly technique was used by Artyukhin et al..[106] Sequential adsorption of carbon nanotubes and polyelectrolytes onto substrates was carried out in order to obtain polymer/carbon nanotubes with modified surface properties.[107,108] More studies on the surface modification have been reported.[109-112] Fabrication of a new class of nano/microtubes, poly(p-xylylene) nano/microtubes, by using degradable polymer template fibers (TUFT process) has been reported.[113] Poly(L-lactide) electrospun fibers was used as template and were coated by PPX using chemical deposition process (CVD).[114-116] After selective removal of template fibers the PPX tubes were obtained.

In this presentation, the polyelectrolyte multilayers (PEMs) formation on the surface of the PPX-tubes were reported by using layer-by-layer self-assembly technique. Altering the surface properties of PPX-tubes make them suitable for varieties of applications. For instance, PPX-tubes can be subject to surface modification, making them potentially applicable in electronic devices and sensors by coating respectively conductive and pH-sensitive polymers onto their surfaces.

2.4.1. H_2SO_4-treated PPX tubes

In order to obtain the surface of PPX tubes modified somehow that be able to use them as substrate for deposition of polyelectrolytes, the PLLA-PPX core-shell fibers were treated with sulfuric acid as described in experimental section. After H_2SO_4 treatment, the H_2SO_4-treated PPX tubes were obtained. To investigate how the surface was effected by sulfuric acid treatment, a simple experiment was carried out. A PPX film, which was prepared by CVD process was treated with concentrated sulfuric acid (as was mentioned in experimental section) and contact angle measurements was performed at the surface of PPX films before

and after acid treatment. The water contact angle of H_2SO_4-treated PPX film was conducted resulting a value of Θ ~ 12°, whereas the value of Θ = 95° was obtained for the film before sulfuric acid treatment.

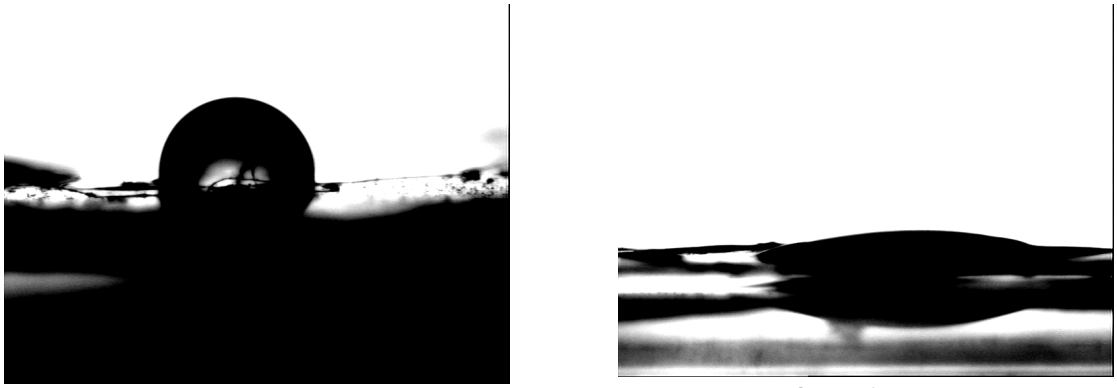

Figure 23. The ware droplets on PPX coated films: left, before H_2SO_4 treatment; right, H_2SO_4-treated film.

ATR-FTIR was carried out from the H_2SO_4-treated PPX film. As can be seen from figure 24, the IR spectra of the PPX films before and after H_2SO_4 treatment. The band of the $–SO_2O–$ centred at 1200 cm^{-1}, which is overapped with other peaks, is another proof to emphsis that the sulfunation reaction is performed.

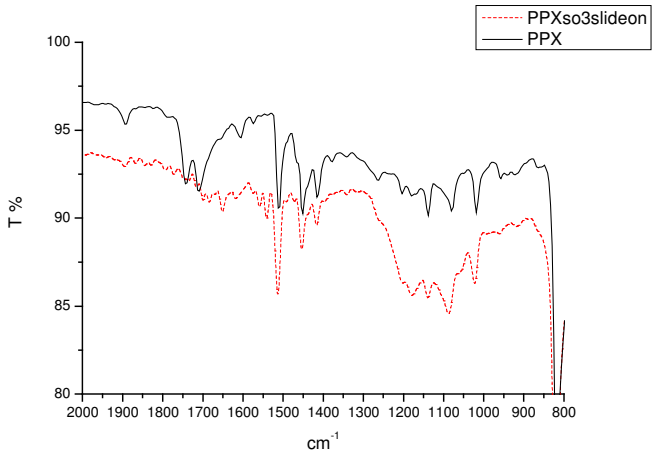

Figure 24. Shown ATR-FTIR spectra of PPX films: solid line, IR spectrum of PPX film; dashed line, IR spectrum of H_2SO_4-treated PPX film.

2.4.2. PEM formation on the H_2SO_4-treated PPX tubes

The oppositely charged polyelectrolytes were deposited on the surface of the tubes by using LbL self-assembly technique. the PEMs deposited on the surface of the tubes were (PEI-$PSS_{SDS})_{30}$ and PEI(PAA-PAH)$_{29}$PAA.

SEM spectroscopy and ATR-FTIR was used to prove the formation of PEMs on the surface of the tubes. Figure 25 shows the SEM images of H_2SO_4-treated PPX tubes before and after PEMs deposition. The surface of the tubes after deposition of PEMs of either (PEI-$PSS_{SDS})_{30}$ or PEI(PAA-PAH)$_{29}$PAA display significant changes, insisting the successful formation of PEMs on the surfaces.

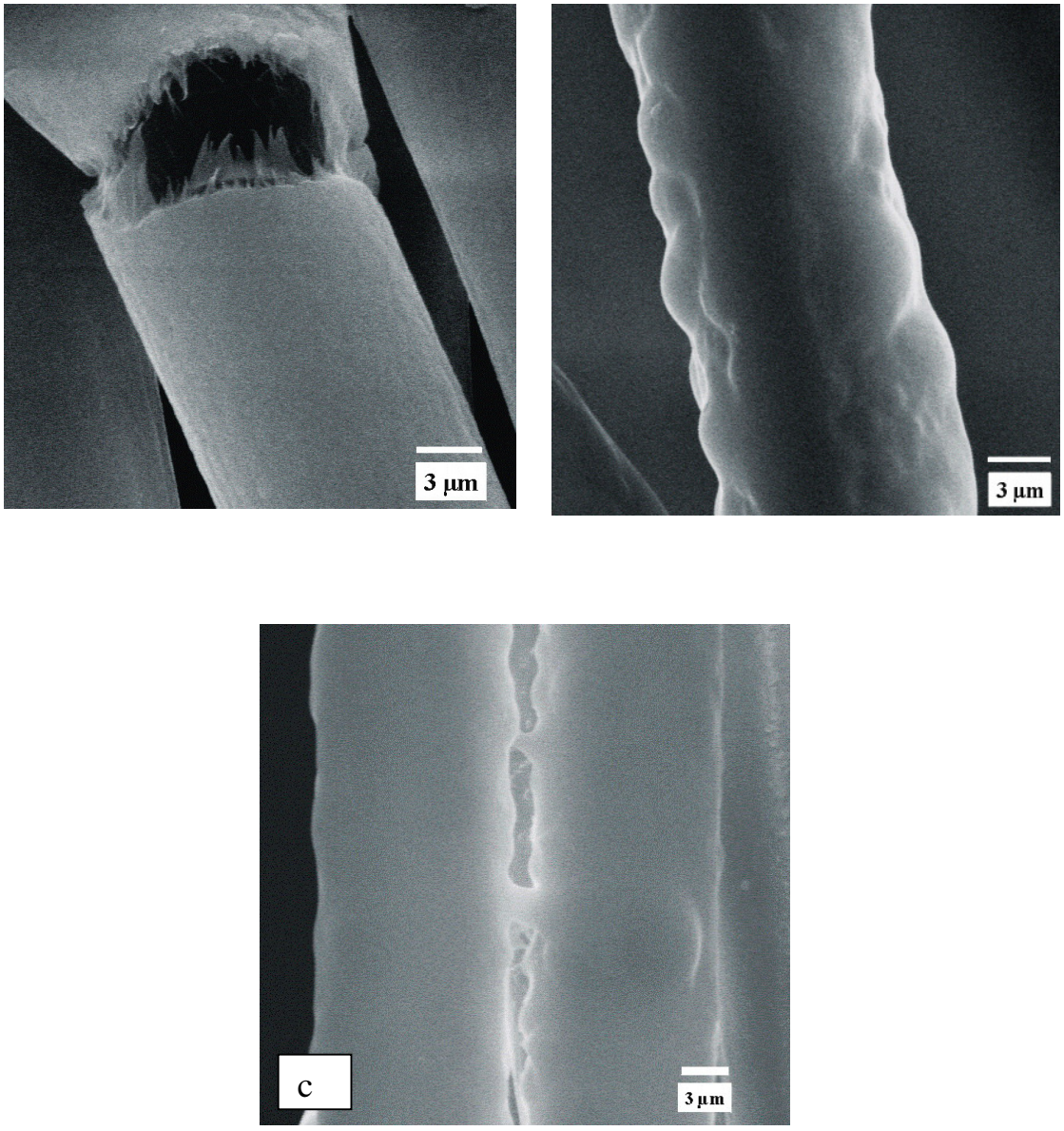

Figure 25. Shown PPX tubes after H_2SO_4 treatment and PEMs coated tubes: (a) H_2SO_4-treated PPX tubes: after H_2SO_4 treatment the fiber templates of PLLA are removed automatically ; (b) PEM-coated-PPX tubes (PEMs: $(PEI\text{-}PSS_{SDS})_{30}$); (c) PEM-coated-PPX tubes (PEMs: $PEI(PAA\text{-}PAH)_{29}PAA$.

Furthermore, to get more proofs on the modified surfaces, the ATR-FTIR spectroscopy was performed. As can be seen from figure 2, the IR spectrum of the tubes coated with PEMs of $(PEI\text{-}PSS_{SDS})_{30}$ shows the peaks signed for PEMs of $(PEI\text{-}PSS_{SDS})_{30}$ on the surface of the H_2SO_4 treated-PPX tubes. In the case of the tubes coated with multilayers of PEI(PAA-PAH)$_{29}$PAA, the peaks responsible for PEMs PEI(PAA-PAH)$_{29}$PAA can be observed.[117] A comparison of ATR-FTIR spectra of H_2SO_4-treated PPX tubes before and after coating with PEMs: $(PEI/PSS_{SDS})_{30}$, PEI(PAA/PAH)$_{29}$PAA has been shown in figures 26 and 27.

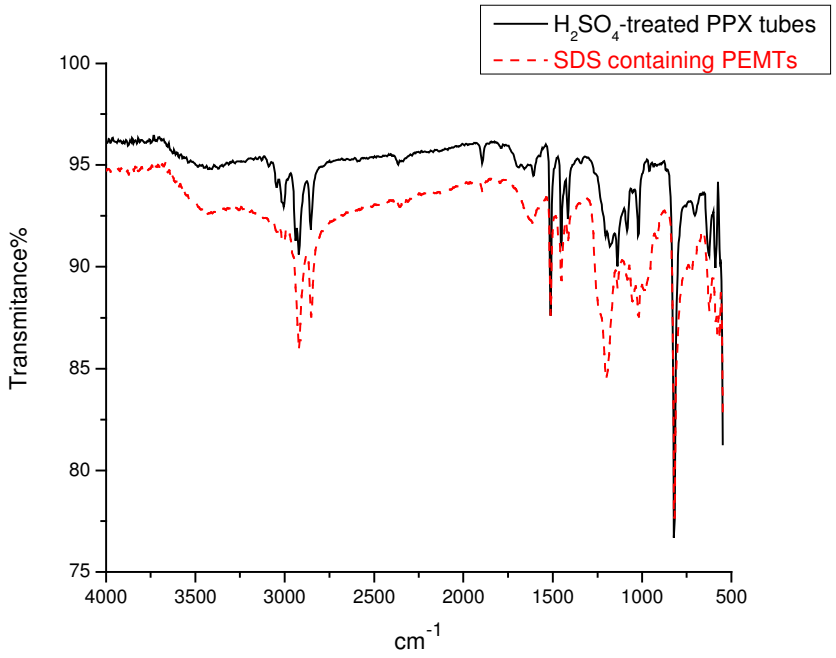

Figure 26. Solid line, ATR-FTIR spectrum of the H_2SO_4 treated-PPX tubes; dashed line, ATR-FTIR spectrum of the tubes coated with multilayers of $(PEI\text{-}PSS_{SDS})_{30}$.

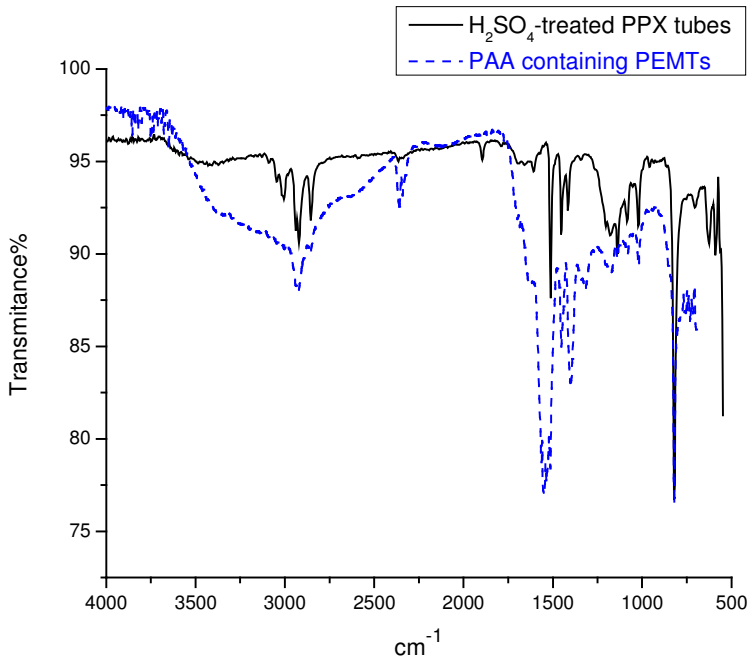

Figure 27. Solid line, ATR-FTIR spectrum of the H_2SO_4 treated-PPX tubes; dashed line, ATR-FTIR spectrum of the tubes coated with multilayers of PEI(PAA/PAH)$_{29}$PAA.

2.4.3. HCl treatment

In order to study the effect of a low pH of environment on PEM-coated-tubes, they were kept in the solution of 0.5 M HCl for 40 min and then dried in air. SEM and ATR-FTIR spectroscopy from the tubes after HCl treatment were performed.

2.4.3.1. HCl treatment of the PPX tubes coated with PEMs of (PEI/PSS$_{SDS}$)$_{30}$

To see how tubes coated with PEMs are effected after introducing them into a solution of 0.5 M HCl, SEM images and ATR-FTIR spectra of HCl treated tubes were provided. As can be seen from figure 28, the surface of the tubes coated with PEMs of (PEI-PSS$_{SDS}$)$_{30}$ after HCl

treatment shows changes comparing to the tubes before acid treatment. Nevertheless, the structural changes of the surface (PEMs) here is not pronounced. The reason for this observation that the PEMs do not show a high structural changes can be due to the rigidity of the PPX tubes uses as substrate for the deposition of polyelectrolyte layers.

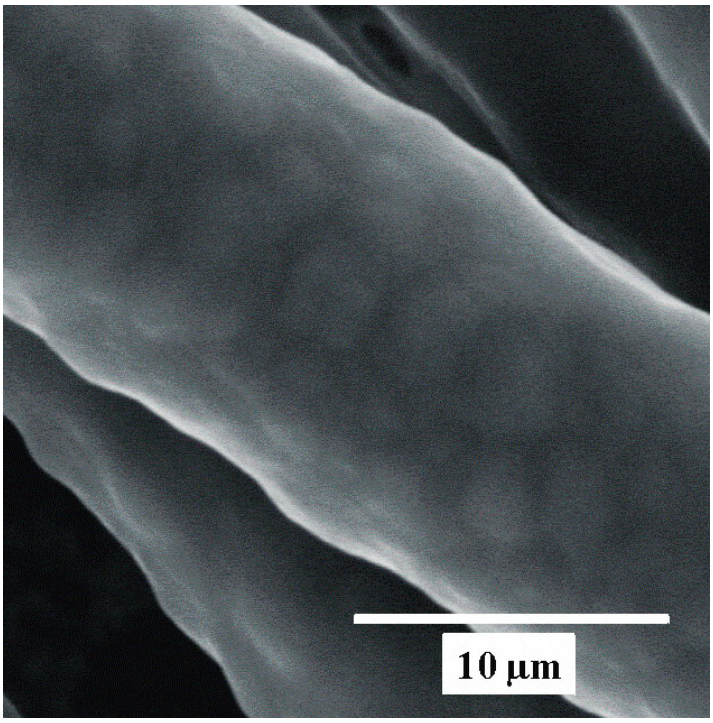

Figure 28. SEM images of tubes coated with PEMTs of (PEI-PSS_{SDS})$_{30}$ after HCl treatment.

The IR spectra of the PEMTs after and before HCl treatment indicate that the PEM coating at the surface of the tubes did not removed after HCl treatment, indicating that the (PEI-PSS_{SDS})$_{30}$ multilayers are stable against acidic environment (see figure 29).

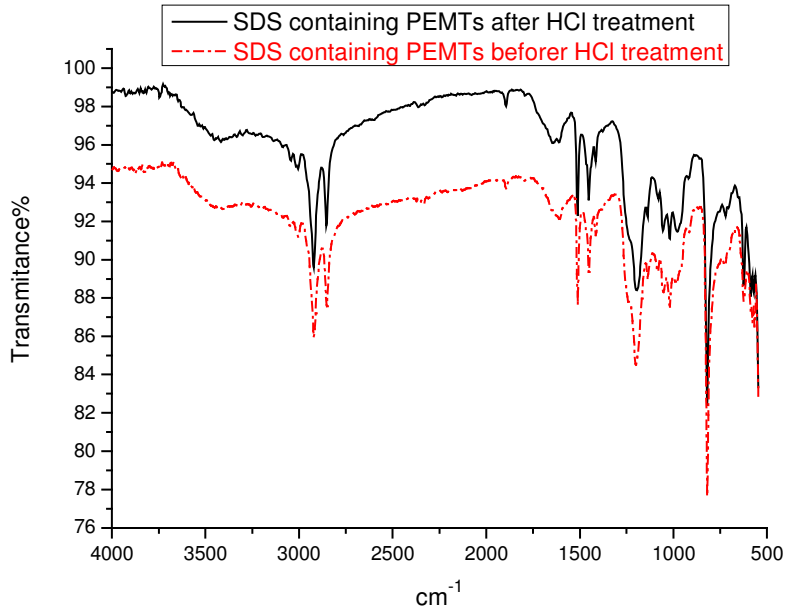

Figure 29. ATR-FTIR spectra of PPX tubes coated with PEMs of (PEI/PSS_{SDS})$_{30}$ before and after treatment with 0.5 M HCl.

2.4.3.2. HCl treatment of the PPX tubes coated with PEMs of PEI(PAA/PAH)$_{29}$PAA

If the tubes coated with PEMs of PEI(PAA/PAH)$_{29}$PAA are treated with 0.5 HCl solution, the surface of the tubes looks similar to the surface before coating (see figures 25 and 30), which could mean that the PEMs were decomposed and washed out in the solution of 0.5 M HCl.[117]

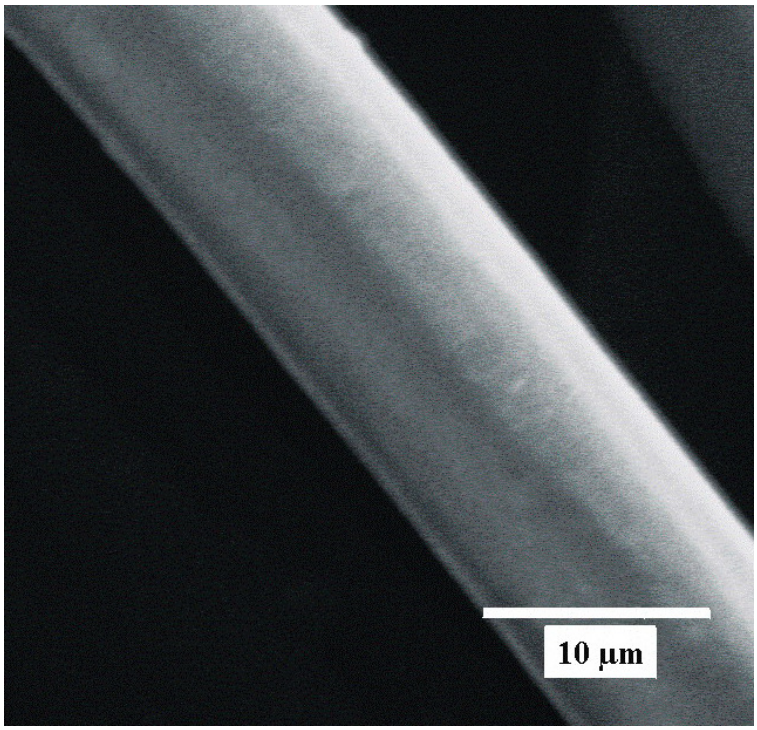

Figure 30. SEM images of PPX tubes coated with PEMTs of PEI(PAA/PAH)$_{29}$PAA after HCl treatment.

In addition, ATR-FTIR spectrum of the HCl-treated-tubes coated with PEMs of PEI(PAA/PAH)$_{29}$PAA indicates that the PEMs were removed from the surface of the PPX tubes after HCl treatment while for the case of the tubes coated with PEMs of (PEI/PSS$_{SDS}$)$_{30}$, the IR spectra before and after HCl treatment almost similar, insisting that PEMs of (PEI/PSS$_{SDS}$)$_{30}$ deposited on the surface of the PPX tubes are stable at low pH (see figure 4). The reason for the stability of PEI/PSS$_{(SDS)}$ multilayers has been described in our publication.[125]

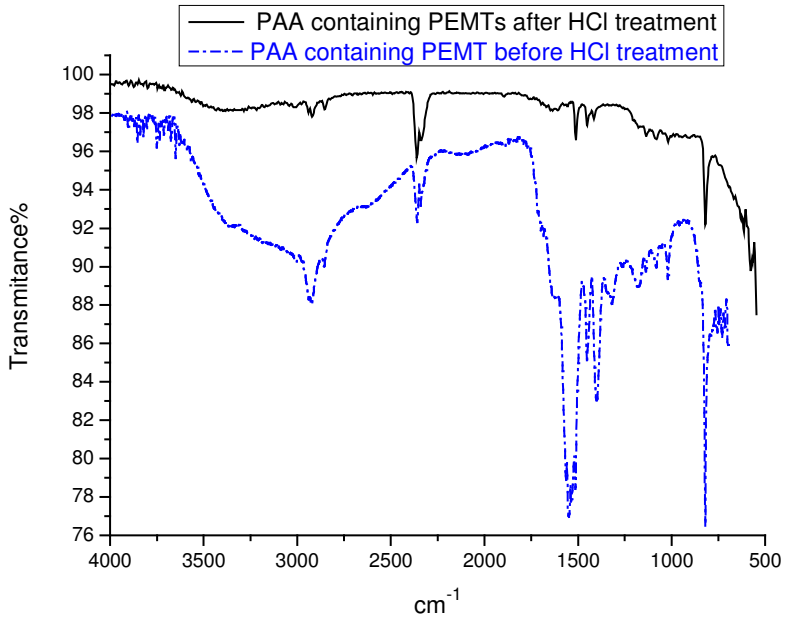

Figure 31. ATR-FTIR spectra of PPX tubes coated with PEMs of PEI(PAA/PAH)$_{29}$PAA before and after treatment with 0.5 M HCl.

2.5. Sealing process of PPX tubes

In this section, methods for sealing the tubes at the ends (top and bottom of the tubes) are described. The idea is to seal the tubes at the ends with materials sensitive to different environments. If the sealing materials are pH sensitive, by changing pH of media it is possible to signal the tubes to make them open or closed at the ends. Therefore, this tubes are suitable for releasing materials such as drugs into the specific environments. Here in this work, the PPX tubes were sealed with three different materials. The sealing polymers are pH sensitive or thermosensitive.

2.5.1. PPX tubes sealed with pH sensitive polymer by using ATRP

The preparation of the PPX tubes sealed at the ends (top and bottom) with polyacrylic acid (PAA), a pH sensitive polymer, is described. The pH sensitivity is because PAA is a weak polyelectrolyte and the charge density of the PAA chains can be varied by changing pH. In the case of low pH, the carboxyl groups of the chains are protonated. This cause the less charge density of the polymer chains, leading to less electrostatic repulsion forces within the chains. This is why PAA chains are more coiled at low pH. On the other hand, if pH is high, the highly charged chains are more extended.

PAA at the ends of the tubes can act as gates,which can be opened and closed by variation of pH. The sealing procedure was carried out, first by bromination of the tubes at the ends as described in the experimental section. The brominated PPX (BrPPX) was used as ATRP initiator. There are some other reports on suface-initiated-ATRP, which was perormed successfully. Usually, PAA can not be used in ATRP because of its poisoning effect on the ATRP catalyst. A work was performed in order to make ATRP of PAA by using a macroinitiator at a basic pH (pH 8-9).[71] The work introduced in this section is a successful ATRP of the PAA monomers at the ends of tubes. In order to prevent the poisoning effect, PAA was used in its salt form of N,N-diisopropyl ammonium acrylate (NNDIAAc). To performe the polymerization at the ends of the tubes, the tubes were placed into MMA monomers and then by polymerization of the MMA monomers, a supporting layer of PMMA obtained around the tubes. After, the solid support of PMMA containing PPX tubes inside was cut into slices to get 2 mm cut-supported-tubes. The bromination reaction was carried out at this ends and then the cut-supported-tubes brominated at the ends were used as initiator for ATRP and target polymers were obtained at the ends of the tubes, see figures 32 and 33.

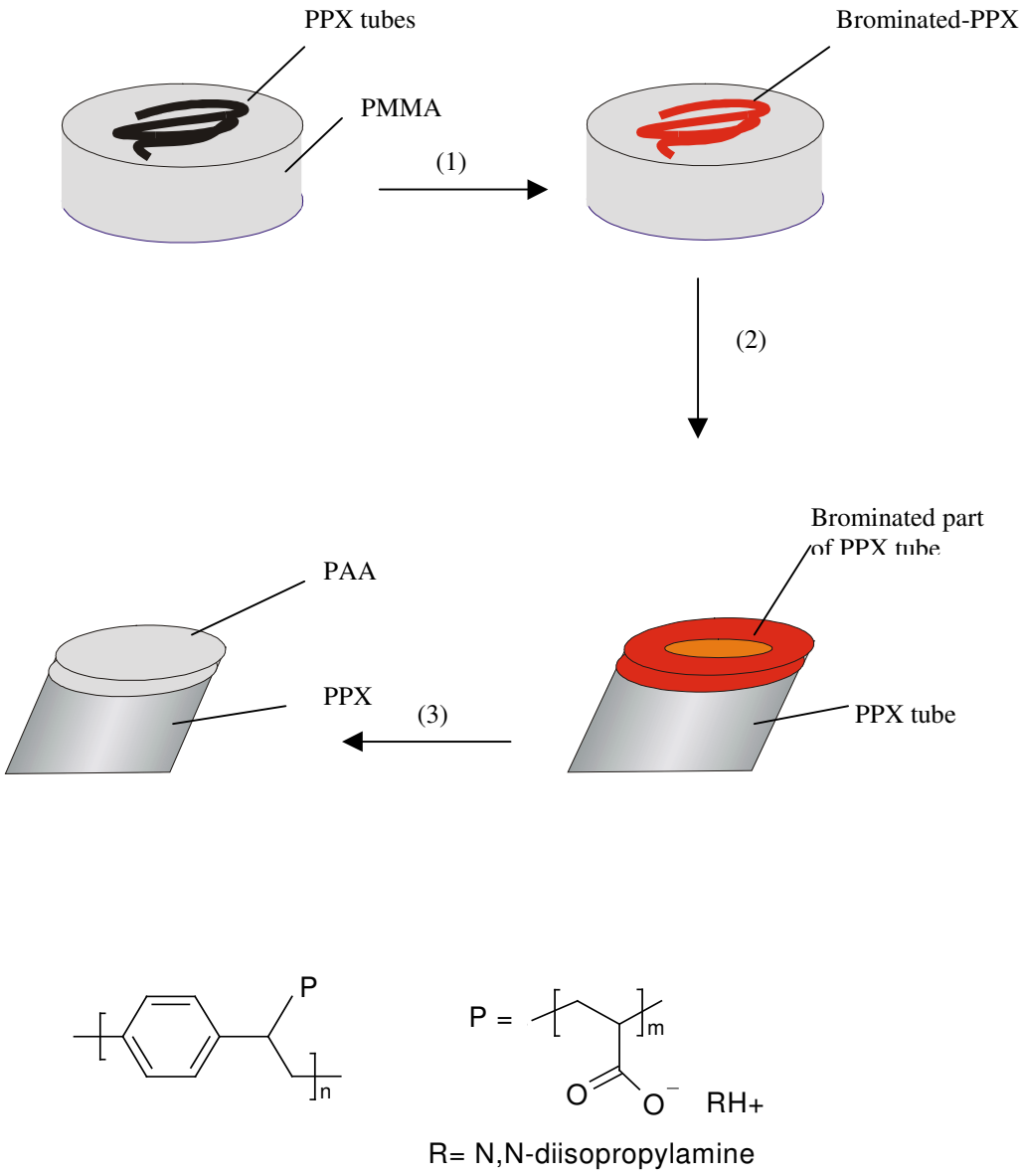

Figure 32. Schematic illustration of the ATRP at the end of the PPX tubes.

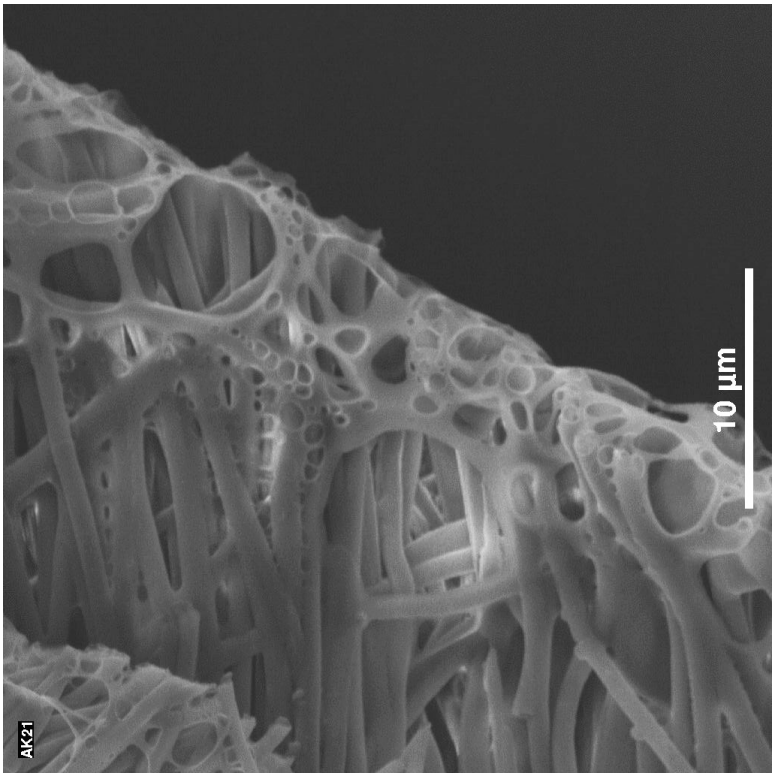

Figure 33. SEM image of the PPX tubes with polyacrylate N,N-diisopropyl ammonium at the ends.

NaOH treatment

The above tubes after sealing with polyacrylate N,N-diisopropyl ammonium were treated with the solution of 0.1 M NaOH. Since N,N-diisopropyl ammonium can be deprotonated in a basic environment, It was expected that Na^+ is replaced instead as counter ion for carboxyl groups of the PAA. Furthermore, PAA is a polyelectrolyte and the PAA chains are in a extended form so that it is expected the sealed tubes to be opened after NaOH treatment. The SEM image below is showing the result after the tubes were treated by NaOH solution.

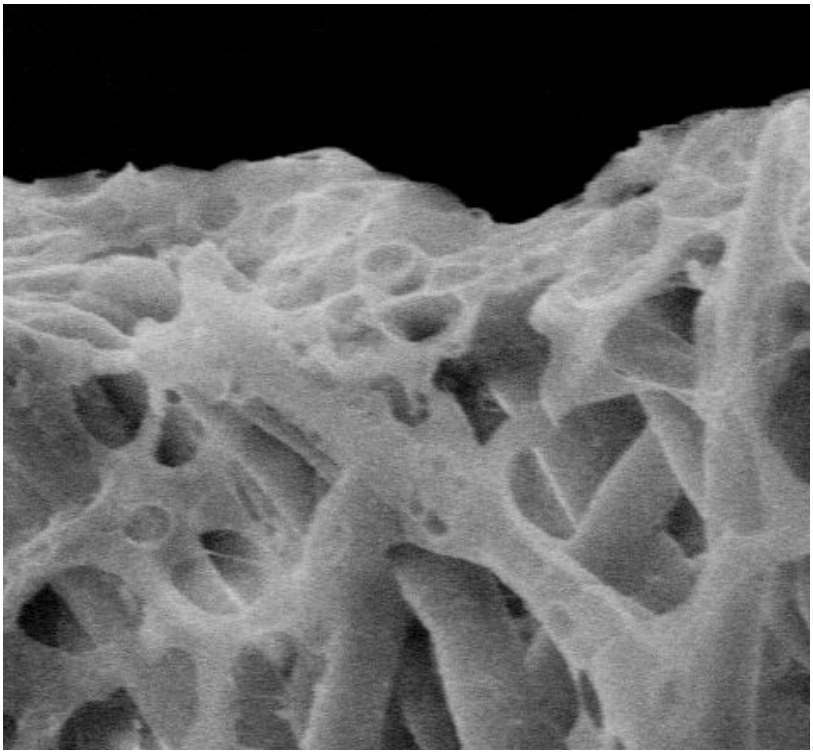

Figure 34. SEM image of the sealed-PPX tubes after NaOH treatment.

Figure 35 shows EDX spectra of the sealed tubes, which were performed from the top (before NaOH treatment) and from the middle (after NaOH treatment).

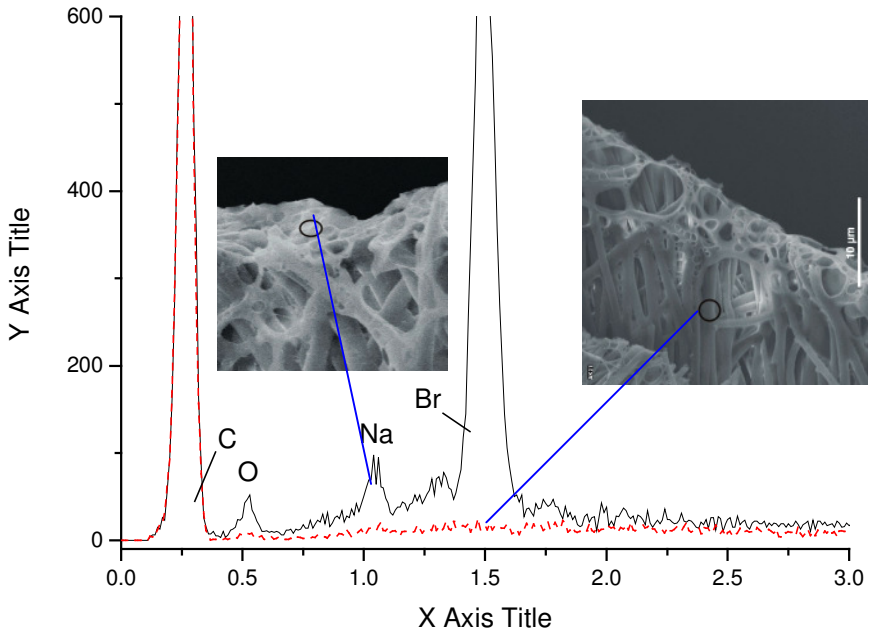

Figure 35. Shown EDX spectra of polymer-sealed-PPX tubes : solid line, EDX from the end of the tubes after NaOH treatment; dashed line, EDX from the end of the tubes before NaOH treatment.

2.5.2. PPX tubes sealed with thermo-sensitive polymer by using ATRP

The same procedure as section 2.5.1 was also performed in order to seal PPX tubes with PNIPAM by using ATRP. PNIPAM has special thermal properties and is sorted as a thermo-sensitive polymer. Figure 36 shows SEM image of the tubes sealed with PNIPAM by ATRP.

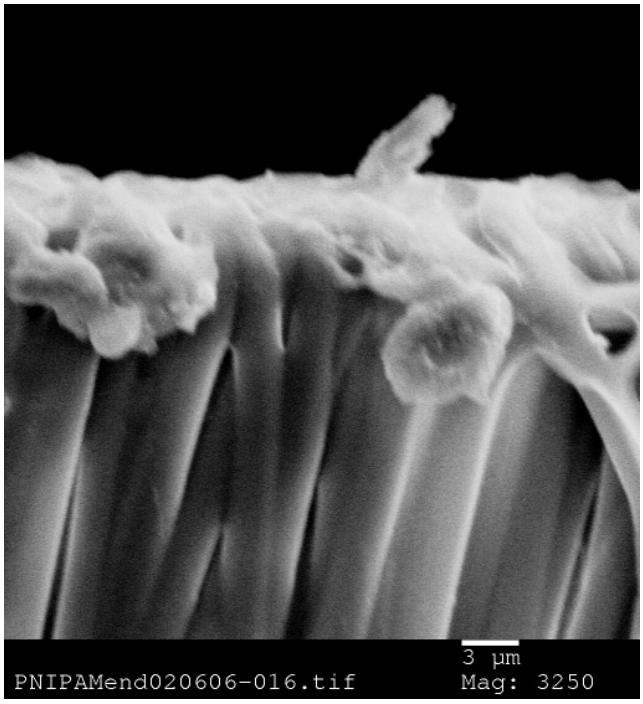

Figure 36. SEM image of the tubes sealed with PNIPAM.

The EDX spectra shown in figure37 were performed from the top and the middle of the tubes, representing the peaks of oxygen and bromine while EDX was performed from the end of the tubes. When EDX was performed from an area on the middle of the tubes, the peaks of O and Br do not exist.

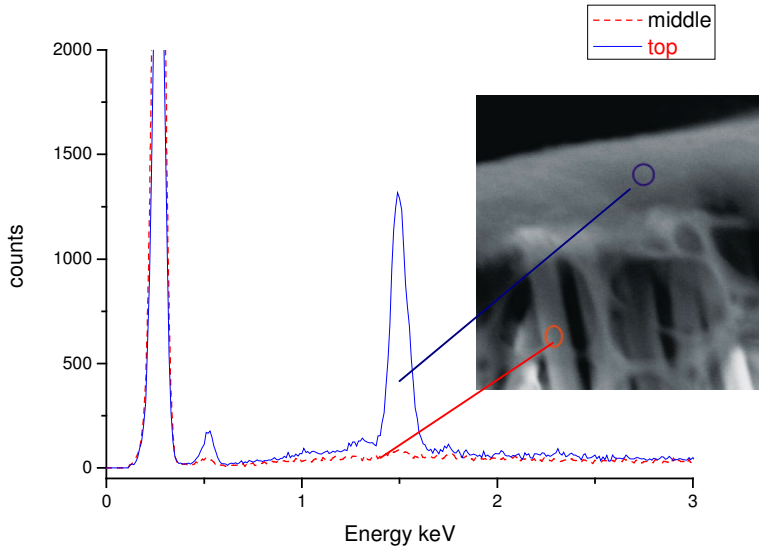

Figure 37. Shown EDX spectra of polymer-sealed-PPX tubes (polymer:PNIPAM): solid line, EDX from the end of the tubes; dashed line, EDX from the end of the tubes before NaOH treatment.

These sealed tubes have potential application in sensors because of the thermosensitivity of the PNIPAM. It was previously investigated that PNIPAM is a thermo-sensitive polymer, showing temperature dependent behavior. In the range of 30-35˚C, it shows a transition (LCST) and forms random coils in water so that the aqueous solution of PNIPAM become turbid. The behavior of the water (PNIPAM gels in water) has been investigated by NMR spectroscopy, indicating the temperature dependent water hydrogen bonding.[127-130] The phase transition of PNIPAM can be also observed within adsoption layers of PNIPAM.[131]

2.5.3. PPX tubes sealed with PEMs by self-assembly

Again, the self-assembly based technique was employed, this time in order to seal PPX tubes. The procedure of the PEM coating was like before. PEMs of PEI(PAA/PAH)$_{29}$PAA were deposited at the top of the tubes. At first, the PPX tubes were supported by PMMA. After

cutting the supporting PMMA containing tubes inside in 2 mm slices, in order to obtain good PEM coating on the tubes they were treated with sulfuric acid. Before coating, the supporting PMMA was removed by solvent, which was chloroform, (see experimental section).

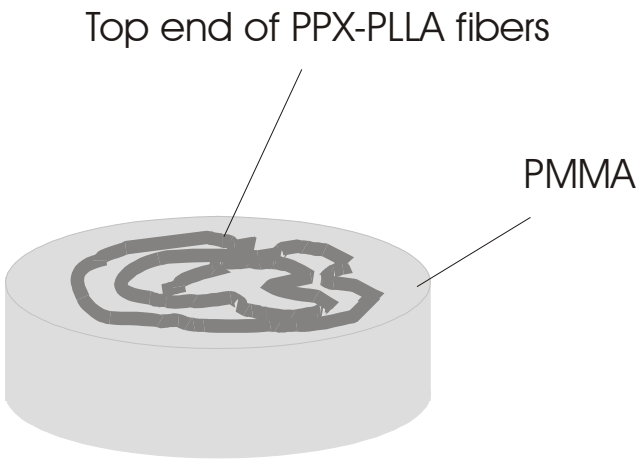

Figure 38. Schematic representation of a sliced-PMMA supported-PPX tubes.

The polyelectrolytes after coating were swelled, so that PEMs are observed not only at the ends of the tubes, but to a larger area of the surface of the tubes. Figure 39 shows the tubes sealed with PEMs of $PEI(PAA/PAH)_{29}PAA$.

The interesting behavior of the mutilayers made of PAA-PAH bi-layers is that they can be removed at low pH (pH < 1) or at high pH (e.g. pH 13). Therefore, by variation of the pH the tubes sealed with this multilayers can be switched to be opened (see figure 39). Moreover, this method make us to be able to seal the tubes with PEMs with varieties of properties. For example, by using particular polylelectrolytes within the structure of PEMs, the PEMs sensitive to pH or temperature can be obtained. Moreover, the self-assembly technique is very easy to be applied in the lab.

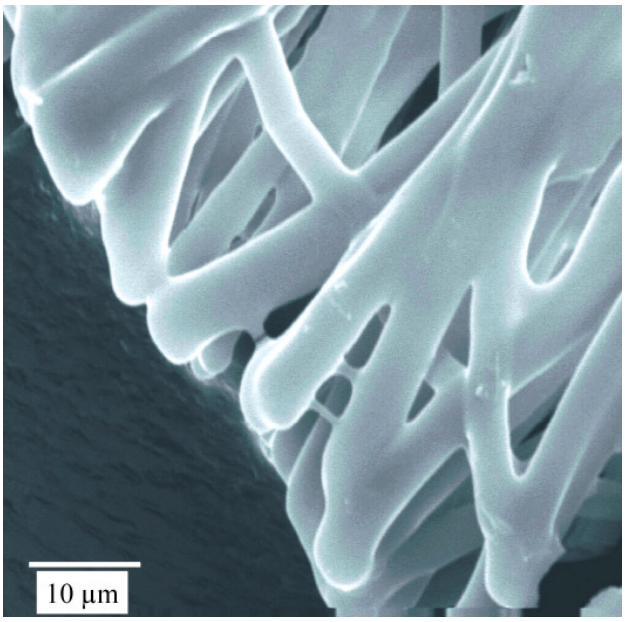

Figure 39. SEM image of the PPX tubes sealed with PEMs of PEI(PAA/PAH)$_{29}$PAA.

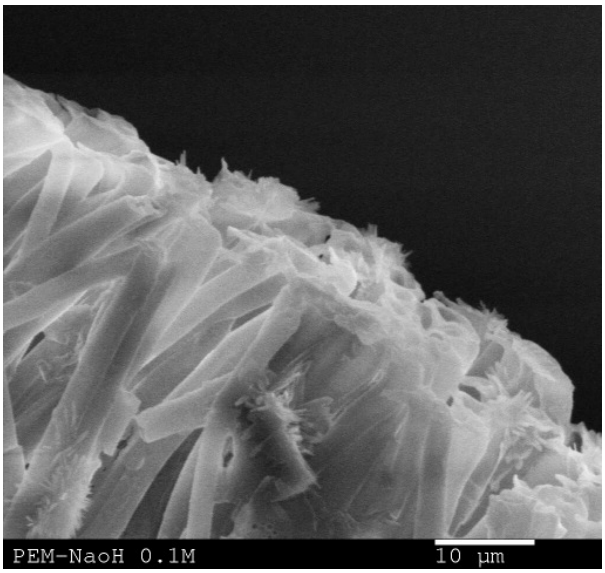

Figure 40. SEM image of the PEM-seald-PPX tubes(PEMs : PEI(PAA/PAH)$_{29}$PAA) after NaOH 0.1 M for 15-30 min maybe dont need because in acid already said that removed.

2.6. ATRP of N,N-diisopropyl ammonium acrylate in presence of air[72]

ATRP of N,N-diisopropyl ammonium acrylate was performed in the presence of air according to Scheme 7. Conversion was followed by quantification of olefinic double bonds of NNDIPAAc via ^{1}H NMR spectroscopy. ^{1}H NMR spectra of NNDIPAAC and poly(N,N-diisopropyl ammonium acrylate) are shown in figures 41.

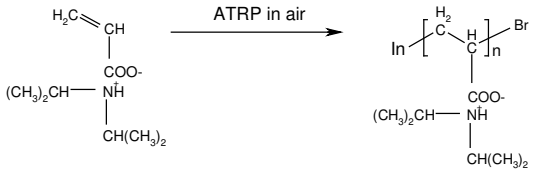

Scheme 7.

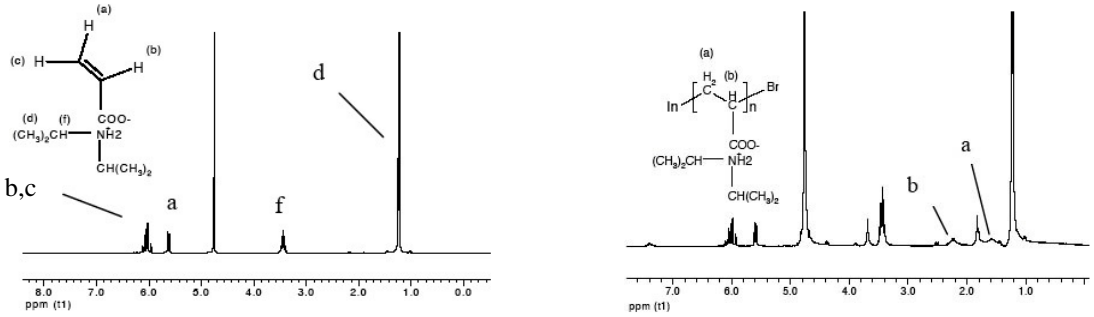

(1) **(2)**

Figure 41. (1) ^{1}HNMR of N,N-diisopropyl ammonium acrylate; (2) ^{1}HNMR of poly(N,N-diisopropyl ammonium acrylate) (Table 1: entry 2), which was synthesised by controlled polymerisation.

Conversions, molecular weights, and molecular weight distributions of poly(N,N-diisopropyl ammonium acrylate) are presented in table 1. Conversion of the polymerization was followed by quantification of olefinic double bonds of NNDIPAAc via ^{1}H NMR spectroscopy. ^{1}H NMR spectra of NNDIPAAC and poly(N,N-diisopropyl ammonium acrylate) are shown in figure 40 and 41.

Linear growth of molecular weight as a function of conversion and narrow molecular weight distributions indicated that controlled polymerisations (Fig. 42).

Table 1. Molecular weights, polydispersities and conversions of poly (N,N-diisopropyl ammonium acrylate) synthesised by CuBr/bipy catalysed ATRP in different polymerization conditions.

polymer	oxygen	time (min)	M_n(GPC)	M_w/M_n (GPC)	conversion %*
1	a	10	12900	1.14	44
2	a	30	14600	1.19	56
3	a	90	17400	1.32	75
4	a	110	18000	1.46	81
5	b	10	5800	1.24	42
6	b	15	7900	1.23	48
7	b	40	8900	1.35	60
8	b	65	10000	1.40	65

a: Reaction was carried out in presence of controlled amounts of air (reaction was sealed in air and air was introduced to the reaction in designated times as described above).

b: Reaction was carried out open to air.

*** Conversion of the polymerization was followed by quantification of olefinic double bonds of NNDIPAAc via ^{1}H NMR spectroscopy.**

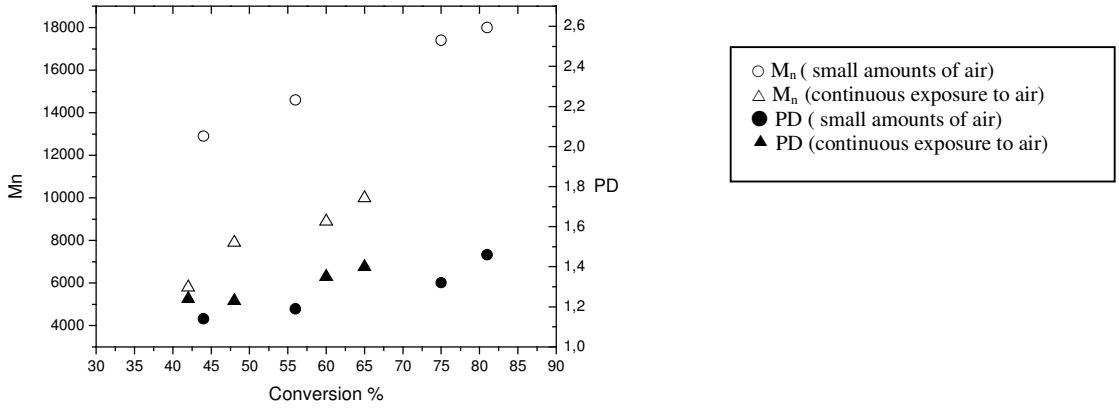

Figure 42. Molecular weights and polydispersities (PD) of poly(N,N-diisopropyl ammonium acrylate)as a function of conversion.

The molecular weights obtained from GPC indicates that the initiator efficiency is low, which can be due to inactivation of BzBr and propagating chains containing terminal bromine by amine. The polymerization with continuous exposure to air occured at higher rate and lower molecular weights than those in presence of small (controlled) amounts of air indicating the role of oxygen in the polymerization (see Tab. 1 and Fig. 42). Polydispersities increased not unexpectedly with monomer conversion in the presence of oxygen but clearly, polydispersities are lower with reactions performed in air (Fig. 42). Oxygen may act as co-catalyst in a complex of CuBr/bipy/O_2. Since the catalyst solution was prepared before starting the polymerisation, most of Cu(I) can be stabilized by the formation of the complex of CuBr/bipy.

$$Cu^{2+} + Cu + 2n\ bipy \rightleftharpoons 2\ Cu^{+}/(bipy)_n$$

The reason for the higher rate of polymerization after introducing more oxygen to the reaction is not clear. An explanation for this observation is that the complex of CuBr/bipy/O_2 plays more significant role as catalyst after introducing more oxygen to the reaction and therefore results the higher rate of polymerization (see Fig. 43).

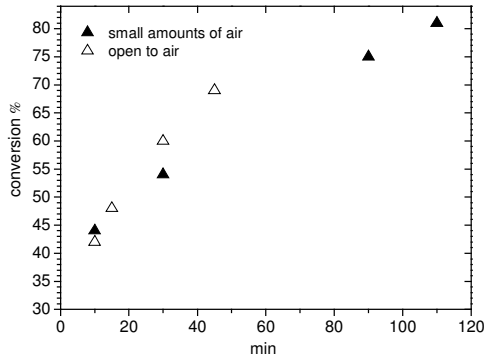

Figure 43. Conversion of N,N-diisopropyl ammonium acrylate in the presence of small amounts of oxygen and open to air as a function of time (min).

2.7. Immobilization of Gold Particles on the thiol-modified-PPX Films/tubes by using self-assembly

In this section, the goal is to immobilize gold particles on the surfaces modified by self-assembly technique. Gold have tendency to react with thiol (mercapto) groups. In order to provide suitable substrate for gold immobilization a monolayer of 1-dodecanthiol was self-assembled onto surface. The substrate used were either PPX film or PPX tubes. In order to obtain suitable surfaces deposition of the monolayer of 1-dodecanthiol, the PPX films/tubes were treated with sulfuric acid and then a polycation, PEI, was self-assembled onto the surface. The positively charged surface is suitable for the deposition of 1-dodecanthiol. As is described in experimental section, three solutions of 1-dodecanthiol with different pH was prepared. It should be noted that because of low solubility of 1-dodecanthiol in water, α-CD was used to make a complex of 1-dodecanthiol/CD, which is soluble in water.

Three gold sols were prepared were: 1) gold sol prepared from reduction of $HAuCl_4$ ($Au_{redAu(III)}$); 2) Thiol-stabilized gold sol; 3) DMAP-modified-gold sol. The gold particles in different forms were immobilized on the surface of the thiol-modified films/tubes from the above gold sols.

2.7.1. Gold particles immobilized using the gold sol prepared by reduction of $HAuCl_4$ ($Au_{redAu(III)}$) onto the thiol-modified surfaces of the films/tube

Au (III) were reduced to Au (0) in toluene by using sodium borohydrite (BH_4Na) as reduction agent. The films/tubes were placed in the Au sol. Since, Au clusters are not stable, therefore, right after the preparation of gold sol, it should be used in the next step for immobilization of gold onto the previously prepared thiol-modified surfaces.

2.7.1.1. Gold particles from $Au_{redAu(III)}$ immobilized on the SH-mod-Sur-1

in order to make a suitable substrate for immobilizing the gold on the surface, the H_2SO_4-treated-PPX film/tubes were coated with a PEI layer (see figure 44).

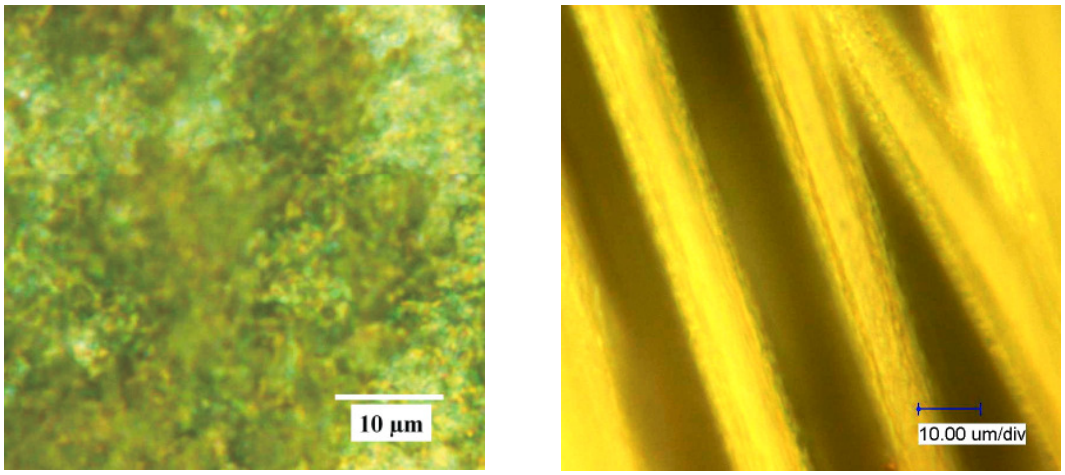

Figure 44. Shown the H_2SO_4- treated-PPX film/tubes coated with a monolayer of PEI.

Figure 45, shows the IR spectra of the H_2SO_4- treated-PPX film before and after the PEI coating.

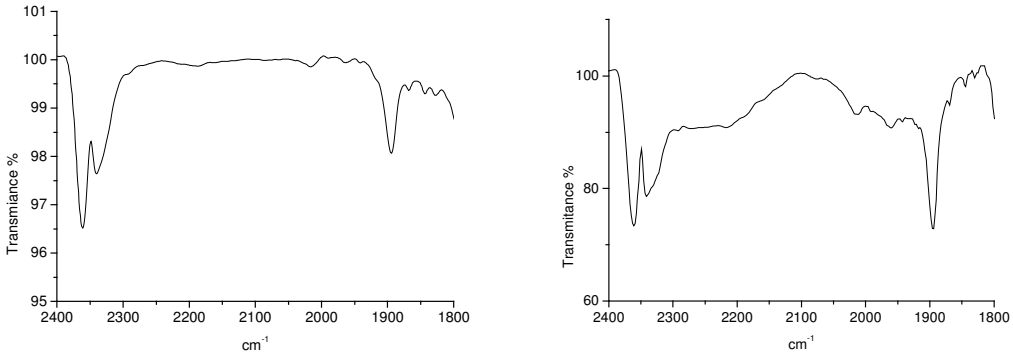

Figure 45. ATR-FTIR spectra of the films: left, H_2SO_4- treated-PPXfilm; right, H_2SO_4- treated-PPX film coated with a monolayer of PEI.

The water contact angle measurements were carried out on the surfaces of the H_2SO_4- treated-PPX film and H_2SO_4- treated-PPX film coated with a monolayer of PEI. The contact angle of H_2SO_4- treated-PPX film was obtained as average value of 12˚, whereas for the film after coating with a monolayer of PEI, the average value of the contact angle was 22˚.

Figure 46. Water droplets on the films for one of the measurements: left, the contact angle of the H_2SO_4- treated-PPX film θ = 12˚; right, the contact angle of the H_2SO_4- treated-PPX film coated with a monolayer of PEI θ = 22˚.

Figure 47 shows EDX performed from the H_2SO_4- treated-PPX film.

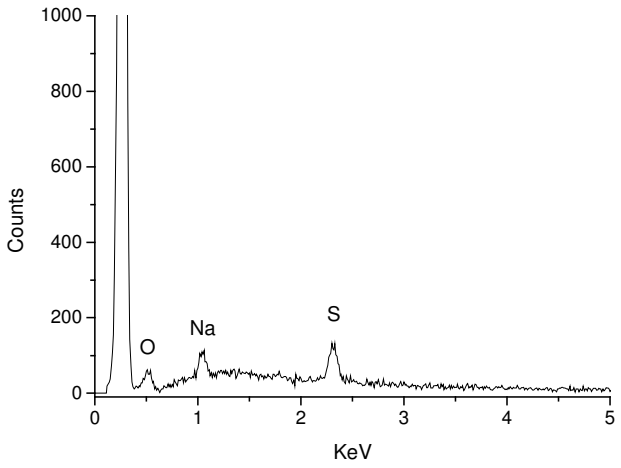

Figure 47. Shown EDX performed from the H_2SO_4- treated-PPX film.

After deposition of the PEI layer, a monolayer of 1-dodecanthiol was on the SH-mod-Sur-1 (the preparation procedure in experimental section).

Figure 48 shows the IR spectra of the PEI-coated-PPX film before and after the deposition of the monolayer of 1-dodecanethiol. The IR spectrum of 1-dodecanethiol exhibits a broad band centered at 1300 cm^{-1}.

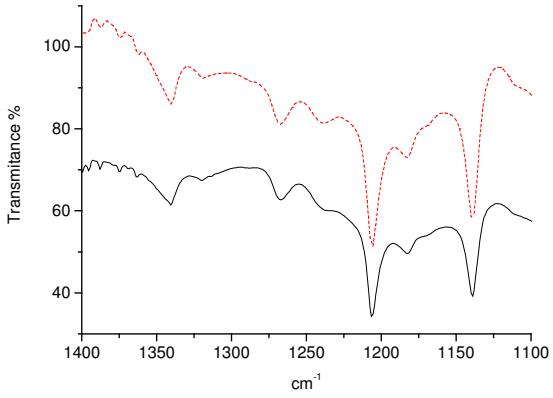

Figure 48. ATR-FTIR spectra of the films: solid line, H_2SO_4- treated-PPX film coated with a monolayer of PEI; dashed line, SH-mod-Sur-1.

.

The above SH-mod-Sur-1 was placed into $Au_{redAu(III)}$ in order to immobilize the gold particles on the surface of the film. Au(0) can react with thiol groups to have gold chemically bounded (—S—Au) to the surface.

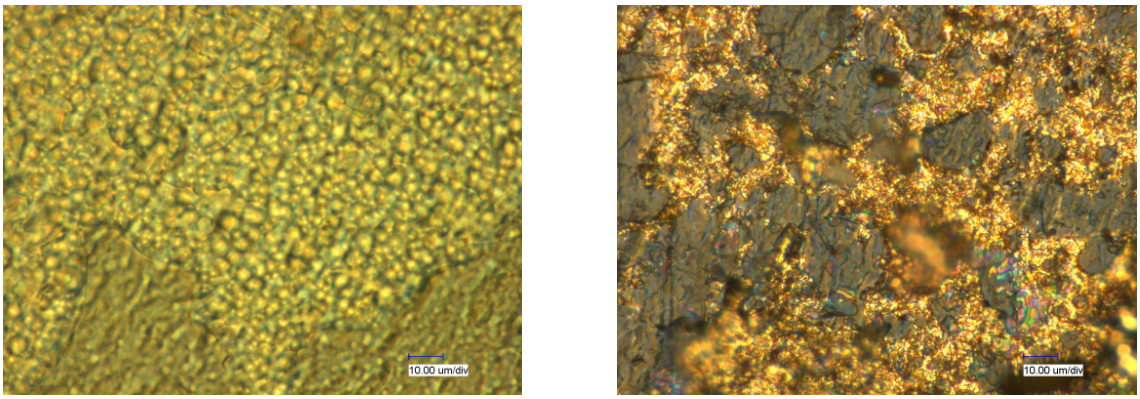

Figure 49. Digital microscope images were performed from the surface of the films: left, thiol-modified film; right, gold immobilized onto the surface of the film.

The IR spectra from the surface of the film before and after gold immobilization indicate a decrease in the intensity of the stretchs of aromatic and saturated hydrocarbons (3100-2830 cm $^{-1}$) after gold assembly are much weaker than those before gold assembly onto the surface.

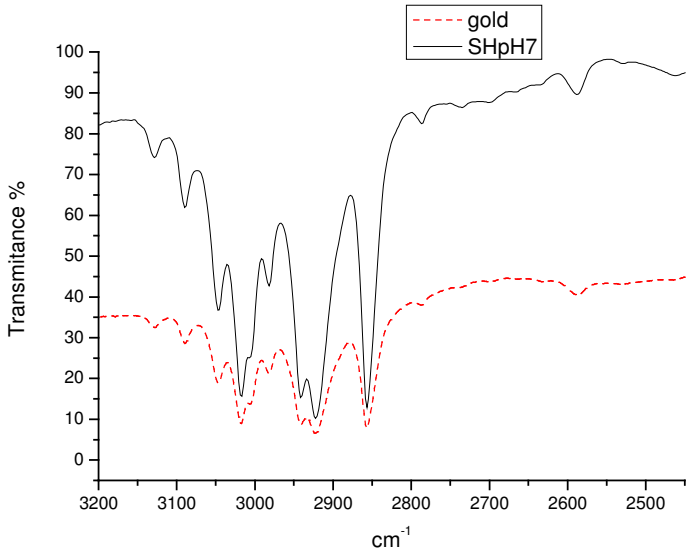

Figure 50. ATR-FTIR spectra of the films: solid line, thiol-modified film; dashed line, the film after gold immobilization.

2.7.1.2. Gold particles from $Au_{redAu(III)}$ immobilized on the SH-mod-Sur-2

The PEI modified film/tubes were coated with a monolayer of 1-in order to obtain SH-mod-Sur-2. PH of the dipping solution of 1-dodecanthiol was varied to investigate that how the changes at the thiol-modified surface can be influence the immobilization of Au.

Figure 51 indicates the SH-mod-Sur-2.

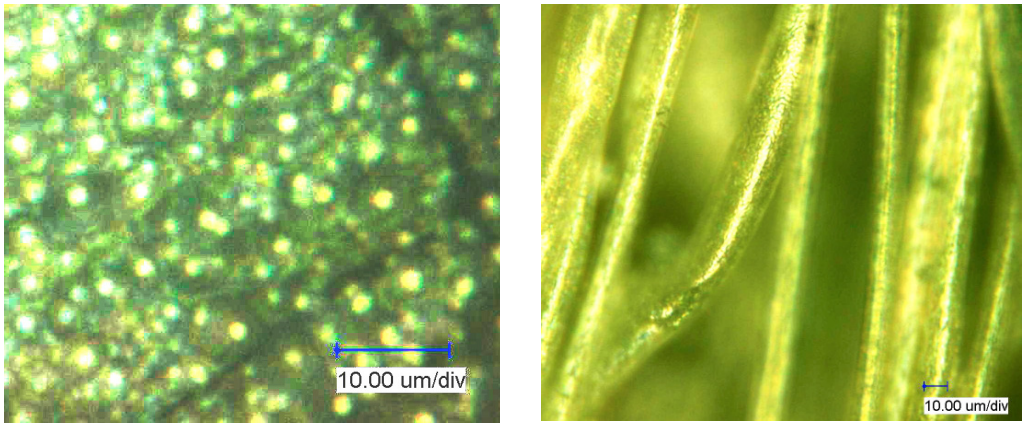

Figure 51. Shown digital microscope images of thiol-modified^{pH8} surfaces of film on the left and of the tubes on the right.

Figure 50 shows the IR spectra of the PEI-coated-PPX film before and after the deposition of the monolayer of 1-dodecanethiol. The reference IR spectrum of 1-dodecanethiol exhibits a broad band centered at 1300 cm^{-1}. As can be seen from figure 46, comparing the IR spectra, the spectra of the SH-mod-Sur-2, exhibits an increase in intensity about 1300 cm^{-1}, insisting the existance of the 1-dodecanethiol on the surface.

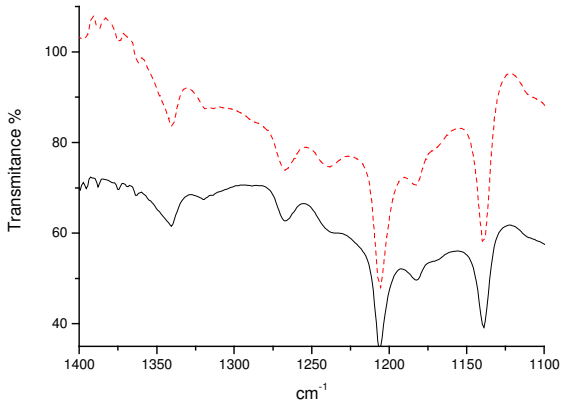

Figure 52. ATR-FTIR spectra of the films: solid line, H_2SO_4-treated-PPX film coated with a monolayer of PEI; dashed line, SH-mod-Sur-2.

The water contact angle measurement from the SH-mod-Sur-1 was performed, resulting a contact angle of 72˚. The surface is less hydrophile comparing to the PEI coated surface. This is because of the hydrophobe feature of the hydrocarbon chains of 1-dodecanethiol.

Figure 53. A water droplet on the SH-mod-Sur-2, θ = 72˚.

As can be seen from figure54, gold clusters have been successfully self-assembled onto the surface of the film and tubes. By increasing the pH of the dipping solution of 1-dodecanthiol, the gold coverage looks more effective. As can be seen from figure 48, the aggregation of the gold clusters was taken place at the surface of the film.[82]

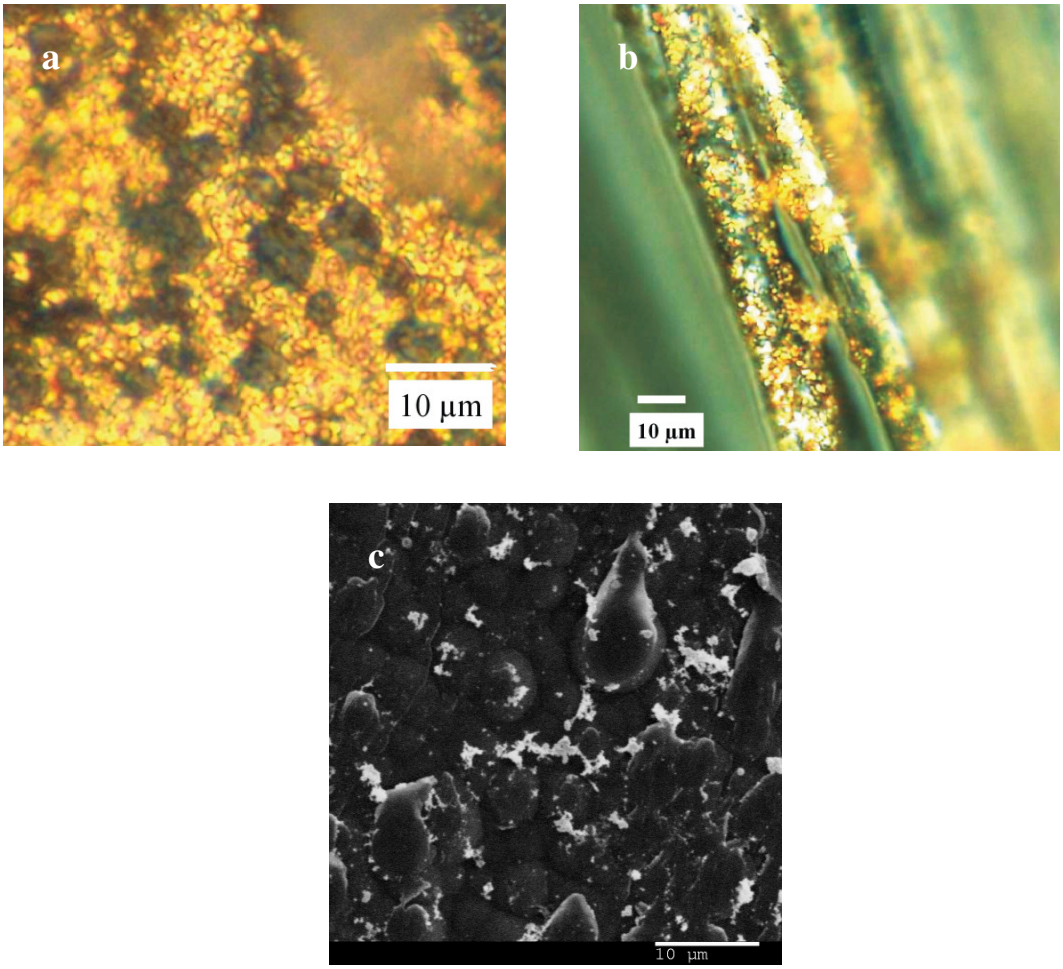

Figure 54. Shown digital microscope and SEM images of the films and tubes: (a) digital microscope image of gold immobilized onto the surface of the SH-mod-Sur-2 of film; (b) digital microscope image of gold immobilized onto the surface of the SH-mod-Sur-2 of tubes; (c) SEM image of gold immobilized onto the surface of the SH-mod-Sur-2 of film.

figure 55 shows the IR spectra of the films before and after gold coating. After immobilization of gold on the SH-mod-Sur-2, C-H stretches of aromatic and saturated hydrocarbons (3100-2830 cm $^{-1}$) became weaker, which is consistent with the fact that the surface is coated with gold particles.

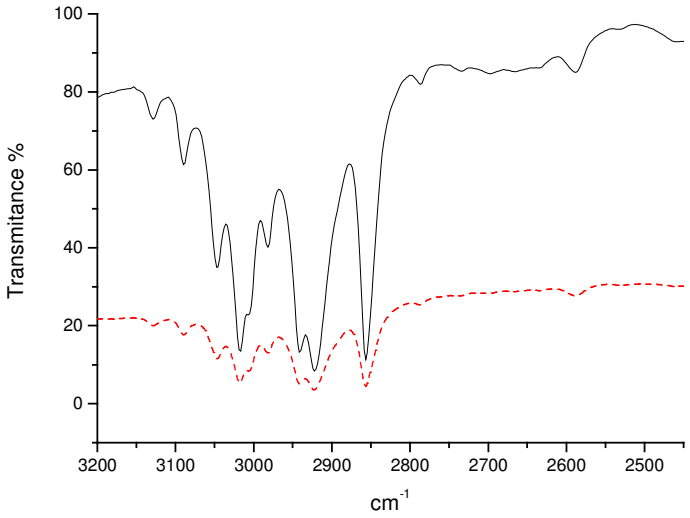

Figure 55. ATR-FTIR spectra of the films: solid line, SH-mod-Sur-2 of film; dashed line, the film after gold immobilization.

2.7.1.3. Gold particles from $Au_{redAu(III)}$ immobilized on SH-mod-Sur-3

The PEI modified film/tubes were coated with a monolayer of to provide SH-mod-Sur-3. Figure 56 shows the digital microscope image of SH-mod-Sur-3 of film.

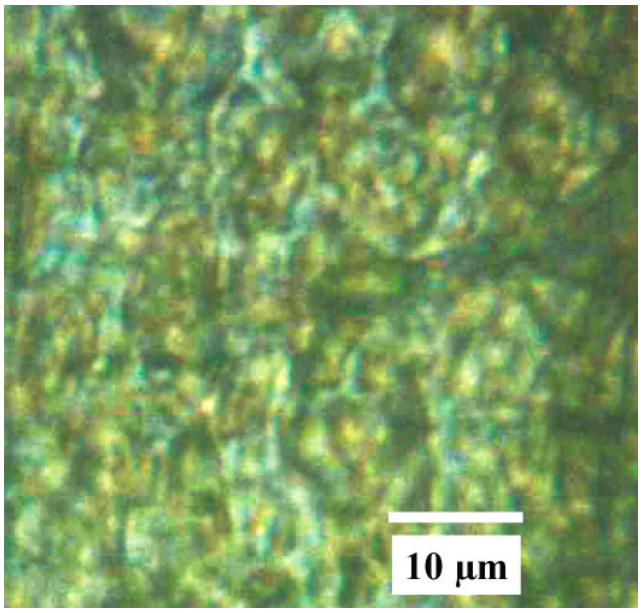

Figure 56. Shown digital microscope images of SH-mod-Sur-3 of film.

Figure 55 shows the IR spectra of the PEI-coated-PPX film before and after the deposition of the monolayer of 1-dodecanethiol. As reference, the IR spectrum of 1-dodecanethiol exhibits a broad band centered at 1300 cm^{-1}. As can be seen from figure 57, comparing the IR spectra, the SH-mod-Sur-3 film exhibits an increase about 1300 cm^{-1}, insisting the existance of the 1-dodecanethiol at the surface.

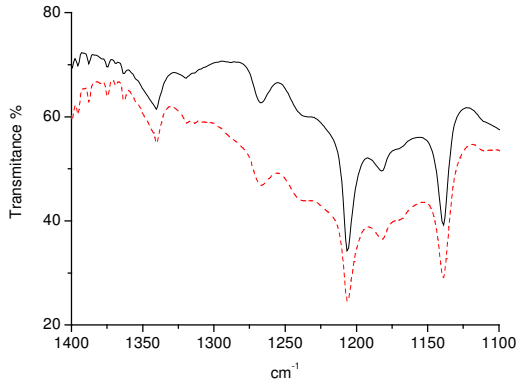

Figure 57. ATR-FTIR spectra of the films: solid line, H_2SO_4- treated-PPX film coated with a monolayer of PEI; dashed line, SH-mod-Sur-3 of the film.

As can be seen from figure 58, gold clusters have been successfully self-assembled onto the surface of the film and tubes.

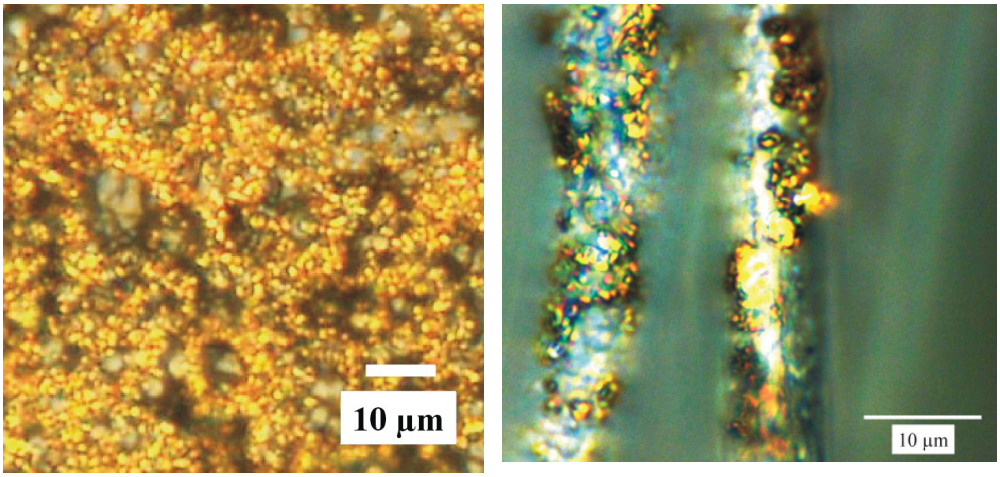

Figure 58. Shown digital microscope images of the films and tubes: left, digital microscope image of gold immobilized onto SH-mod-Sur-3 of the film; right, digital microscope image of gold immobilized onto SH-mod-Sur-3 of the tubes.

The IR spectra before and after immobilization of gold give the similar information about the effectiveness of the gold self-assembly like what it was observed for the case of the lower SH-mod-Sur-2. Again, a significant decrease can be observed from the IR spectrum after gold self-assembled on the surface.

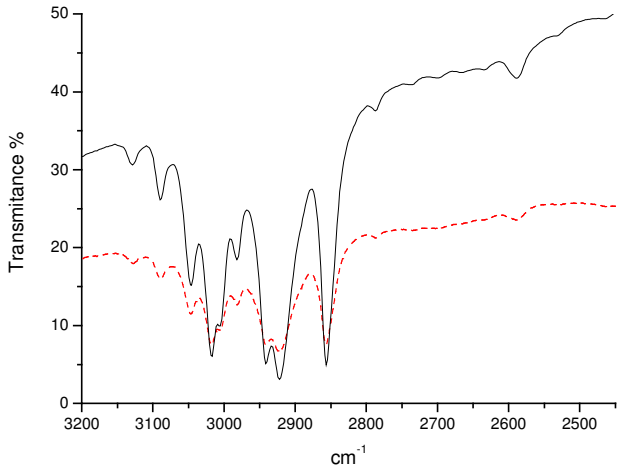

Figure 59. ATR-FTIR spectra of the films: solid line, SH-mod-Sur-3 o the film; dashed line, the film after gold immobilization.

2. 7.1.4. Contact angle measurement of the modified-surfaces

The water contact angle measurements of the films after immobilization of the Au particles indicates that the surface become more hydrophilic comparing the contact angle of the thiol-modified-films, which is consistent with literature data.[81] Figure 60 shows a comparison of the water contact angles of SH-mod-Sur-3 of the film before and after Au particles were self-assembled onto the surface.

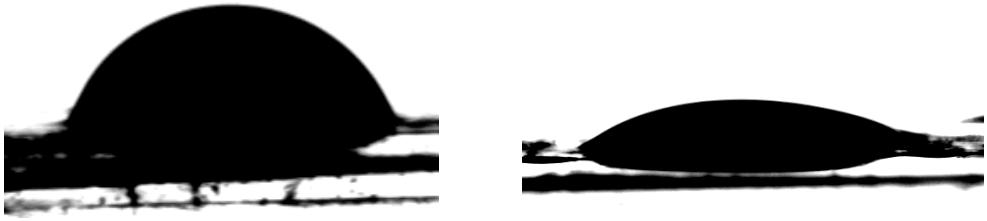

Figure 60. Water droplets on the films; left, the contact angle of the SH-mod-Sur-3 of the film, θ = 72˚; right, the contact angle of the film after Au particles were immobilized onto the surface, θ = 34˚.

2.7.2. 4-(dimethylamino)pyridine-stabilized-Gold (DMAP-stabilized-Gold) particles immobilized on the thiol-modified surfaces of films/tubes

DMAP-stabilized-gold particles[135-137] were immobilized onto the surfaces modified previously by 1-dodecanethiol, means of exchange reaction of DMAP at the surface of the gold particles with thiol groups at the surface of the film/tubes.

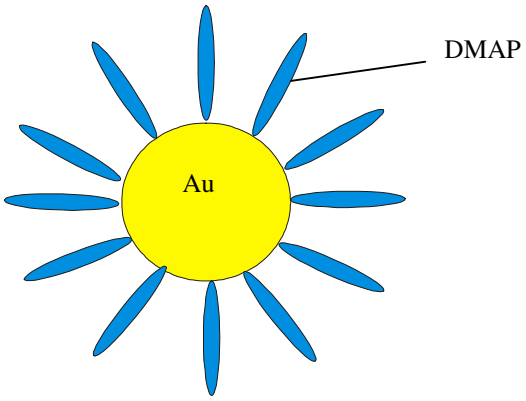

Figure 61. A DMAP-stabilized-gold particle.

The size of the DMAP-stabilized-gold particles was in range of 2-6 nm. As can be seen from figure 62, in spite of the stabilization of the surface of the gold particles, the aggregation of the DMAP-stabilized-gold particles is partly observed . This is because of the polar feature of the DMAP molecules, which were used as a protection layer at the surface of the gold particles.

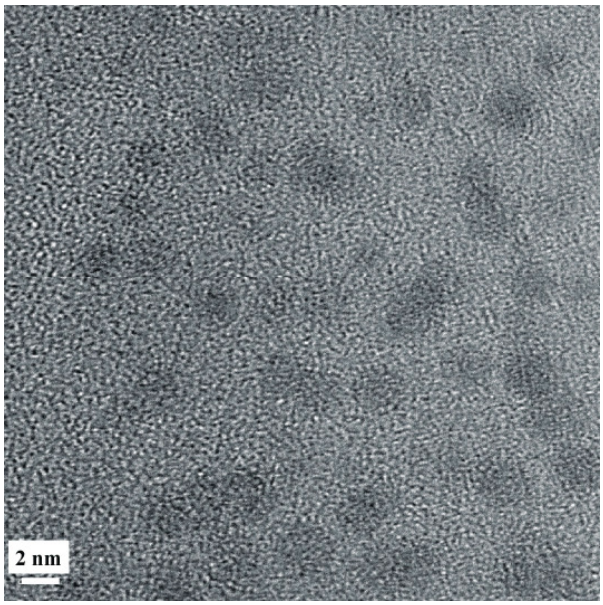

Figure 62. TEM image of the DMAP-stabilized-gold particles.

2.7.2.1. DMAP-stabilized-gold particles immobilized on SH-mod-Sur-2

As can be seen from figure 63, DMAP-stabilized-gold particles have been successfully self-assembled onto the surface of the film.

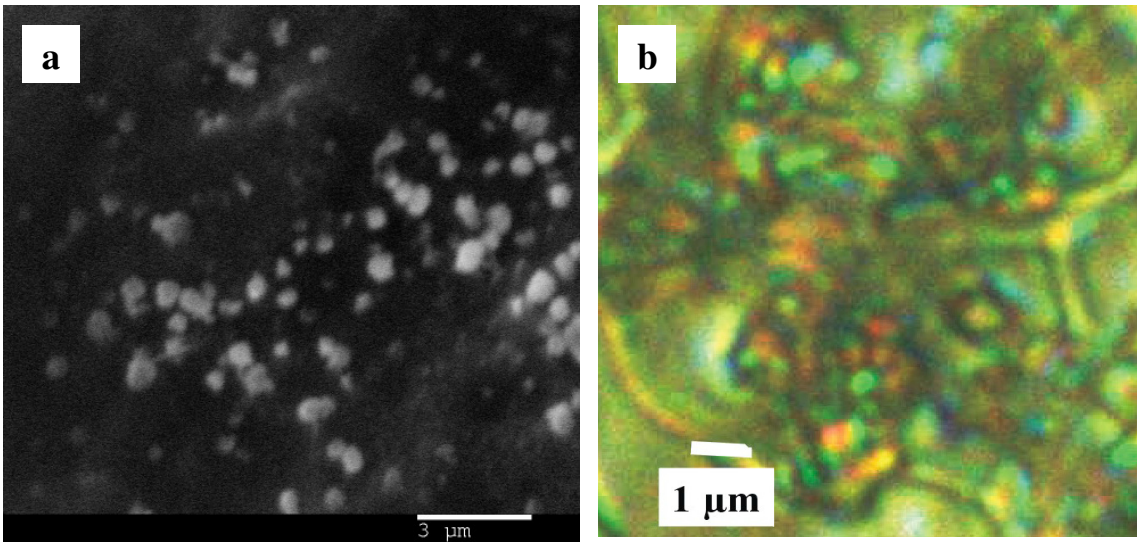

Figure 63. Shown SEM and digital microscope and images of the films: (a) SEM image of DMAP-stabilized-gold particles immobilized onto the surface of SH-mod-Sur-2 of the film; (b) digital microscope image of DMAP-stabilized-gold particles immobilized onto the surface SH-mod-Sur-2 of the film.

figure 64 shows the IR spectra of the films before and after DMAP-stabilized-gold particles were immobilized on the surface. After the surface was self-assembled with DMAP-stabilized-gold particles, C-H stretches of aromatic and saturated hydrocarbons (3100-2830 cm^{-1}) became weaker, which is consistent with the fact that the surface is coated with gold particles.

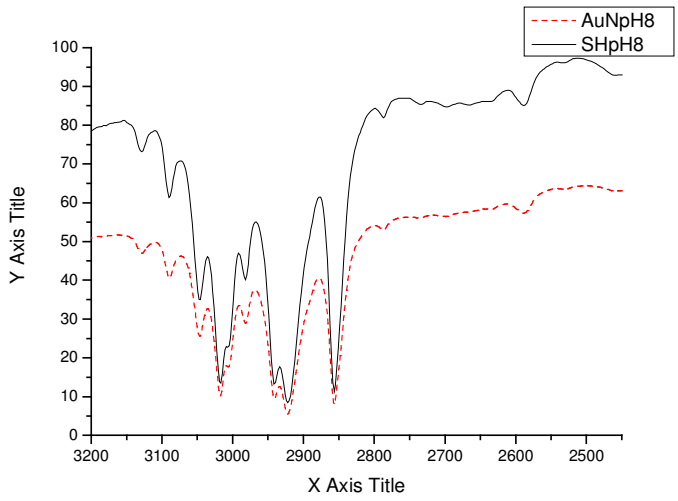

Figure 64. ATR-FTIR spectra of the films: solid line, SH-mod-Sur-2 of the film; dashed line, the film after DMAP-stabilized-gold particles immobilization.

EDX was performed from gold particles immobilized on the surface of the sample $Au_{DMAP\text{-}stab\text{-}2}$.

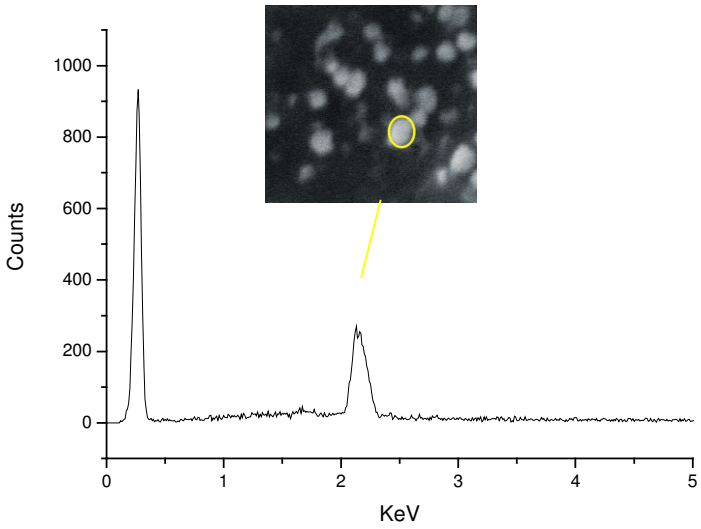

Fugure 65. EDX of the $Au_{DMAP\text{-}stab\text{-}2}$ of the film.

2.7.2.2. DMAP-stabilized-gold particles immobilized on SH-mod-Sur-3

As can be seen from figure 66, DMAP-stabilized-gold particles have been successfully self-assembled onto the surface of the films/tubes.

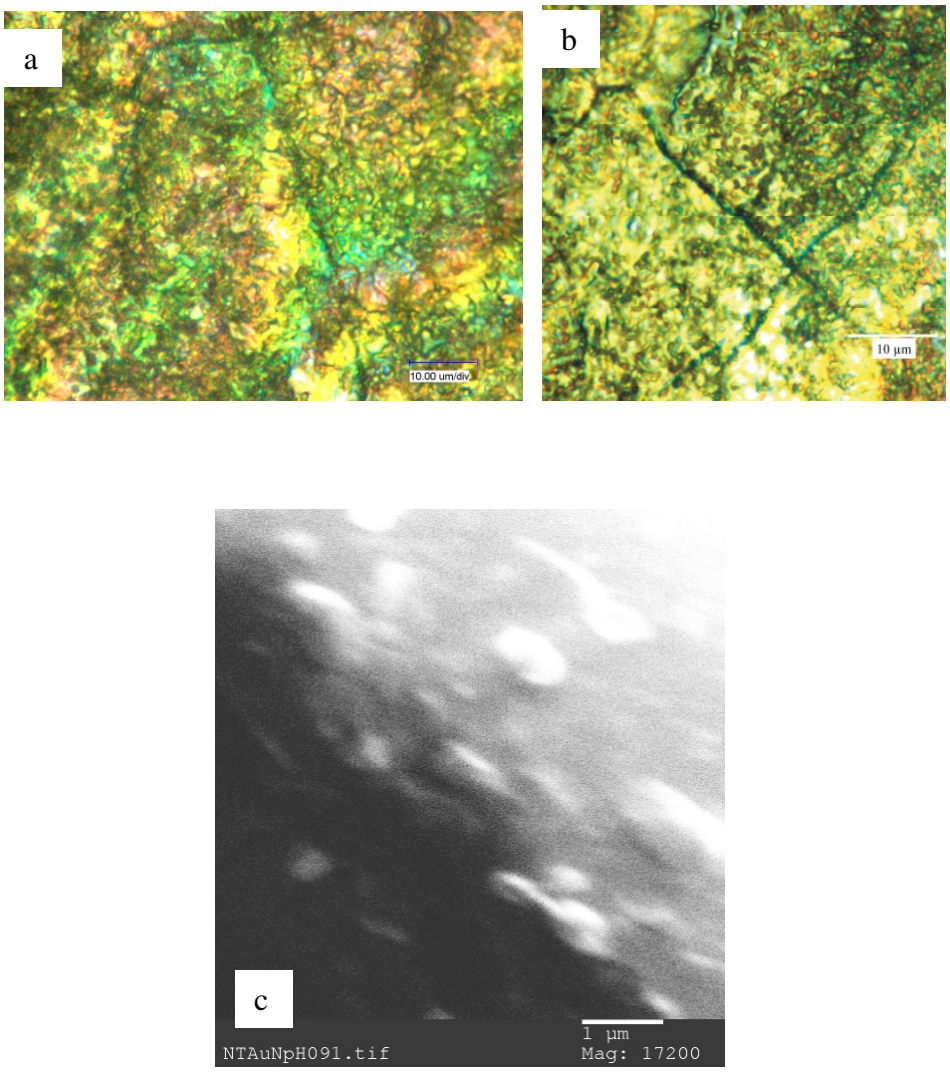

Figure 66. Shown digital microscope and SEM images of the films and tubes: (a) digital microscope image of DMAP-stabilized-gold particles immobilized onto SH-mod-Sur-3 of the film; (b) digital microscope image of gold immobilized onto SH-mod-Sur-3 of the film; (c) SEM image of DMAP-stabilized-gold particles immobilized onto SH-mod-Sur-3 of the tube.

figure 67 shows the IR spectra of the films before and after DMAP-stabilized-gold particles coating. After the surface was self-assembled with DMAP-stabilized-gold particles, C-H stretches of aromatic and saturated hydrocarbons (3100-2830 cm $^{-1}$) became weaker, which is consistent with the fact that the surface is coated with gold particles.

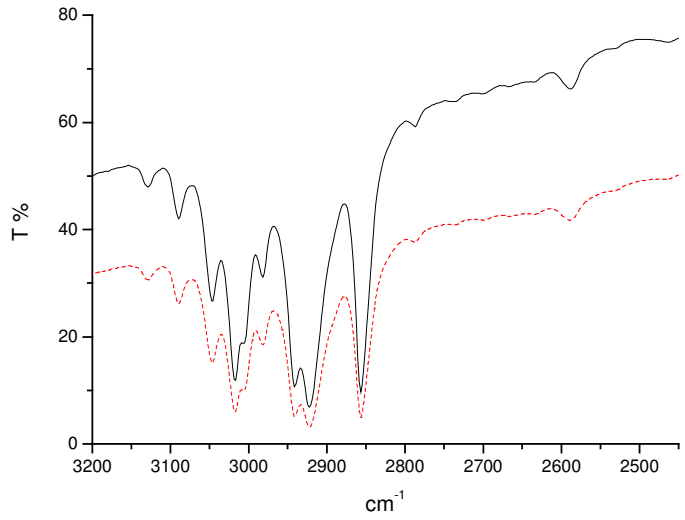

Figure 67. ATR-FTIR spectra of the films: solid line, SH-mod-Sur-3 of the film; dashed line, the film after gold immobilization.

2.7.2.3. Contact angle measurement of the modified-surfaces

The water contact angle measurements of the films after immobilization of the DMAP-stabilized particles indicates that the surface become more hydrophilic comparing the contact angle of the thiol-modified-films. Figure 68 shows a comparison of the water contact angles SH-mod-Sur-3 of the film before and after DMAP-stabilized particles were self-assembled onto the surface.

Figure 68. water droplets on the films; left, the contact angle of SH-mod-Sur-3 of the film, θ = 72˚; right, the contact angle of the film after DMAP-stabilized gold particles particles were immobilized onto the surface, θ = 39˚.

Optical Spectroscopy

UV/Vis measurements were carried out in order to monitor the optical properties of the self-assembled monolayer of the DMAP-stabilized gold particles. As can be seen from figure 69, a broad band centered at 564 nm appears. The broadening of the band responsible for the DMAP-stabilized gold particles immobilized on the thiol-modified surfaces occurs because of the aggregation of the particles and consequently wide particles size distribution. For the samples of $Au_{redAu(III)-x}$ and $Au_{thiol-stab-x}$, the UV spectroscopy is not a proper method because the particles at the surface respectively are highly aggregated for the case of $Au_{redAu(III)-x}$ and are isolated for $Au_{thiol-stab-x}$.

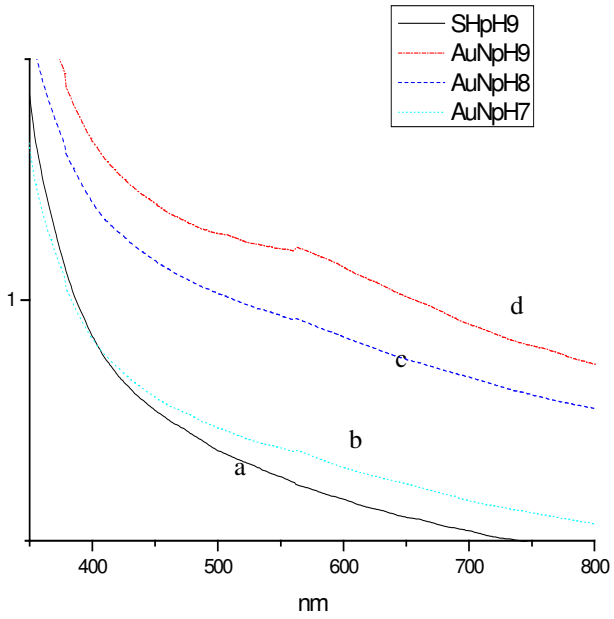

Figure 69. UV/VIS spectra of the films after DMAP-stabilized gold particles were immobilized on their surfaces: a, SH-mod-Sur-3 of the film; b, $Au_{DMAP\text{-}stab\text{-}1}$; b, $Au_{DMAP\text{-}stab\text{-}2}$; c, $Au_{DMAP\text{-}stab\text{-}3}$.

2.7.3. Thiol-stabilized-gold particles immobilized on the thiol-modified surfaces of films/tubes

In this section, thiol-stabilized-gold particles were immobilized onto the surface of SH-mod-Sur-x by means of exchange reaction between the thiol groups on the surface of the gold particles and the thiol groups on SH-mod-Sur-x.[138] The size of the tiol-stabilized-gold particles was in range of 2-5 nm. As can be seen from figure 70, the thiol-sstabilized gold particles are well-distributed.

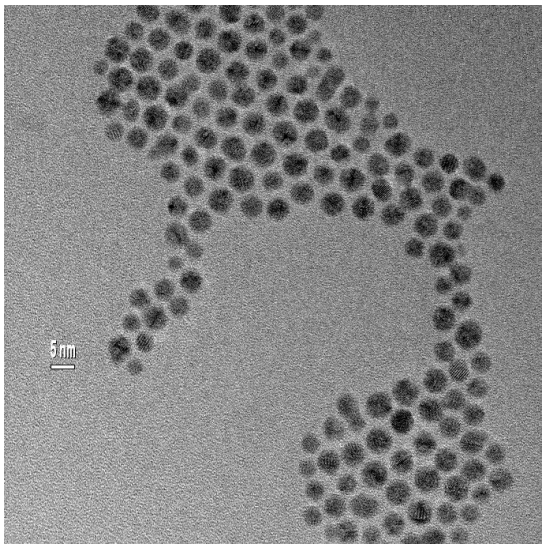

Figure 70. TEM image of the DMAP-stabilized-gold particles.

2.7.3.1. Thiol-stabilized-gold particles immobilized on SH-mod-Sur-1

Figure 71. shows thiol-stabilized-gold particles have been self-assembled onto SH-mod-Sur-1 of the film.

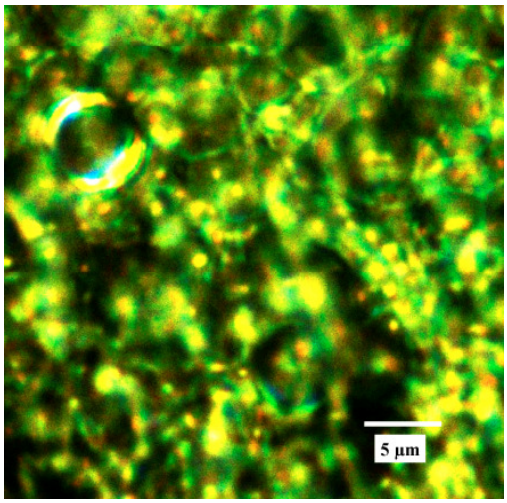

Figure 71. Shown digital microscope image of the films thiol-stabilized-gold particles immobilized onto SH-mod-Sur-1 of the film.

figure 72 shows the IR spectra of the films before and after thiol-stabilized-gold particles coating. After the surface was self-assembled with thiol-stabilized-gold particles, C-H stretches of aromatic and saturated hydrocarbons (3100-2830 cm $^{-1}$) became weaker, which is consistent with the fact that the surface is coated with gold particles. But the slight decrease in the intensity of the IR after the immobilization process was carried out on the surface insists a low surface coverage of the particles.

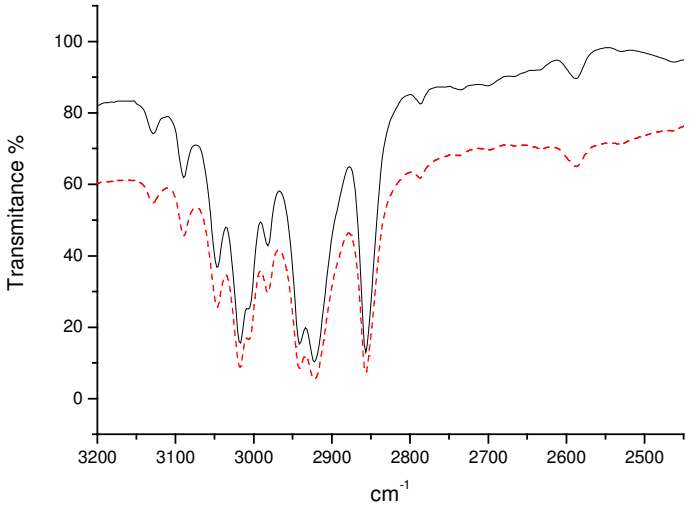

Figure 72. ATR-FTIR spectra of the films: solid line, SH-mod-Sur-1; dashed line, the film after thiol-stabilized-gold particles immobilization.

2.7.3.2. Thiol-stabilized-gold particles immobilized on SH-mod-Sur-2

As can be seen from figure 73, thiol-stabilized-gold pa the particles have been successfully self-assembled onto SH-mod-Sur-2. After self-assembly on the surface, the particles indicate the growth in the their size. This could be because of aggregation of the particles either in the solution (the solution of the thiol-stabilized particles stored in the refregerator for a while) or

during the self-assembly process while the exchange reaction ocurrs. Nevertheless, because of the surface protection, the particles shows a good destribution on the surface.

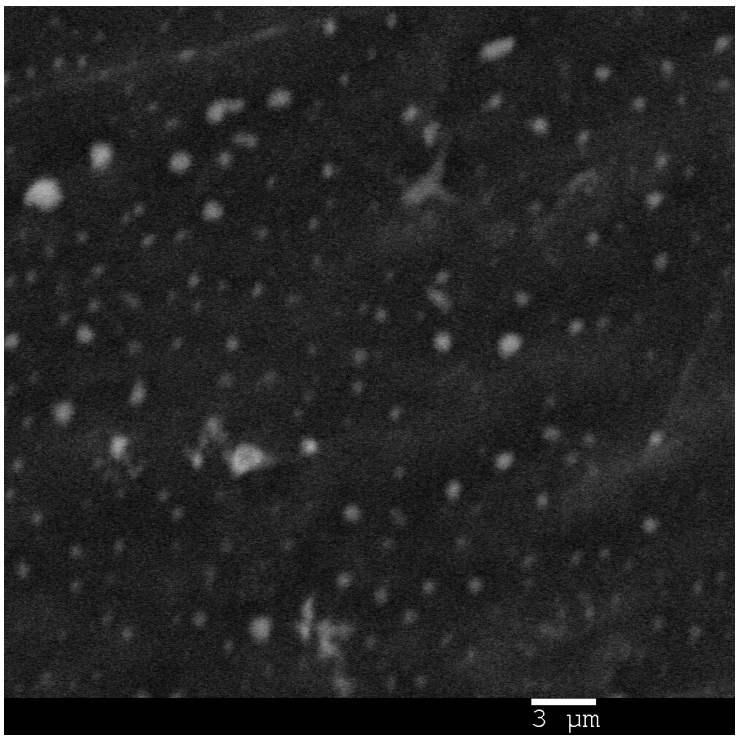

Figure 73. SEM image of thiol-stabilized-gold particles immobilized onto SH-mod-Sur-2 of the film.

Figure 74 shows the IR spectra of the films before and after thiol-stabilized-gold particles immobilized on the surface. After the surface was self-assembled with thiol-stabilized-gold particles, C-H stretches of aromatic and saturated hydrocarbons (3100-2830 cm^{-1}) became weaker, insisting the fact that the surface is coated with a gold particles.

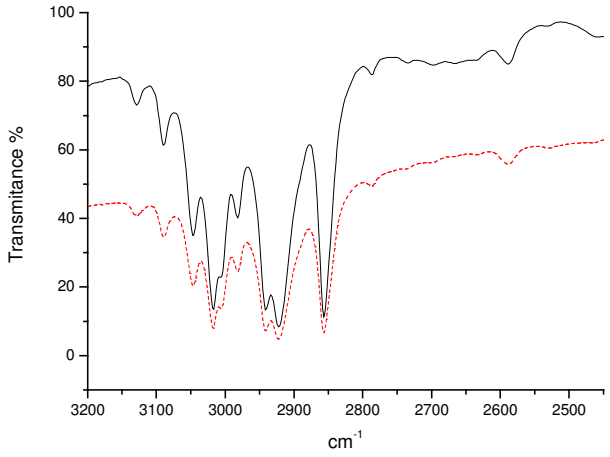

Figure 74. ATR-FTIR spectra of the films: solid line, SH-mod-Sur-2 of the film; dashed line, the film after thiol-stabilized-gold particles immobilization.

Figure 75 shows EDX performed from gold particles immobilized on the surface of the SH-mod-Sur-2 (sample $Au_{thiol\text{-}stab\text{-}2}$).

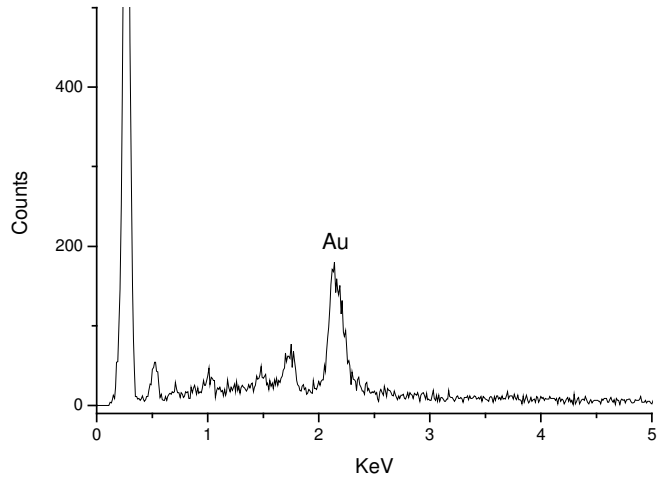

Fugure 75. EDX of the $Au_{thiol\text{-}stab\text{-}2}$ of the film.

2.7.3.3. Thiol-stabilized-gold particles immobilized on SH-mod-Sur-3

As can be seen from figure 76, thiol-stabilized-gold particles have been successfully self-assembled onto SH-mod-Sur-3 of the films.

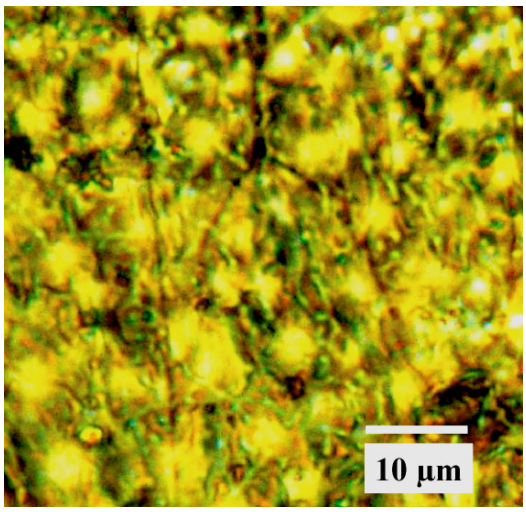

Figure 76. Shown digital microscope image of the thiol-stabilized-gold particles immobilized onto SH-mod-Sur-3 of the film.

Figure 77 shows the edge-on image of SH-mod-Sur-3 of the film before and after thiol-stabilized-gold particles were immobilized onto the surfece.

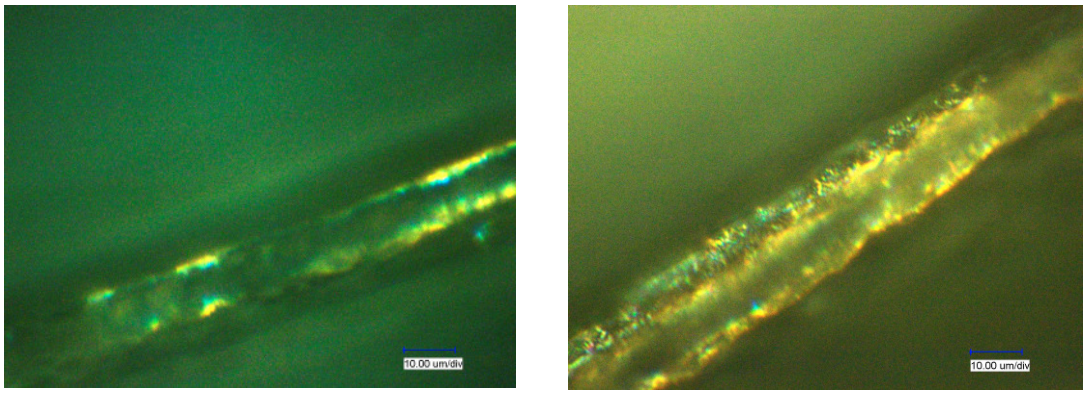

Figure 77. (a) edge-on image of SH-mod-Sur-3 of the film; (b) edge-on image SH-mod-Sur-3 of the film after the thiol-stabilized-gold particles were immobilized onto the the surface.

Figure 78 shows the IR spectra of the films before and after thiol-stabilized-gold particles immobilized on SH-mod-Sur-3 of the film. After the surface was self-assembled with thiol-stabilized-gold particles, C-H stretches of aromatic and saturated hydrocarbons (3100-2830 cm $^{-1}$) became weaker, insisting the fact that the surface is coated with a gold particles.

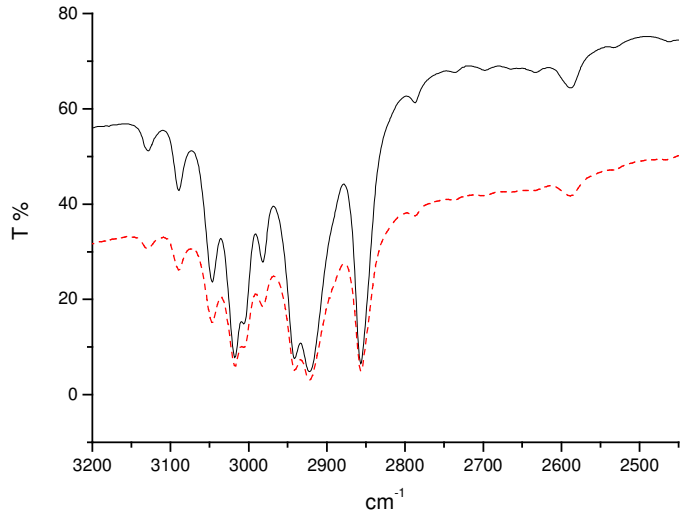

Figure 78. ATR-FTIR spectra of the films: solid line, SH-mod-Sur-3 of the film; dashed line, the film after thiol-stabilized-gold particles immobilization.

2.7.3.4. Contact angle measurement of the modified-surfaces

Figure 79 shows a comparison of the water contact angles of SH-mod-Sur-2 of the film before and after thiol-stabilized particles were self-assembled onto the surface. The water contact angle measurements of the films after immobilization of the thiol-stabilized particles indicates that the surface does change its feature (hydrophilisity) or if there are some changes, they are negligible, which is consistent with what is expected. The reason for this observation if that the gold particles have 1-dodecanethiol molecules, so that the feature of the surface after gold immobilization does not change.

Figure 79. water droplets on the films; left, the contact angle of SH-mod-Sur-2 of the film, θ = 72˚; right, the contact angle of the film after thiol-stabilized-gold particles were immobilized onto the surface, θ = 79˚.

2.7.4. Immobilized gold particles at the ends of the tubes

In order to immobilized gold particles on a specific area of the PPX tubes (at the ends of the tubes), the thiol functionalization at the ends of the tubes was performed. Here, the method used was simple, having the thiol-modified-tubes (the procedure of modification of the tubes with 1-dodecanethiol was previously mentioned) and then a layer of PPX was coated on the modified surface using CVD technique. After this step, the tubes were freezed in liquid nitrogen and then cut in smaller species. In this way, at the ends of the cut-tubes ($PPXT_{end\text{-}thiol\text{-}mod.}$), the monolayer of 1-dodecanethiol bearing thiol fuctionalities are out.

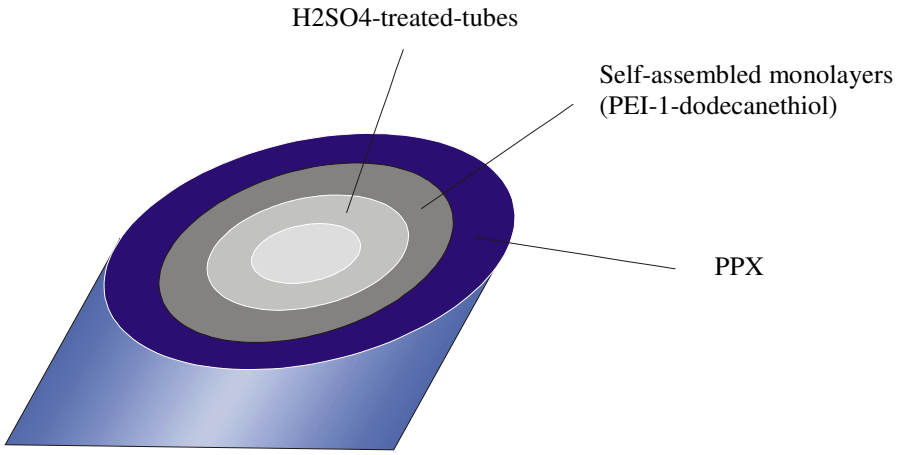

Figure 80. Schematic representation of cut-tubes; the thiol layer is out after cutting the tubes.

By placing the cut-tubes in colloidal gold sols, gold particles can react with thiol grops at the end of the tubes and immobilized there.

2.7.4.1. Gold particles immobilized using thiol-stabilized gold sol and gold sol prepared by reduction of $HAuCl_4$ ($Au_{redAu(III)}$) at the ends of $PPXT_{end\text{-}thiol\text{-}mod.}$

Gold particles were immobilized at the ends of the tubes with a monolayer of 1-dodecanethiol, which were deposited from thiol-solution-3. The preparation of the tubes bearing a monolayer of 1-dodecanethiol is mentioned in experimental section. The tubes placed either into the $Au_{redAu(III)}$ in order to immobilized gold at the ends of the tubes.

Figure 81 shows $PPXT_{end\text{-}thiol\text{-}mod\text{-}3}$ with gold particles self-assembled at the ends of the tubes.

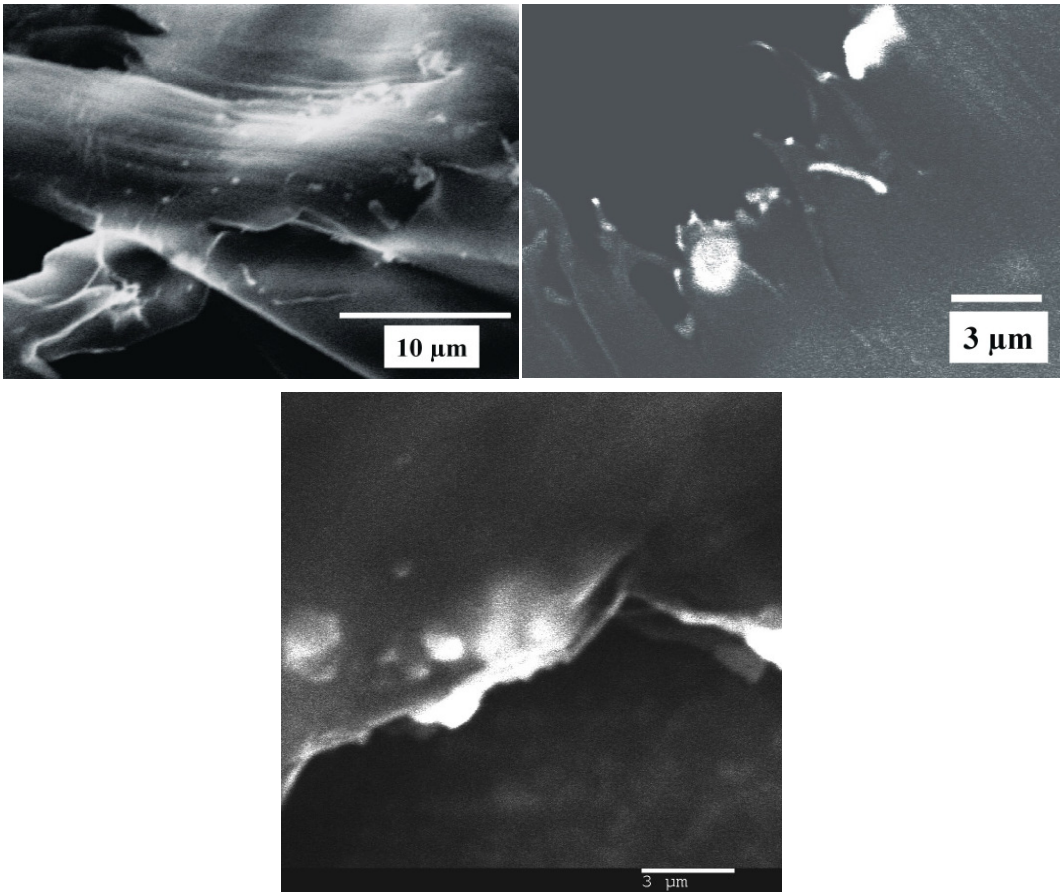

Figure 81. Gold particles immobilized onto the end of the $PPXT_{end\text{-}thiol\text{-}mod\text{-}3}$; (a) gold particles immobilized from the $Au_{redAu(III)}$; (b) gold particles immobilized from the thiol-stabilized-gold sol.

The following is EDX from $PPXT_{end\text{-}thiol\text{-}mod\text{-}3}$ after gold particles were immobilized at the ends ($PPXT_{end\text{-}gold\text{-}mod\text{-}3}$).

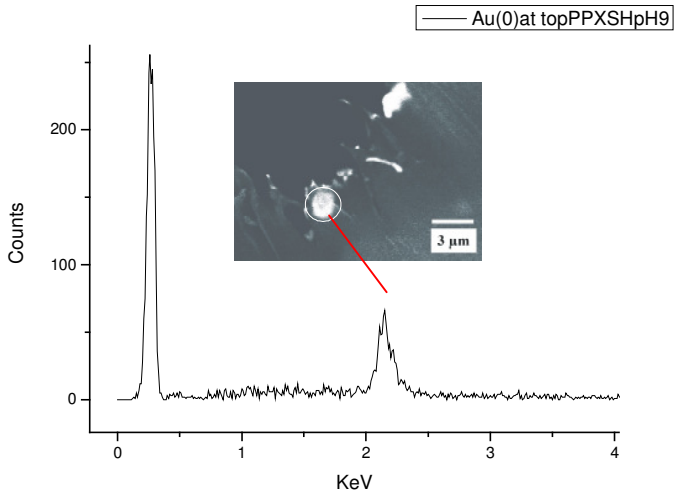

EDX made from the gold immobilized at the end of the tube.

Figure 82. EDX performed from the end of the $PPXT_{end\text{-}gold\text{-}mod\text{-}3}$ (gold particles immobilized from $Au_{redAu(III)}$).

3. Experimental section

3.1.Materials

A-174 Silane	Speedline Technology, Specially coating Systems
Acrylic acid	Acros organics, stabilized, 99.5%
AIBN	Aldrich
Benzylbromide (BzBr)	Acros organics, 98%
2,2´-bipyridyl	Lancaster synthesis
Bromine	Acros
Chloroform	Acros
Copper (I) bromide (CuBr)	Acros, 98%
α-cyclodextrine	Acros
4-(dimethylamino)pyridine-stabilized goldparticles (Nr. 84)	Aldrich
N,N-diisopropylamine	Aldrich, 99.5%
1-dodecanethiol	Merk
Ethanol	Lenz, distilled
Hydrochloric acid (HCl)	Riedel-deHaen, 37%
Hydrogene tetrachloroaurate(III) hydrate ($HAuCl_4$)	Nano solutions, Aldrich, used as received
N-isopropylamine	NIPAM, Acros
[2,2]Paracyclophane	Cookson Electronics, Specially Coating Systems
Poly(acrylic acid)	PAA, Aldrich, M_w = 100 000 35 % (w/w) in water, used as received
Poly(allylamine- hydrochloride)	PAH, Aldrich, M_w = 50 000 - 65 000, used as received
Poly(ethyleneimine)	PEI, Aldrich, M_w = 55 000, 50 % (w/w) in water, used as received
Poly-L-lactide	Boehringer Ingelheim, Resomer L214, M_w = 400 000 used as received
poly(styrene sulfonate sodium salt)	PSS, Aldrich, M_w = 70 000, used as received
Sodium dodecyl sulfate	SDS, Aldrich, ACS + 99%, used as received
Sodium hydroxide (NaOH)	Aldrich

Sodium borohydride ($NaBH_4$)	Aldrich
Sulfuric acid	Bayer, concentrated
Tetrachloromethane	CCl_4, dried over P_2O_5 and distilled
Tetraethylorthosilicate	TEOS, Fluka, + 98 %
Tetrahydrofurane	BASF, dried over potasium and distilled
Tetraoctylammoniumbromide	Aldrich
Toluene	BASF, distilled
Water	Ultrapure, resistivity higher than 18.2 Ω/cm
Water	Deionised
Water-d_1	Deuter GmbH, Kalsruhe

The pH of PAA solution was adjusted with HCl to 4 and in the case of PAH solution the pH was adjusted with NaOH to 5.3. The other polyelectrolyte solutions were used without adjusting the pH. SDS was added to the 0.01 M PSS solution at a concentration of 0.02 M.

3.2. Instrumentation

3.2.1. Contact angle measurement

Water contact angle measurements were carried out using a Kruess contact angle system G10.

3.2.2. Differential scanning calorimetry (DSC)

DSC measurement was carried out using a DSC 821e Mettler in order to obtain glass transition temperature (T_g) and melting point (T_m). The measurements were performed with temperature programming (heating- and cooling rate of 10 ºC/min.

3.2.3. Digital microscope

A VHX digital microscope (Keyence) was used to provide optical images.

3.2.4. Dipping robbot

A robot programmed for a time-dependent sequence of x-, y- and z- displacements were used for dipping the substrates into the polyelectrolyte solutions at Muenster university, department of physical chemistry in Prof. M. Schönhoff's group.

3.2.5. Elemental analysis

Elemental analysis was performed in the analytic center of department of chemistry in Philipps-Universität Marburg.

3.2.6. Energy-dispersive X-ray microanalysis (EDX)

EDX analysis was performed with a scanning electron microscope CamScan series 4 equipped with an EDX microanalysis system from Thermo Noran Company.

3.2.7. Infrared spectroscopy (IR)

Using a DJ-Lab IR spectrometer (Excalibur series) IR spectroscopy was performed:

- **ATR-IR**

Attenuated total reflection (ATR) IR spectroscopy

- **IR microscope (Digilab UMA 600).**
  - Mesurements in reflection mode
  - Slide-on ATR (microscope-ATR)

3.2.8. Gel permeation chromatography (GPC)

GPC measurements was performed using a GPC, Polymer Standards Service, PSS, with an IR detector.

3.2.9. NMR spectroscopy

^{1}H and $^{13}CNMR$ spectra were obtained using a Bruker AC300 and WH400.

3.2.10. Scanning electron microscope (SEM)

SEM images of the samples were obtained using a CamScan series 4.

3.2.11. Thermogravimetry analysis (TGA)

Thermogravimetry analysis was carried out using a Mettler Toledo TGA/SDTA 851e. The heating range of 25 ºC to 800 ºC and rate of 10 ºC/min was used.

3.2.11. UV/VIS specroscopy

UV/VIS spectra were obtained using a Perkin Elmer Lambda spectrometer.

3.3. Electospinning

3.3.1. Electrospinning device

Nanofibers were prepared by electrospining technique. As can be seen from figure 83 ,the instrument set up includes a syringe to load polymer solutions for the electrospinning. A piston with which the presure on the syringe and consequently the speed of the injection of the polymer solution through a capillary with a inner diameter of 0.3 mm for the electrospinning process can be controlled. By creating a high intensity electric field with an anode connected to the capillary and grounded with a cathode connected to a metal plate placed with a X distance below the capillary. The distance between the capillary and the metal plate is variable, so that a proper distance between the capillary and the metal plate for electrospinning of different polymers can be optimized.

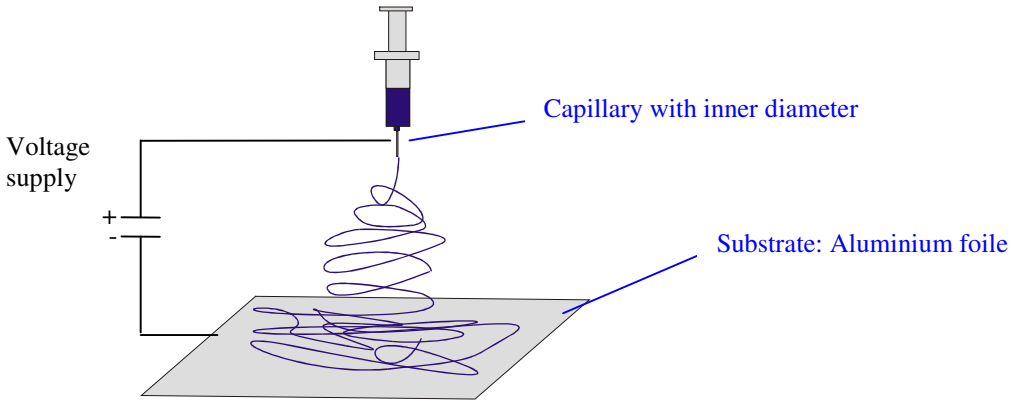

Figure 83. Schematic representation of electrospinning.

3.3.2. General procedure of electrospinning

In this work, nanofibers were fabricated from the polymer solutions at room temperature. A 2 ml syringe with a needle with inner diameter of approximately 0.3 mm, which was placed 20 cm above a surface of aluminiun foil, was used. A voltage difference of 20 kV was applied.

3.3.3. Fabrication of oriented-electrospun fibers

In order to have the fibers well-oriented, the electrospinning was carried out in the way that during the electrospinning process, instead of collecting fibers onto the plannar surface, the fibers were collected on a rotating cylinder substrate (3000-3500 cycle per minute) with a diameter about 15 cm,which was covered by aluminium foil.

3.4. Chemical vapor deposition process (CVD)

3.4.11. CVD apparatus

One of convenient method of production of PPX derivatives is CVD. As was mentioned in the introduction section the apparatus includes five major parts: vaporization chamber, pyrolysis furnace, deposition chamber, cooling dewar and vacuum pump.

3.4.12. CVD process

The CVD machine was switched on. After reaching the desired temperature of the pyrolysis furnace, a monomer, [2,2]paracyclophane (Parylene N), on a self-made Al-frame, was placed into the vaporization chamber. And the samples for PPX coating were placed in the deposition chamber. The vacuum pump was switched on and liquid nitrogen was filled into the cooling dewar. After reaching the appropriate pressure of below 8 mTorr, the temperature of the vaporization chamber was raised up to an appropriate temperature. The coating was started automatically after the vapor pressure of the monomers was reached to an appropriate value. At this stage, by evaporation of the monomers the vapor pressure is raised and the coating is taken place. Finally, the deposition process will be stopped by finishing the monomer supply and consequently, the vapor pressure decreases down to 20 mTorr.

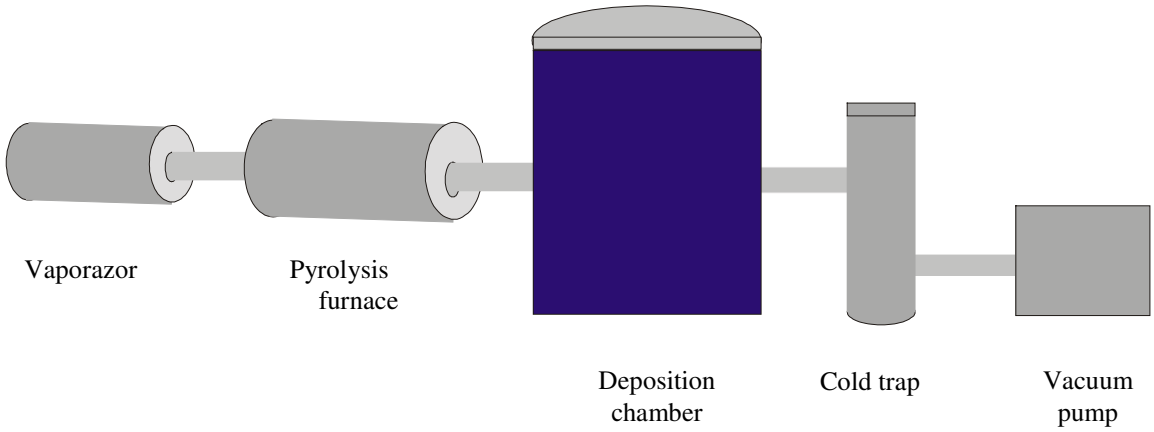

Figure 84 . Schematic illustration of set up of CVD machine.

3.5. Preparation of PPX-PLLA core-shell fibers

In this section the fiber templates were fabricated and as for the next step, the fibers can be coated with different polymers in order to get them as core-shell fibers from which the hollow fibers can be produced.

3.5.1. Preparation of PLLA fiber templates

Electrospun PLLA fibers were used as template for preparation of PPX tubes.[4] PLLA nanofibers were fabricated from the polymer solutions at room temperature. A 2 mL syringe with a needle with inner diameter of approximately 0.3 mm, which was placed 20 cm above a surface of aluminium foil. A voltage difference of 20 kV was applied. In order to obtain oriented PLLA fibers, the fibers were collected on a rotating cylinder substrate with a diameter of about 15 cm, which was covered by aluminium foil.

3.5.2. PPX-coated fiber templates by CVD

The PLLA fibers were coated by PPX using chemical vapor deposition (CVD) process as described above.[4,58,115] The fibers were placed into a CVD machine and all the PPX coating process was carried in the CVD machine. [2,2]paracyclophane was used as starting material for coating.

Slide-on ATR-FTIR

ν / cm^{-1} : 3090 (w), 3040 (w), 3000 (w), 2930 (m), 2850 (m), 1890 (w), 1790 (w), 1750 (m), 1710 (m), 1520 (m), 1450 (m), 1400 (m), 1270 (w), 1175 (w), 1130 (w), 1070 (w), 1015 (w), 925 (w), 820 (s), 720 (m), 580 (m), 545 (m).

3.6. Preparation of Tubes Made of Polyelectrolyte Multilayers (PEMs)

The TUFT process was employed in order to obtain hollow fibers made PEMs.[4]

3.6.11. Fabrication of the SiO_2 fibers

SiO_2 nanofibers prepared by electrospining: Our strategy to fabricate the fibers is similar to the preparation procedure published by Zhang et al.[141] The milky solution of 1 M tetraethylorthosilicate (TEOS), 2 M H_2O and 0.01 M HCl in ethanol was placed in an oven at 60˚C to get a proper viscosity (50-100 cP) of the polymerized solution. The electrospun SiO2 nanofibres were fabricated from the above solution at ambient temperature. The solution was charged into a 2 ml syringe with a needle with inner diameter of approximately 0.3 mm, which was placed 20 cm above a surface of aluminiun foil. A voltage difference of 20 kV was applied for this performance.

3.6.2. Formation of PEMs on the surface of SiO_2 nanofibres (PEM-coated SiO_2 nanofibers)

The PEMs were formed on the surface of silica nanofibres by sequential deposition of oppositely charged polyelectrolytes. Fibers were fixed in a sample holder and immersed into the appropriate solutions using a robot, which could be programmed for a time-dependent sequence of x-, y- and z- displacements. The first deposited layer (precoating layer) for all samples prepared here, was a PEI layer. The adsorption time for the precoating layer was 30 min, for all other layers it was 20 min. After each deposition, the samples were washed by immersion into ultrapure water three times (two min each washing). After each layer deposition the samples were not dried and when the deposition process were finished the samples were dried in air. In this work, two multilayers were formed on the surface of the nanofibers: $(PEI/PSS_{SDS})_{30}$ and $PEI(PAA/PAH)_{29}PAA$.

Core dissolution: In order to obtain PEMHFs, the silica template fibers were dissolved in 0.5 M HF solution. The PEMHFs (remained from HF treatment) were washed with water and dried in air.

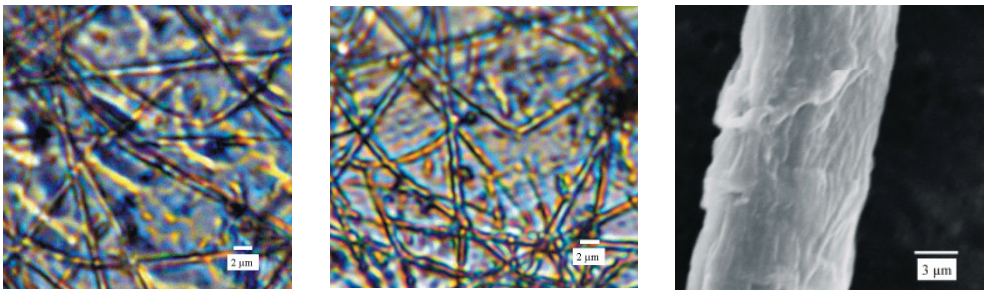

(1) **(2)** **(3)**

Figure 85. (1) Digital microscope image of PEM-SiO_2 nanofibres coated with $PEI(PAA-PAH)_{29}PAA$; (2) PEM-SiO_2 nanofibres coated with $(PEI-PSS/SDS)_{30}$; (3) SEM images of PEMHFs coated with $(PEI-PSS_{SDS})_{30}$ after HF treatment.

3.7. Sealing Process of the Tubes (PPX tubes sealed with polymers synthesized at their ends using ATRP)

In order to perform ATRP of acrylic acid monomers at the ends of the tubes, the PPX tubes must be selectively functionalized so that they can be used as macro-initiator of undergoing ATRP. In this section, the technique employed to limit the polymerization at the selected area of the tubes (the ends of the tubes) is described:

3.7.1. PMMA as supporting material for PPX-PLLA core-shell fibers

The core-shell fibers were placed into a test tube in the way that the fibers were vertically positioned inside the test tube, which was previously filled with 0.05 mol% of intiator, AIBN, in methylacrylate (see figure86). The reaction was placed in an oven at 40 ˚C for 5 days. After the reaction was cooled down to room temperature, the solid PMMA surrounding the PLLA-PPX core-shell fibers (PMMA-protected-PLLA-PPX_{CSF}) was obtained and cut into 2 mm slices (small disks with 2 mm thickness). The cut-slices of PMMA-protected-PLLA-PPX_{CSF} are ready for the next step in which the functionalization of the core-shell fibers can be carried out, in order to convert PPX to a suitable ATRP initiator at the ends, the bromination of PPX was carried out. Since the whole body of the fibers were supported by PMMA, the only contact of the fibers with the surrounding environment was the cut-surface of the slice or in other words, the ends of the fibers.

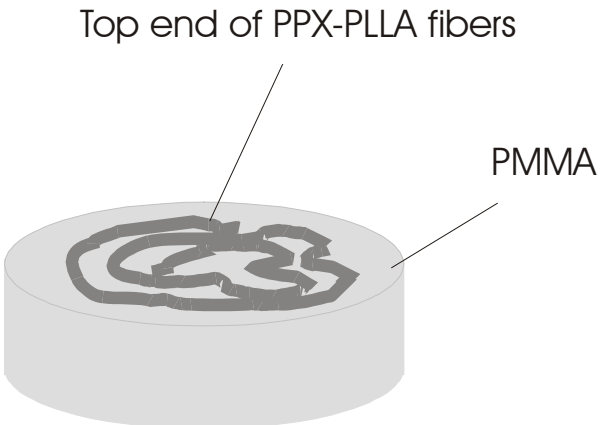

Figure 86. Shown schematic representation of cut-slice of PMMA-protected-PLLA-PPX_{CSF}.

3.7.2. Bromination reaction at the ends of the PPX-PLLA core-shell fibers

The bromination reaction was carried out in 20 mL tetrachloromethane containing 32 mg (0.2 mmol) AIBN, the cut-slice of PMMA-protected-PLLA-PPX_{CSF} and 0.1 mL (2 mmol) of bromine (Br_2) and the reaction refluxed for 5 h. After the reaction was finished, the sample was rinsed in THF and chloform until the solvent remains colorless.

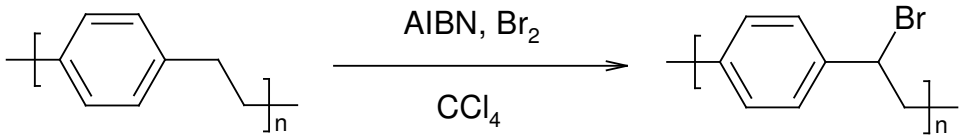

Scheme 8. Shown the bromination reaction of PPX.

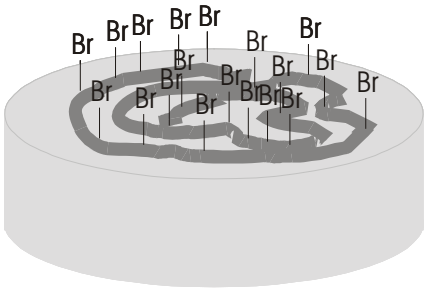

Figure 87. Shown schematic representation of cut-slice of PMMA-protected-PLLA-PPX_{CSF} after performance of the bromination reaction (PMMA-protected-PLLA-$BrPPX_{CSF}$).

3.7.3. ATRP of N,N-diisopropyl acrylate (NNDIPAAc) at the ends of the PPX tubes

a catalyst mixture was prepared by adding 2 mg (0.014 mmol) of CuBr to 4 mg (0.026 mmol) of 2,2´-bipyridyl (bipy). 5 ml THF was quickly charged into the flask containing the catalyst mixture and the flask was sealed in air. The catalyst mixture was stirred for 15 min. After 15 min stirring, there was a clear colourless-light pink solution and still a green insoluble solid at the bottom of the flask. The catalyst solution was injected into another flask containing a cut-

slice of PMMA-supported-PLLA-BrPPX_{CSF}. The flask was sealed and stayed for 45-60 min at room temperature. The above solution and the disk was charged into a flask containing 420 mg (mmol) of NNDIPAAc salt. After dissolving NNDIPAAc, solvent was evaporated at 40 °C using a Rotary evaporator. The slide was covered by the reaction mixture. The flask was placed into an oil bath for 2 h at 60 °C.

3.7.4. ATRP of N-isopropylacrylamide (NIPAM) at the ends of the tubes

The synthesis procedure was similar to what was performed above for ATRP of NNDIAAc. NIPAM was used as monomer in order to obtain PNIPAM a thermosensitive polymer at the ends of the tubes.

3.7.5. Removal of PMMA from the PMMA-protected-PLLA-BrPPX_{CSF} sealed either with PAA or PNIPAM

After the reaction, the PMMA-protected-PLLA-BrPPX_{CSF} was placed into the chloroform in order to remove the PMMA and dried in air to obtain the PPX tubes sealed with poly acrylate N,N-diisopropyl ammonium.

3.7.6. NaOH treatment of the PPX tubes sealed with N,N-diisopropyl acrylate

The sealed PPX-PLLA tubes were kept in the 0.1 M solution of NaOH. After NaOH treatment, the carboxyl groups of PAA at the ends of PPX tubes can be partly deprotonated and sodium cations can act as conterions of the carboxyl groups of PAA. The existence of Na on the PPX tubes can be monitored by EDX, which can be considered as a proof for the successfull performance of the ATRP of NNDIPAAc salt at the end of the tubes. The discussion about the results of the EDX was indicated in discussion part.

3.8. PPX tubes sealed with PEMs

To seal the tubes with PEMs, the layer by layer (LbL) self-assembly of PEs was performed on

the PPX tubes. The self-assembly procedure mentioned in the sections 3.5.1.1, 3.5.1.2 and 3.7.1 were repeated to obtain cut- slices of PMMA-protected-PLLA-PPX_{CSF}.

3.8.1. H_2SO_4-treatment of PMMA-protected-PLLA-PPX_{CSF}

The treatment of the PMMA-protected-PLLA-PPX_{CSF} with sulfuric acid was carried out under following conditions: 20 mL concentrated H_2SO_4 (96%) was added into a 250 ml round-flask containing PMMA-protected-PLLA-PPX_{CSF} . The flask was sealed and ultra-sonicated at 60 ºC for 5 h. Every 30 min, the stopper was carefully removed under Hood for a short time to release possible gasses produced during the reaction. After the reaction was kept to be cooled down to room temperature. The tubes were washed in a solution of 9 M H_2SO_4 (cooled down in an ice bath) and then were sequentially placed into a solution of 3 M HCl and 1 M NaOH and ultra-sonicated respectively for 15 min and 5 min at room temperature. After, the tubes were dried in air. It should be noted that the PLLA template fibers (as core of the PLLA-PPX fibers) were removed by the H_2SO_4-treatment automatically because of the solubility of PLLA in sulfuric acid so that the H_2SO_4-treated PPX tubes were obtained directly after the reaction without performing further experiments for the PLLA template fibers removal.

3.8.2. The removal of PMMA from the H_2SO_4-end-treated PMMA-protected- PPX tubes

H_2SO_4-treated PMMA-protected-PPX tubes was placed into the chloroform in order to remove PMMA and dried in air to obtain the PPX tubes treated with H_2SO_4 at their ends H_2SO_4-end-treated PPX tubes, which can be used in the next step to obtain tubes sealed with PEMs.

3.8.3. Sealing the H_2SO_4-end-treated PPX tubes with PEMs by self-assembly technique

In order to seal H_2SO_4-end-treated PPX tubes, the layer by layer (LbL) self-assembly deposition technique was employed. To get the H_2SO_4-end-treated PPX tubes with PEMs, the L-b-L self-assembly was carried out following the procedure mentioned previously in section 3.6.

3.9. Coating PPX tubes with PEMs

Modified-PPX tubes were coated with PE layers using the self-assemby based technique. To make the surface of the PPX tubes suitable for self-assembly coating, the surface need to be modified to bear electrostatic charges so that the electrostatic forces as well as entropic forces can act to stabilize the PE layers on the surface of the fibers.

3.9.1. H_2SO_4-treatment of the PLLA-PPX core-shell fibers

The treatment of the PPX-PLLA fibers with sulfuric acid was carried out under following conditions: 20 mL concentrated H_2SO_4 (96%) was added into a round-flask containing PPX-PLLA fibers. The reaction was sealed and ultra-sonicated at 60 ºC for 5 h. Every 30 min, the stopper was removed for a short time to release possible gasses produced during the reaction. After the reaction was kept to be cooled down to room temperature. The tubes were washed in a solution of 9 M H_2SO_4 (cooled down in an ice bath) and then were sequentially put into solutions of 3 M HCl and 1 M NaOH and ultra-sonicated respectively for 15 min and 5 min at room temperature. After, the tubes were dried in air. It should be noted that the PLLA template fibers are desolved during the treatment with sulfuric acid so that the H_2SO_4-treated PPX tubes were obtained directly after the reaction without performing further experiments for the PLLA template fibers removal.

3.9.2. Self-assembly of polyelectrolytes onto the H_2SO_4-treated PPX tubes

In order to coat H_2SO_4-treated PPX tubes, the self-assembly deposition technique was employed. The self-assembly deposition procedure of PEMs on the surface of tubes is described as follows:

3.9.3. Polyelectrolyte solutions

Polyelectrolyte dipping solutions of 0.01 M (here concentrations refer to the concentration of the monomer repeat unit) were prepared by using ultrapure water (resistivity higher than 18.2 Ω/cm). The pH of PAA solution was adjusted with HCl to 4 and in the case of PAH solution the pH was adjusted with NaOH to 5.3. Other polyelectrolyte solutions were used without adjusting the pH. SDS was added to the 0.01 M PSS solution at a concentration of 0.02 M.

3.9.4. Deposition of the first layer

The first deposited layer (precoating layer) was PEI layer. The adsorption time for this precoating layer was 30 min, for all other layers it was 20 min. After each deposition, the samples were washed by immersion into ultrapure water three times (two min each washing). After each layer deposition the samples were not dried and when the deposition process were finished the samples were dried in air. Two different PEMs of $((PEI/PSS_{SDS})_{30}$ or $PEI(PAA/PAH)_{29}PAA)$ were formed on the surface of the tubes to obtain respectively PPX tubes coated with $((PEI/PSS_{SDS})_{30}$, SDS containing PEMTs or PPX tubes coated with $PEI(PAA/PAH)_{29}PAA)$, PAA containing PEMTs.

3.9.5. Washing Procedure

After deposition of the layer of PEI, the samples were rinsed in ultrapure water. The washing was done by immersing the tubes in the water for 2 minutes. This had to be done three times to remove access unstable non-adsorbed polyelectrolytes from the surface.

3.9.6. Deposition of Multilayers

The deposition procedure was similar to the deposition of the first layer. By knowing that the surface is now positively charged, an anionic polyelectrolyte was needed to deposit a

negatively charged layer on the surface. For this, the solution of PSS or PAA was used. The time of immersion was 20 minutes. After each layer deposition, the washing process was done. For the next layer deposition, the solution of PEI or PAH (polycation solution) was used to have a positively charged layer deposited on the surface. The slides were kept in polycation solutions for 20 min. After this stage, depending on the number of layers needed, the consecutive deposition of the PE layers with oppsite charges was carried out. the PEMs were coated onto the substrates were $(PEI/PSS_{SDS})_{30}$ or $PEI(PAA/PAH)_{29}PAA$.

3.9.7. Hydrochloric acid treatment

In order to study the effect of a low pH of environment on PEM coated tubes, they were kept in the solution of 0.5 M HCl for 40 min and then dried in air. SEM and ATR-FTIR spectroscopy from the tubes after HCl treatment were performed.

3.9.8. HCl treatment of H_2SO_4-treated PPX tubes coated with $(PEI/PSS_{SDS})_{30}$

After the $(PEI/PSS_{SDS})_{30}$ coated tubes were treated with HCl following the procedure above, the SEM and IR spectroscopy were performed in order to get information about the surface changes after acid treatment (see discussion section).

3.9.9. HCl treatment of H_2SO_4-treated PPX tubes coated with $PEI(PAA/PAH)_{29}PAA$

After the $PEI(PAA/PAH)_{29}PAA$ coated tubes were treated with HCl, the SEM and IR spectroscopy were performed in order to get information about the surface changes after acid treatment (see discussion section for the results).

3.10. Atom transfer radical polymerization (ATRP) of N,N-diisopropyl ammonium acrylate (NNDIPAAc)[72]

The atom transfer radical polymerization (ATRP) of N,N-diisopropyl ammonium acrylate (NNDIPAAc) was successfully carried out either with continuous exposure to air or in presence of small amounts of air.

3.10.1. ATRP of N,N-diisopropyl ammonium acrylate in presence of controlled amount of air

In this polymerization, small amounts of air was introduced to the reaction mixture during the polymerization. The preparation of NNDIPAAc consists of adding (2.28 g, 0.023 mol) of N,N-diisopropyl amine to (2 g, 0.028 mol) of freshly (under vacuum) distilled acrylic acid in a round bottom flask. The above mixture was washed with an appropriate amount of hexane, which was charged into the flask containing the mixture. After removing hexane, white salt was dried under vacuum at room temperature and kept in freezer. Controlled polymerisation was carried out in the following described procedure: all preparation steps were in presence of air.

3.10.1.1.Catalyst preparation

A catalyst mixture was prepared by adding 2 mg (0.014 mmol) of CuBr to 4 mg (0.026 mmol) of 2,2´-bipyridyl (bipy). 5 mL THF was quickly charged into the flask containing the catalyst mixture and the flask was sealed in air. The catalyst mixture was stirred for 15 min. After 15 min stirring, there was a clear colourless-light pink solution and still a green insoluble solid at the bottom of the flask. The solution part was taken by a syringe and used as the catalyst solution.

If the polymerization is carried out in a large scale (e.g. polymerization of 4 g of NNDIPAAc using the complex of CuBr/bipy as the catalyst), the preparation of the catalyst solution in the larger scale takes longer time due to the longer mixing time required to get the right complex of $Cu^{+}(bipy)_n$, which is able to catalyze the polymerization. In this case, the procedure of the catalyst preparation is described as follows: A catalyst mixture was prepared by adding 28.6 mg (0.20 mmol) of CuBr to 57.1 mg (0.37 mmol) of bipy. 70 mL THF was quickly charged into the flask containing the catalyst mixture and the flask was sealed in air. The mixture was stirred for 1 h. During mixing, the colour of the catalyst mixture changes

from a brown colour to a green colour. After 1 h stirring, there was a green mixture. In order to precipitate the insoluble part (green solid), the mixture was left for 4 h. The green insoluble part of the mixture was precipitated at the bottom of the flask and the solution above was nearly colourless. This solution was used as the catalyst for the polymerization.

3.10.1.2. Polymerization

The catalyst solution was injected into another flask containing 7 mg (0.041 mmol) of BzBr in 1 mL of THF, which was prepared previously. The flask was sealed and the solution was stirred for 30 min at room temperature. The above solution was added into a pear–shaped flask containing 280 mg (mmol) of NNDIPAAc salt. After dissolving NNDIPAAc, solvent was evaporated at 40 °C using a Rotary evaporator. The reaction mixture was placed into an oil bath at 60 °C. After this stage, the reaction was followed in presence of small amounts of air. After designated times, small samples were taken from the reaction mixture. In the case of introducing controlled amount of air to the reaction, the flask was sealed in presence of air using a stopper and was placed into the oil bath . Since each time for taking samples from the reaction the stopper has to be removed and therefore to have the same reaction conditions during the whole reaction time, after taking the first sample, air was introduced to the reaction by opening the flask in air every 10 min for 30 sec. The samples, which have been taken from the reaction, were quenched in liquid nitrogen.

Table 1. Molecular weights, polydispersities and conversions of poly (N,N-diisopropyl ammonium acrylate) synthesised by CuBr/bipy catalysed ATRP presence of small amounts of air (reaction was sealed in air and air was introduced to the reaction in designated times as described above).

For more detailes on NMR spectroscopy see discussion section.

Table 2. Molecular weights, polydispersities and conversions of poly (N,N-diisopropyl ammonium acrylate) synthesised by CuBr/bipy catalysed ATRP in different polymerization conditions. Reaction was carried out in presence of controlled amounts of air (reaction was sealed in air and air was introduced to the reaction in designated times as described above).

polymer	time (min)	M_n(GPC)	M_w/M_n (GPC)	Conversion%
1	10	12900	1.14	44
2	30	14600	1.19	56
3	90	17400	1.32	75
4	110	18000	1.46	81

3.10.2. ATRP of N,N-diisopropyl ammonium acrylate with continuous exposure to air.

The above procedure was followed. The only difference with the previous synthesis was that the reaction was carried out open to air. After evaporation of the solvent, the reaction mixture was placed in an oil bath to air at 60 °C with continuos exposure. After designated times, small samples were taken from the reaction and were quenched in liquid nitrogen.

Table 3. Molecular weights, polydispersities and conversions of poly (N,N-diisopropyl ammonium acrylate) synthesised by CuBr/bipy catalysed ATRP open to air.

polymer	time (min)	M_n(GPC)	M_w/M_n (GPC)	Conversion%
5	10	5800	1.24	42
6	15	7900	1.23	48
7	40	8900	1.35	60
8	65	10000	1.40	65

3.11. Modification of surfaces: Surface-initiated ATRP

In order to modify a surface of a given substrate, surface-initiated ATRP can be used. To achieve this goal, ATRP of different monomers was carried out using a surface initiator, which was chemically bonded to a pre-coating layer of A-174[140] at the surface of a glass substrate.

3.11.1. Surface initiated ATRP of N-isopropyl acrylamide (NIPAM)

The ATRP of NIPAM was carried out using a glass substrate bearing the brominated PPX (BrPPX), G_{BrPPX}, as suface initiator.

3.11.2. Preparation of the surface initiator

The pre-coating layer was deposited on a glass slide in order to stabilize the next layer (initiator layer) on the substrate. The deposition of the pre-coating layer (A-174) was performed according to the procedure described in the reference.[140] A layer of PPX with a thickness of 1500 nm was deposited on the previously coated-substrate (precoating layer: A-174) by means of chemical vapour deposition (CVD). In order to obtain the surface initiator, G_{BrPPX}, the deposited-PPX was converted to BrPPX. The PPX-coated substrate was placed into a flask containing 20 ml of CCl_4 and asobis(isobutironitrile) AIBN (32 g, 0.2 mmol) and bromine (0.1 ml, 2 mmol). The reaction mixture was refluxed for 5 h (ref 13.) and after, was left to cool down to room temperature. The modified slide was rinsed with chloroform and THF and dried in air.

To obtain the efficiency of bromination reaction, the reaction was carried out using a PPX film prepared by CVD process. Elemental analysis of the PPX film indicated that about 85 percent of the film is brominated.

Elemental analysis:

C 53.25% H 4.40% Br 42.35%

Slide-on ATR-FTIR:

ν / cm^{-1} : 3140 (w), 3020 (w), 2920 (w), 2840 (w), 1890 (w), 1790 (w), 1690(m), 1605 (w), 1570 (w), 1510 (m), 1450 (w), 1405 (m), 1270 (w), 1210 (w), 1170 (w), 1130 (w), 1085 (w), 1010 (w), 960 (w), 825 (s), 751 (w), 700 (w), 595 (s), 535(s).

3.11.3. Preparation of catalyst

For the catalyst preparation the procedure described in section 3.2.1.1 was followed.

3.11.4. ATRP procedure

The catalyst solution was injected into another flask containing the G_{BrPPX}. The flask was sealed and kept for 60 min at room temperature. The above solution together with the slide was charged into a flask containing 0.5 g (mmol) of NIPAM. After dissolving NIPAM, solvent was evaporated at 35 °C using a Rotary evaporator. The slide was covered by the reaction mixture after the solvent was evaporated. The flask was placed into an oil bath at 50 °C for 1.5 h. After the reaction was finished, the substrate was rinsed in water and THF and dried in air.

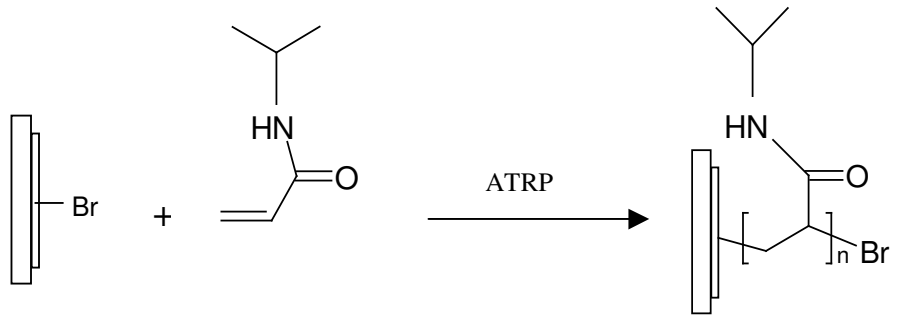

Scheme 9. Schematic illustration of the surface-initiated ATRP of NIPAM.

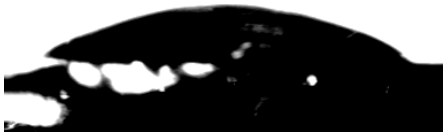

Figure 88. A water droplet on the PNIPAM-modified surface , θ = 26˚.

3.12. Immobilization of gold Particles on the Surface of PPX Films and PPX tubes

In order to coat the surface of the PPX films and tubes with a monolayer of gold series of experiments were carried out. The aim was to immobilize gold onto the surface of the substrate, which were previously coated with a monolayer of 1-dodecanthiol by using self-assebly technique. As gold can make covalent bound with thiol functional groups, it must be immobilized on the surface modified by a monolayer bearing thiol goups. 3.12.1. Preparation of modified surfaces suitable for gold immobilization.

3.12.1. Preparation of modified surfaces suitable for gold immobilization

3.12.1.1. H_2SO_4-treated PPX films/tubes

The same procedure as described in section 3.8.1 was followed to obtain suitable surfaces of the PPX film/tubes for self-asembly. After, the H_2SO_4-treated PPX films/tubes were used as substrate for self-assembly process.

3.12.1.2. Deposition of a monolayer of PEI on the surface of the H_2SO_4-treated PPX films/tubes (PEI- H_2SO_4-treated PPX films/tubes)

The H_2SO_4-treated PPX films/tubes were kept in a 0.01 M aqueous solution of PEI for 60 min. after deposition, the film/tubes were extensively rinsed in deionized water.

3.12.1.3. Deposition of a monolayer of 1-dodecanthiol deposition on the surface of the PEI- H_2SO_4-treated PPX films/tubes

The deposition of the monolayer of 1-dodecanthiol was performed by keeping the PEI-H_2SO_4-treated PPX films/tubes in different solutions of 1-dodecanthiol for 60 min. the reparation procedure of 1-dodecanethiol solutions is described as follows:

Aqueous solution of 1-dodecanthiol. The stock solution of 0.01 M of 1-dodecanthiol (thiol-solution-1) was prepared [131,132] by adding 1-dodecanthiol to the aqueous solution of CD at room temperature with a molar ratio of 1:2. The resulting mixture was stirred in a water bath at 40 ˚C for 48 h and then was cooled down to room temperature. A milky solution obtained was used to prepare the solution with different pHs. The pH of the solutions was adjusted by adding appropriate amounts of 10^{-6} and 10^{-5} M NaOH solution to the stock solution prepared above.

Therefore, as dipping solution to assemble a monolayer of 1-dodecanethiol on the PEI coated surfaces the solutions of 1-dodecanethiol as indicated in table 3 were prepared.

Table 4. Different solutions of 1-dodecanethiol prepared are shown here.

1-dodecanethiol solution	Stock solution	NaOH solution	
		10^{-6}	10^{-5}
Thiol-solution-1	x mL	-	-
Thiol-solution-2	1 mL	2 mL	-
Thiol-solution-3	1 mL	-	2 mL

3.12.2.4. Gold particles immobilized using the gold sol prepared by reduction of $HAuCl_4$ ($Au_{redAu(III)}$) onto the thiol-modified surfaces of the films/tube

The immobilization of gold particles on the thiol-modified surfaces is based on the reaction of gold with thiol (-SH) groups at the surface. Since gold particles prepared from $Au_{redAu(III)}$ are not stable and can aggregate therefore, as soon as gold particles were prepared, the immobilization process was performed.

The immobilization of gold on the thiol-modified surfaces was carried out as follows[130]:

0.75 g of tetraoctylammoniumbromide was added into 40 mL toluene in a 250 mL round-bottom and was stirred vigorously. 0.16 g $HAuCl_4.xH_2O$ (1 equiv) was dissolved in 12.5 mL deionized water and was added into the solution of tetraoctylammoniumbromide. The aqueous phase became colorless and the color of the organic phase changed from a bright yellow to a red-brown color as the $HAuCl_4$ was transferred to the organic phase. The organic phase was separated and the thiol-modified film/tubes were placed into the solution and kept for 10 min. The reaction was followed by the addition of previously prepared solution of 0.19 g $NaBH_4$ (10 equiv) in 12.5 mL deionized water. The reaction was then ultra-sonicated at room temperature for 3 h. After, the film/tubes were rinsed in toluene and water extensively and dried in air. The gold particles were immobilized onto the thiol-modified surfaces as are mentioned in table 4, which were prepared according to the discription in the section 3.4.1.

Table 5. Summarized data for preparation of the surfaces on which gold particles were immobilized.

Samples*	Thiol-modified-surfaces	1-dodecanethiol solution**
$Au_{redAu(III)-1}$	SH-mod-Sur-1	Thiol-solution-1
$Au_{redAu(III)-2}$	SH-mod-Sur-2	Thiol-solution-2
$Au_{redAu(III)-3}$	SH-mod-Sur-3	Thiol-solution-3

* After gold immobilization onto the surface

** 1-dodecanethiol solution, which was used as dipping solution for the preparation of the thiol-modified surfaces

The characterization of the surfaces is discussed in discussion section.

3.12.2.5. Imobilization of thiol-stabilized-Gold particles on the thiol-modified surfaces of films/tubes

Thiol-stabilized-gold particles were immobilized onto the surfaces by means of the exchange reactions between 1-dodecanthiol at the surface of the thiol-stabilized gold particles and 1-dodecanethiol at the surface of the thiol-modified fibers/tubes.

The thiol-modfied film/tubes were placed into the gold sol containing thiol-stabilized gold particles in toluene at room temperature for 48 h. After, the film/tubes were rinsed extensively in toluene and deionized water, and then dried in air. The thiol-stabilized-gold particles were immobilized onto the thiol-modified surfaces as are mentioned in table 5.

Table 6. Summarized data for preparation of the surfaces on which thiol-stabilized gold particles were immobilized.

Samples*	Thiol-modified-surfaces	1-dodecanethiol solution**
$Au_{thiol\text{-}stab\text{-}1}$	SH-mod-Sur-1	Thiol-solution-1
$Au_{thiol\text{-}stab\text{-}2}$	SH-mod-Sur-2	Thiol-solution-2
$Au_{thiol\text{-}stab\text{-}3}$	SH-mod-Sur-3	Thiol-solution-3

* After gold immobilization onto the surface

** 1-dodecanethiol solution, which was used as dipping solution for the preparation of the thiol-modified surfaces

The characterization of the surfaces were discussed in the discussion section.

3.12.2.6. Imobilization of DMAP-stabilized-gold particles on the thiol-modified surfaces of films/tubes immobilized on the thiol-modified surfaces of films/tubes

DMAP-stabilized-gold particles were immobilized onto the surfaces by means of the exchange reactions between DMAP at the surface of the gold particles and at the surface of the thiol-modified fibers/tubes.

The thiol-modfied film/tubes were placed into the gold sol containing DMAP-stabilized gold particles (0.01 g gold paticles in 2 mL deionized water) at room temperature for 48 h. After, the film/tubes were rinsed extensively in deionized water and dried in air. The DMAP-stabilized-gold particles were immobilized onto the thiol-modified surfaces as are mentioned in table 6.

Table 7. Summarized data for preparation of the surfaces on which DMAP-stabilized gold particles were immobilized.

Samples*	Thiol-modified-surfaces	1-dodecanethiol solution**
$Au_{DMAP\text{-}stab\text{-}1}$	SH-mod-Sur-1	Thiol-solution-1
$Au_{DMAP\text{-}stab\text{-}2}$	SH-mod-Sur-2	Thiol-solution-2
$Au_{DMAP\text{-}stab\text{-}3}$	SH-mod-Sur-3	Thiol-solution-3

* After gold immobilization onto the surface

** 1-dodecanethiol solution, which was used as dipping solution for the preparation of the thiol-modified surfaces

3.13. Immobilization of gold Particles at the end of PPX tubes

3.13.1. Thiol (mercapto) functionalities at the ends of the tubes

PPX tubes after H_2SO_4 treatment were used as substrate. Monolayers of PEI and 1-dodecanthiol were respectively self-assembled onto the surface of the tubes. The formation of

the monolayers were previously described in section 3.12.1.3. Then, a new layer of PPX were deposited onto the thiol-modified surface of the tubes by using CVD. If these tubes are cut (tubes first were freezed in liquid nitrogen and then were cut), at the end of the tubes, the inner layers will be out so that the gold particles can be self-assembled at the ends of the cut tubes, where the thiol groups exist.

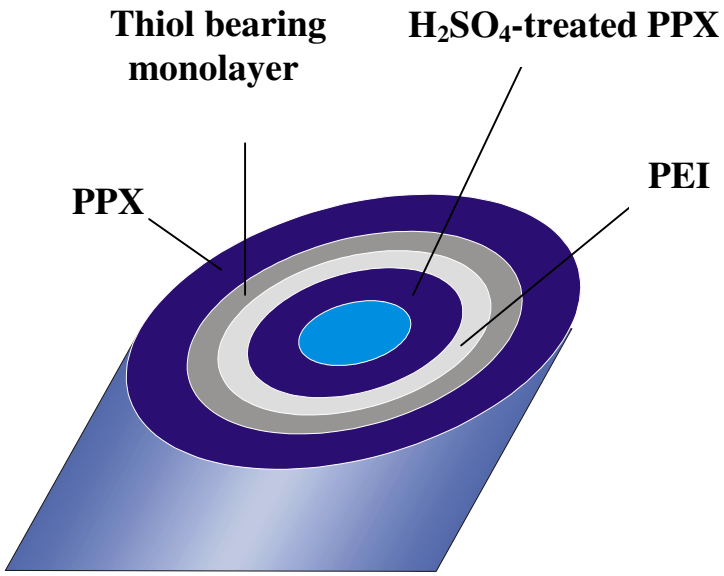

Figure 89. Schematic representation of a cut-tube.

Table 8. Summarized data for preparation of the tubes on which a monolayer of the 1-dodecanethiol was self-assembled.

Thiol-modified-end- tubes*	1-dodecanethiol solution**
Thiol-mod-end-tubes-3	Thiol-solution-3

* Thiol-modified-end-tubes stands for the cut tubes with Thiol (mercapto) functionalities at the ends (also see figure 84).

** 1-dodecanethiol solution, which was used as dipping solution for the preparation of the thiol-modified surfaces

3.13.2. Immobilization of Au particles from the $Au_{redAu(III)}$ at the ends of $PPXT_{end\text{-}thiol\text{-}mod\text{-}3}$

Because of the existence of the thiol functionalities at the ends of the tubes, the gold particle can be self-assembled onto the ends of the tubes to obtain $PPXT_{end\text{-}gold\text{-}mod\text{-}3}$. The preparation of the gold sols and the self-assembly process were performed by following the description mentioned previously.

3.13.3. Imobilization of thiol-stabilized-Gold particles at the ends of $PPXT_{end\text{-}thiol\text{-}mod\text{-}3}$

The preparation of the gold sols and the self-assembly process were performed by following the description mentioned previously.

Zusammenfassung

Als ein Ergebnis das in dieser Arbeit erzielt worden ist, können versiegelte Nano-Mikrorohrchen mit unterschiedlichen Polymerschichten als Versiegelung erwähnt werden. PPX-Hohlfasern wurden mit N,N-Diisopropylammonium-polyacrylate und PNIPAM unter Anwendung von ATRP versiegelt. PAA ist ein schwacher Polyelektrolyt, welcher pH-Sensitivität aufweist und PNIPAM ist ein hitse-emfindliches Polymer. Folglich können die Nanorohre, die mit diesen Materialien versiegelt werden, für pH-Wert-Bestimmungen oder zur Messung sehr geringer Temperautänderungen eingesetzt werden.

Selbstorganisation (self-assembly) wurde eingesetzt, um PPX –Nanorohre mit PEM zu versiegeln. Da PPX-Nanorohre nicht verwendbare Substrate für Selbstorganisation sind, musste der Polyelektrolyt zuerst mit H_2SO_4 behandelt werden, um negative Ladungen an kleinen ausgewählten Bereichen der Oberfläche der PPX-Nanorohre zu erhalten. Die PPX-Nanorohre wurden mit PEMs aus PEI $(PAA/PAH)_{29}PAA$ versiegelt. Diese Art von PEM kann durch Einführen in Lösungen mit $pH < 1$ oder $pH > 13$ entfernt werden. Dadurch besteht die Möglichkeit die versiegelten Nanorohre zu schalten. Bei einem sehr niedrigem oder einem sehr hohem pH können sie geöffnet werden.

Die Anordnung von PEM-SiO_2 Nanofasern und von PEMHFs wurde demonstriert. Die Herstellung von PEMHF gelang mit einzigartiger pH-Empfindlichkeit und mit hoher Strukturflexibilität. PEMHF sind in der Lage, ihre Größe nach Behandlung der ursprünglichen Fasern mit HF um das zehnfache zu erhöhen. Die hohe Flexibilität und die Stabilität der röhrenförmigen Fasern bei niedrigem pH-Wert ist aufgrund des Einbaus von SDS innerhalb der Struktur der Fasern möglich. Die extreme Zunahme des Durchmessers von PEMHF, im Vergleich zu PEM-Silica-Fasern, liegt am hohen Grad protonierter PEI Schichten innerhalb der Struktur von PEMT. Die elektrostatischen Abstoßungskräfte der PEI-Schichten verursachen möglicherweise eine Vergrößerung des Abstandes zwischen den Ketten. Diese Entdeckung, dass alternierende Polyelektrolytschichten innerhalb von PEMHF die Eigenschaften der röhrenförmige Fasern verändern, könnte zur Optimierung der Eigenschaften wie pH-Empfindlichkeit und Thermosensitivität genutzt werden.

Die kontrollierte Polymerisation von N,N-Diisopropylammoniumacrylat wurde erfolgreich bei 60 ºC bei Vorhandensein von Luft durchgeführt. Die ATRP wurde entweder in Anwesenheit von etwas Sauerstoff oder vollkommen unter Luft mit NNDIPAAc als Monomer durchgeführt. Die niedrigsten Polydisperisitäten und die höchsten Reaktionsraten wurden für die Reaktionen beobachtet, die ohne Schutzgas durchgeführt wurden. Es ist denkbar, dass Sauerstoff bei dieser Reaktion als Cokatalysator dient. Für eine eindeutige Aussage über die Funktion des Sauerstoffs sind quantitative Experimente nötig, die in Bearbeitung sind. Die ATRP wurde an einer Oberfläche. durchgeführt, um die Oberfläche der Substrate zu ändern. Es wurden beschichtete Glassubstrate mit BrPPX als Oberflächeinitiator eingesetzt, so dass die ATRP von NIPAM stattfand. Der Wasserkontaktwinkel der Filme verringerte sich auf 26º, nachdem die Polymerisierung durchgeführt wurde und PNIPAM auf der Oberfläche adsorbiert war.

Goldpartikel wurden erfolgreich auf den selbstorganiiserten Oberflächen der Filme und der Nanorohre immobilisiert. 1-Dodecanethiol wurden durch die Anwendung der Selbstorganisations-Technik auf die Oberflächen aufgebracht. Die Goldpartikel, die auf der Oberfläche immobilisiert wurden, waren $Au_{redAu(III)}$, thiol-stabilisierte Goldpartikel und DMAP-stabilisierte Goldpartikel. In einem anderen Versuch wurden die Goldpartikel am Ende der Nanorohre aufgebracht. Dafür wurden die Enden der Nanorohre mit Thiol-Gruppen zunächst funktionalisiert und in einem zweiten Schritt die Goldpartikel angebracht.

References

[1] A, Formhals, *US Patent* 1934, 1,975,504.

[2] A, Formhals, *US Patent* **1939,** 2,160,962.

[3] A, Formhals, *US Patent* **1940,** 2,187, 306.

[4] M. Bognitzki, H. Hou, M. Ishaque, T. Freese, M. Hellwig, C. Schwarte, A. Schaper, J. H. Wendorff, A. Greiner, *Adv. Mater.* **2000,** 12, 637.

[5] M. Szwarc, *Nature* **1947,** 160, 403.

[6] M. Szwarc, *Faraday Society Discussions* **1947,** 2, 46.

[7] M. Szwarc, *J. Chem. Phys.* **1948,** 16, 128.

[8] W. F. Gorham, *US Patent* **1967,** 3, 342, 754.

[9] W. F. Gorham, *J. Polymer science: part A-1* **1966,** 4, 3027.

[10] Y. L. Yeh, W. F. Gorham, *The J. Organic Chemistry* **1969,** 34(8), 2366.

[11] A. Greiner, S. Mang, O. Schäfer, P. simon, *Acta Polymer.* **1997,** 48, 1.

[12] P. Simon, S. Mang, A. Hasenhindl, W. Gronski, A. Greiner, *Macromolecules* **1998,** 31, 8775.

[13] J. B. Fortin, T.-M. Lu, *Chem. Mater.* **2002,** 14, 1945.

[14] G. Decher, Y. Lvov, J. Schmitt, *Thin Solid Films* **1994,** 244, 722.

[15] G. Decher, *Science* **1997,** 277, 1232.

[16] J. Schmitt, T. Griinewald, G Decher, P. Pershan, K. Kjaer, M. Losche,. *Macromolecules* **1993,** *26*, 7058.

[17] N. A. Kotov, I. Dékány, J. H. Fendler, *J. Phys. Chem.* **1995**, *99*, 13065.

[18] T. Cassagneau, J. H. Fendler, T. E. Mallouk, *Langmuir* **2000**, *16*, 241.

[19] J. H. Rouse, Peter T. Lillehei, *Nano Lett.* **2003***,* 3(1), 59.

[20] A. Carrillo, J. A. Swartz, J. M. Gamba, R. S. Kane, N. Chakrapani, B. Wei, .P. M. Ajayan, *Nano Letters* **2003***,* 3 (10), 1437.

[21] M. Olek, J. Ostrander, S. Jurga, H. Möhwald, N. Kotov, K. Kempa, M. Giersig, *Nano Letters* **2004***,* 4 (10), 1889.

[22] R. Ma, T. Sasaki, Y. Bando, *J. Am. Chem. Soc.* **2004,** 126 (33), 10382.

[23] A. B. Artyukhin, O. Bakajin, P. Stroeve, A. Noy, *Langmuir* **2004,** *20,* 1442.

[24] B. Kim, Wolfgang M. Sigmund, *Langmuir* **2004,** *20,* 8239

[25] P. V. Pavoor, B. P. Gearing, R. E. Gorga, A. j. Bellare, R. E. Cohen, *Journal of Applied Polymer Science* **2004**, 92, 439.

[25] J. Yan, S. Dong, *Langmuir* **1997,** 13, 3251.

[26] J. Liu, R. Xu, A. E. Kaifer, *Langmuir* **1998,** 14, 7337.

[27] A.. Formhals, *US patent,* **1934,** 1, 975, 504.

[28] A.. Formhals, *US patent* **1939,** 2,160,962.

[29] A.. Formhals, *US patent* **1940,** 2,187,306.

[30] A.. Formhals, *US patent* **1943,** 2,323,025.

[31] A.. Formhals, *US patent* **1944,** 2,349,950.

[32] HL. Simons, *US patent* **1966,** 3,280,229.

[33] H. Fong, I. Chun, DH. Reneker, *Polymer* **1999,** 40, 4585.

[34] R. Inai1, M. Kotaki, S. Ramakrishna, *Nanotechnology* **2005,** 16, 208.

[35] X. Zong, K. Kim, D. Fang, S. Ran, B. Hsiao, B. Chu, *Polymer* **2002,** 43, 4403.

[36] T. A. Kowalewski, S. Blonski, S. Barral, *Bulletin of the Polish Academy of Science* **2005,** 53 (4), 358.

[37] M. M. Bergshoef, G. J. Vancso, *Adv. Mater* **1999,** 11(16), 1362.

[38] J. M. Deitzel, J. Kleinmeyer, D. HarrisD, N. C. B. Tan, *Polymer* **2001,** 42, 261.

[39] S. Koombhongse, W. X. Liu, D. H. Reneker, *Polymer Sci J: Part B: Polymer Physics* ***2*001,** 39, 2598.

[40] D. H. Reneker, A. L. Yarin , H. Fong, S. Koombhongse, *J. Appl Phys* **2000,** 87, 4531.

[41] A. L. Yarin, S. Koombhongse, D. H. Reneker, *J. Appl Phys* **2001,** 89(5), 3018.

[42] A. L. Yarin, S. Koombhongse, D. H. Reneker, *J Appl Phys* **2001,** 89(9), 4836.

[43] Y. M. Shin, M. M. Hohman, M. P. Brenner, G. C. Rutledge, *Appl Phys Lett* **2001,** 78, 1149.

[44] M. M. Hohman, M. Shin, G. Rutledge, M. P. Brenner, *Physics of Fluids* **2001,** 13, 2201.

[45] M. M. Hohman, M. Shin, G. Rutledge, M. P. Brenner, *Physics of Fluids* **2001,** 13, 2221.

[46] P. K. Baumgarten, *J. Colloid and Interface Science* **1971,** 36, 71.

[47] J. Doshi, D. H. Reneker, *J. Electrostatics* **1995,** 35(2-3),151.

[48] H. Fong, I. Chun, D. H. Reneker, *Polymer* **1999,** 40, 4585.

[49] J. M. Deitzel, J. Kleinmeyer, D. Harris, N. C. B. Tan, *Polymer* **2001,** 42, 261.

[50] M.M. Demir, I. Yilgor, E. Yilgor, B. Erman, *Polymer* **2002,** 43, 3303.

[51] R. Jaeger, H. Schönherr, G. J. Vancso, *Macromolecules* **1996,** 29, 7634.

[52] H. Fong, D. H. Reneker, *J Polym Sci: Part B Polym Phys* **1999,** 37(24), 3488.

[53] E. Zussman, A. L. Yarin, D. Weihs, *Experiments in Fluids* **2002,** 33, 315.

[54] D. Ziegler, K. J. Senecal, C. Drew, L. Samuelson, *New Frontiers in Fiber Science, Spring Meeting* **2001.**

[55] Szwarc, M. *Discuss. Faraday Soc.* **1947**, *2*, 46.

[56] Szwarc, M. *J. Polym. Sci.* **1951**, *6* (3), 319.

[57] Szwarc, M. *J. Chem. Phys.* **1948**, *16* (2), 128.

[58] Gorham, W. *J. Polym. Sci. A-1* **1966**, *4*, 3027.

[59] W. F. Gorham, *J . Polym. Sci.,* **1966,** 4, 3027.

[60] W. F. Corham (UnionCarbide Corp.), *US Patent* **1967,** 3,342,754.

[61] K. Matyjaszewski, J. Xia, *Chem. Rev.* **2001,** 101, 2921.

[62] K. Ohno, T. Morinaga, K. Koh, Y. Tsujii, T. Fukuda, *Macromolecules* **2005,** 38, 2137.

[63] D. Xiao, M. J. Wirth, *Macromolecules* **2002,** 35, 2919.

[64] K. Min, J. Hu, C. Wang, A. Elaissari, *J. Polymer Science: Part A: Polym. Chem.* **2002,** 40, 892.

[65] H. Kong, W. Li, C. Gao, D. Yan, *J. Mater. Chem.* **2004,** 14, 1401.

[66] P. Zhang, C. He, R. D. Craven, J. A. Evans, N. C. Fawcett, *Macromolecules* **1999,** 32, 2149.

[67] Y-P Wang, X-W Pei, X-Y He, Z-Q Lei, *European Polym. J.* **2005,** 41, 737.

[68] M. Bednarek, T. Biedron, P. Kubisa, *Macromol. Chem.Phys.* **2000,** 201, 58.

[69] M. Teodorescu, K. Matyjaszewski, *Macromolecules* **1999**, *32*, 4826.

[70] M. Bednarek, T. Biedron, P. Kubisa, *Macromol. Chem.Phys.* **2000,** 201, 58.

[71] E. J. Ashford, V. Naldi, R. O'Dell, N. C. Billingham, S. P. Arms, S. P. *Chem. Commun.* **1999,** 1285.

[72] A. Kazemi, S. Agarwal and A. Greiner, *Designed Monomers and Polymers* **2005,** 8 (6), 673.

[73] K. Matyjaszewski, T. E. Patten, J. Xia, *J. Am. Chem. Soc.* **1997,** 119, 674.

[74] K. Matyjaszewski, K. Davis, T. Patten, M Wie, *Tetrahedron* **1997,** 53, 15321.

[75] K. Matyjaszewski, K. Nakagava, C. G. Jasieczek, *Macromolecules* **1998,** 31, 1535.

[76] X. wang, N. Luo, S. Ying, *Polymer* **1999,** 40, 4157.

[77] X. S. wang, S. P. Arms, *Macromolecules* **2000,** 33, 6640.

[78] S. Perrier, S. P. Arms, X. S. wang, F. Malet, D. M. Haddleton, *J. polym. Sci., Part A: Polym. Chem.* **2001,** 39, 1696.

[79] J. Chaoyang, S. Dinesh, V. V. T. Kommireddy, *Advanced Functional Materials* **2006,** 16, 27.

[80] G. Decher, J.D. Hong, J. Schmitt, *Thin Solid Films* **1992,** 210, 831.

[81] H-J. Himel, C. Wöll, *Chemie in unserer Zeit* **1998,** 32(6), 294.

[82] K. C. Grabar, R. G. Freeman, M. B. Hommer, M. J. Natan, *Anal. Chem.* **1995,** 67, 735.

[83] G. Decher, Y. Lvov, J. Schmitt, *Thin Solid Films* **1994,** 244, 722.

[84] G. Decher, *Science* **1997,** 277, 1232.

[85] J. Schmitt, T. Griinewald, G Decher, P. Pershan, K. Kjaer, M. Losche,. *Macromolecules* **1993,** *26*, 7058.

[86] M. Schönhoff, *Current Opinion in Coll. Interf. Sci.* **2003,** 8(1), 86.

[87] M. Schönhoff, *J. Phys.: Cond. Matter* **2003**, 15(49), R1781.

[88] M. Park, S. Deng, R. C. Advincula, *J. Am. Chem.Soc.* **2004,** 126 (42), 13723.

[89] S. Y. Yang, M. F. Rubner, *J. Am. Chem. Soc.* **2002,** 124 (10), 2100.

[90] D.M. DeLongchamp, P. T. Hammond, *Langmuir* **2004**, 20 (13), 5403.

[91] D.M. DeLongchamp, P. T. Hammond, *Langmuir* **2004**, 20 (13), 5403.

[92] P. M. Claesson, M. Bergström, A. Dedinaite, M. Kjellin, J. F. Legrand, I. Grillo, *J. Phys. Chem. B* **2000**, 104,11689.

[93] A. F. Thünemann, S. Kubowicz, U. Pietsch, *Langmuir* **2000**, *16*, 8562.

[94] A. F Thünemann, *Langmuir* **2000**, *16*, 824.

[95] M. S. Johal, B. H. Ozer, J. L. Casson, A. St. John, J. M. Robinson, H. L. Wang,. *Langmuir* **2004**, 20, 2792.

[96] K. Müller, J. F. Quinn, A. P. R. Johnston, M. Becker, A. Greiner, F. Caruso, Chem. Mater. 2006, Chem. Mater. 2006, 18, 2397.

[97] N. A. Kotov, I. Dékány, J. H. Fendler, *J. Phys. Chem.* **1995**, *99*, 13065.

[98] T. Cassagneau, J. H. Fendler, T. E. Mallouk, *Langmuir* **2000**, *16*, 241.

[99] J. H. Rouse, Peter T. Lillehei, *Nano Lett.* **2003***,* 3(1), 59.

[100] A. Carrillo, J. A. Swartz, J. M. Gamba, R. S. Kane, N. Chakrapani, B. Wei, .P. M. Ajayan, *Nano Letters* **2003***,* 3 (10), 1437.

[101] M. Olek, J. Ostrander, S. Jurga, H. Möhwald, N. Kotov, K. Kempa, M. Giersig, *Nano Letters* **2004***,* 4 (10), 1889.

[102] R. Ma, T. Sasaki, Y. Bando, *J. Am. Chem. Soc.* **2004,** 126 (33), 10382.

[103] A. B. Artyukhin, O. Bakajin, P. Stroeve, A. Noy, *Langmuir* **2004,** *20,* 1442.

[104] B. Kim, W. M. Sigmund, *Langmuir* **2004,** *20,* 8239.

[105] P. V. Pavoor, B. P. Gearing, R. E. Gorga, A. j. Bellare, R. E. Cohen, *Journal of Applied Polymer Science* **2004**, 92, 439.

[106] C. Déjugnat, G. B. Sukhorukov, *Langmuir* **2004**, 20, 7265.

[107] T. Mauser, C. Déjugnat, G. B. Sukhorukov, *Macromol. Rapid Commun.* **2004,** 25 (20), 1781.

[108] C. Déjugnat, D. Haloan, G. B. Sukhorukov, *Macromol. Rapid Commun.***2005**, 26 (12), 961.

[109] S. Y. Yang, M. F. Rubner, *J. Am. Chem. Soc.* **2002,** 124 (10), 2100.

[110] D.M. DeLongchamp, P. T. Hammond, *Langmuir* **2004**, 20 (13), 5403.

[111] S. S. Shiratori, M. F. Rubner, *Macromolecules* **2000,** 33, 4213.

[112] S. T. Dubas, T. R. Farhat, J. B. Schlenoff, *J. Am. Chem. Soc*. **2001,** 123, 5368.

[113] G. J. Fleer, M. A. Cohen Stuart, J. M. H. M. Scheutjens, T. Cosgrove, B. Vincent, *Polymers at*

interfaces: Chapman and Hall, London, 1993.

[114] N. G. Hoogeveen, M. A. Cohen Stuart, G. J. Fleer, *Langmuir* **1996,** 12, 3675.

[115] A. B. Artyukhin, O. Bakajin, P. Stroeve, A. Noy, *Langmuir* **2004,** 20, 1442.

[116] J. H. Rouse and P. T. Lillehei, *Nano Lett.*. **2003,** 3(1), 59.

[117] M. Olek, J. Ostrander, S. Jurga, H. Möhwald, N. Kotov, K. Kempa, M. Giersig, *Nano Letters* **2004***,* 4 (10), 1889.

[118] P. V. Pavoor, B. P. Gearing, R. E. Gorga, A. j. Bellare, R. E. Cohen, *Journal of Applied Polymer Science* **2004**, 92, 439.

[119] A. Carrillo, J. A. Swartz, J. M. Gamba, R. S. Kane, N. Chakrapani, B. Wei, .P. M. Ajayan, *Nano Letters* **2003***,* 3 (10), 1437.

[120] B. Kim, W. M. Sigmund, *Langmuir* **2004,** *20,* 8239.

[1210] R. Ma, T. Sasaki, Y. Bando, *J. Am. Chem. Soc.* **2004,** 126 (33), 10382.

[122] M. Bognitzki, H. Hou, M. Ishaque, T. Frese, M. Hellwig, C. Schwarte, A. Schaper, J. H. Wendorff, A. Greiner, *Adv. Mater.* **2000,** 12 (9), 637.

[123] W. F. Gorham, *J. Polym. Sci., part A-1* **1966,** 4, 3027.

[124] A. Greiner, S. Mang, O. Schäfer, P. Simon, *Acta Polymer.* **1997,** 48, 1.

[125] S. Iwatsuki, *Adv. Polym. Sci.* **1984,** 58, 93.

[126] A. Kazemi, M. Schönhoff and A. Greiner, *to be submitted to Small.*

[127] E. Díez-Peña, I. Quijada-Garrido, J. M. Barrales-Rienda, M. Wilhelm, H. W. Spiess, *Macromol. Chem. Phys.* **2002,** 203, 491.

[128] M. V. Deshmukh, A. A. Vaidya, M. G. Kulkarni, P. R. Rajamohanan, S. Ganapathy, *Polymer* **2000,** 41, 7951.

[129] H. E. Gottlieb, V. Kotlyar, A. Nudelman, *J. Org. Chem.***1997,** 62, 7512.

[130] I. Calderara, R. Gougeon, L. Delmotte, V. Lemee, D. J. Lougnot, *J. Polym. Sci., Part A: Polym. Chem.* **1997,** 35, 3619.

[131] A. Anders, D. Kuckling, M. Schönhoff, Colloids and surfaces A: Physicochemical and engineering Aspects 2001, 190, 185.

[132] J. Lui, R. Xu, A. E. Kaifer, *Langmuir* **1998,** 14, 7337.

[133] J. Yan, S. Dong, *Langmuir* **1997,** 13, 3251.

[134] V. Ramamurthy, D. F. Eaton, *Acc. Chem. Res.* **1988,** 21, 300.

[135] J. Cho, F. Caruso, *Chem. Mater.* **2005,** 17, 4547-4553

[136] D. V. Leff, L. Brandt, J. R. Heath, *Langmuir* **1996**, *12*, 4723.

[137] X. Y. Chen, J. R. Li, L. Jiang, *Nanotechnology* **2000**, *11*, 108.

[138] A. W. Shaffer, J. G. Worden, Q. Huo, *Langmuir* **2004,** 20, 8343.

[139] M. J. Hostetler, J. E. Wingate, C-J Zhong, J E. Harris, R. W. Vachet, M. R. Clark, J. D. Londono, S. J. Green, J. J. Stocks, G. D. Wignall, G. L. Glish, M. D. porter, N. D. Evans, R. W. Murray, *Langmuir* **1998,** 14, 17.

[140] Speedline Technology, Specially Coating Systems.

[141] G. Zhang, W. Kataphinan, R. Teye-Mensah, P. Katta, L. Khatri, E. A. Evans, G. G. Chase, R. D. Ramsier, D. H. Reneker, *Materials Science and Engineering B* **2005,** 116, 353.

Acknowledgements

I would like to express my sincere appreciation to Prof. Andreas Greiner, who served as my supervisor. Furtheremore, I thank him very much for the valuable discussions about the projects.

My special thanks go to Prof. Monika Schönhoff for the collaboration on the project of the preparation of the polyelectrolyte multilayer hollow fibers and her helpful advice during the work.

My special thanks also go to Dr Michael Bognitzki for the frequent discussions about synthesis.

I would like specially to thank Christian Krüger for his helps and collaboration on the preparation of the gold sols.

I thank the group of Prof. J. H. Wendorff for their helps in the measurements.

I am grateful to Mr. Michael Hellwig for his kind helps and advice during the work with SEM.

Many thanks to the colleagues in the electronik and mechanischen-workstatt for their helps with solving electronical/mechanical problems of the instruments.

I am very thankful to my friends and colleagues in our group for the nice time that I will never forget it.

Last but not least, I would like to thank my family for their support not only during my studies but for their help with my life.